

ScholarWorks@GSU

The Neuroprediction of Recidivism: Validation and Extension of the Error-Monitoring Model

Authors	Allen, Corey
Citation	Allen, Corey. "The Neuroprediction of Recidivism: Validation and Extension of the Error-Monitoring Model." Dissertation, Georgia State University, 2021. https://doi.org/10.57709/23745980
DOI	https://doi.org/10.57709/23745980
Download date	2026-03-10 03:16:12
Link to Item	https://hdl.handle.net/20.500.14694/11408

THE NEUROPREDICTION OF RECIDIVISM: VALIDATION AND EXTENSION OF THE
ERROR-MONITORING MODEL

by

COREY H. ALLEN

Under the Direction of Eyal Aharoni, PhD

ABSTRACT

Despite decades of research examining the brain's contributions to the propensity for antisocial behavior, this process is still poorly understood, owing in part to the highly multivariate relationship between the brain, behavioral phenotypes, and the dynamic environmental contexts in which they operate. An important criterion for evaluating the strength of a given explanation is the degree to which it makes accurate predictions. Prior research has demonstrated that hemodynamic activity related to error-monitoring in the dorsal anterior cingulate cortex (dACC) (Aharoni et al., 2013, 2014) improved predictions of rearrest in a sample of criminal offenders. Yet, it remains unclear how generalizable these results are and whether these effects are task specific.

This dissertation project uses hypothesis-driven approaches to probe the generalizability of the previously demonstrated predictive utility of limbic activity for rearrest, as well as establish and test novel task-based and resting state measures for the same purpose. The first analysis used a large sample ($n = 442$) of criminal offenders to establish new limbic regions of interest in order to increase the predictive accuracy of a model of reoffense risk developed in a previously published male ($n = 95$) inmate sample. The second analysis tested the predictive utility of the resting state functional connectivity between these limbic regions and demonstrated robust resting state & multimodal models for the prediction of rearrest in a subset of the same male ($n = 91$) inmate sample. The final analysis tested the out-of-sample generalizability of the original error-monitoring model tested in Aharoni et al., 2013/2014 in a large sample of male ($n = 290$) and female ($n = 248$) offenders. This analysis provides modest support for the predictive utility of error-monitoring activity in the dACC for predictions of rearrest for felonies in women and violent felonies in men, replicating aspects of the previous studies. Overall, these results reinforce and extend research on limbic predictors of recurrent, impulsive antisocial behavior. Implications for clinical and forensic risk assessment are discussed.

INDEX WORDS: Impulsivity, Recidivism, Risk assessment, Resting state functional connectivity, Forensic population, Violence, Neuroprediction

THE NEUROPREDICTION OF RECIDIVISM: VALIDATION AND EXTENSION OF THE
ERROR-MONITORING MODEL

by

COREY H. ALLEN

A Dissertation Submitted in Partial Fulfillment of the Requirements for the Degree of

Doctor of Philosophy

in the College of Arts and Sciences

Georgia State University

2021

Copyright by
Corey Hill Allen
2021

THE NEUROPREDICTION OF RECIDIVISM: VALIDATION AND EXTENSION OF THE
ERROR-MONITORING MODEL

by

COREY H. ALLEN

Committee Chair: Eyal Aharoni

Committee: Isabelle Buard

Eddy Nahmias

Jessica A. Turner

Electronic Version Approved:

Office of Graduate Services

College of Arts and Sciences

Georgia State University

August 2021

ACKNOWLEDGEMENTS

I owe endless amounts of gratitude to all those who made this project possible, starting with my primary research advisor, *Eyal Aharoni*. Over the past five years, *Eyal* has provided constant support to my academic endeavors and has undoubtedly shaped who I am as a researcher in more fields than one. Without *Eyal*, my broader interests in moral psychology would have gone unexplored, my interests in cognitive neuroscience would lack interdisciplinarity, and the more concrete legal implications of my ongoing research would lack their necessary depth. Simply put, his constant feedback and advice have been the bedrock of my graduate experience and I cannot imagine having a more fitting graduate advisor (nor climbing partner).

Similarly, *Eddy Nahmias*, my secondary graduate advisor and Chair of GSU's Philosophy Department, has been a fantastic mentor since the day I interviewed for my fellowship in Neuroethics. Alongside doling out constant writing advice, *Eddy's* impetus for exploring new research ideas has made me far more comfortable in putting words to a page and at looking towards the world of science-fiction for experimental inspiration.

Jessica Turner, a mentor whose work has left me constantly humbled, has been a guiding force in my graduate career via the courses I've had the fortune of taking from her. Starting with Cognitive Neuroscience and ending with a Neuroimaging Methods course, *Jessica's* teaching has enabled me to be the researcher I am today, and I am incredibly thankful to have been afforded the opportunity to learn from her.

In addition to my phenomenal graduate mentors, *Isabelle Buard* provided me with my first *real* undergraduate research assistantship at the University of Colorado Anschutz Medical Campus. Her confidence in me, and support for me, paved the way for my first peer-reviewed

publication, and gave me my first taste of academic research. Needless to say, I would not have pursued neuroscience at a graduate level if it weren't for *Isabelle* and her support. In a similar vein, I owe great thanks to *Brian Drwecki*, *Mark Bruhn*, *Ted Zenzinger*, and *Jason Taylor*, at my undergraduate institution, Regis University, for supporting my early (and naïve) attempts at integrating neuroscience and philosophy within my undergraduate honors thesis.

Of course, I must also acknowledge the funding sources that made this dissertation research possible. My first four years of research at Georgia State University were generously funded through the *2nd Century Initiative doctoral fellowship in Neuroethics*. My final year of funding has been graciously provided by GSU's Department of Psychology via a Graduate Teaching Assistantship, in which I've had the pleasure of teaching two semesters of *Sensation and Perception* to undergraduate psychology and neuroscience students.

Additionally, I have many non-academic sources of support that are due equal (or more!) amounts of gratitude. First, I have to thank my mother, *Cindy Allen*, who has not only supported me in *every* single one of my endeavors, but also stoked my interest in the sciences at an early age by enrolling me as her impromptu study partner as she was attaining her Pharm.D. Second, I have to thank my brother & sister, and brother-in-law, *Kyle & Kelly Allen*, and *Chris Grawl*, for their constant support and for indulging me in conversations regarding my research far more than is considered obligatorily polite. In a similar vein, I thank my father, *Mark Allen*, for his interest and continued support in my work. Third, I owe much gratitude to Atlanta's bicycling community centered around Loose Nuts Cycles—without them, my time at graduate school in Atlanta would have never felt like home.

Finally, I have to thank my wife, *Hannah Allen*, who has provided me with nothing but constant support before and during my graduate studies. Moving all the way from Colorado to

Atlanta with me, *Hannah* has been my biggest advocate during this entire process. I cannot imagine my last five years in Atlanta without her endless supply of love, outdoor distractions, and compassion during tough times. I love you, *Hannah*.

TABLE OF CONTENTS

ACKNOWLEDGEMENTS		IV
LIST OF TABLES		XIII
LIST OF FIGURES		XIV
LIST OF ABBREVIATIONS		XV
1 INTRODUCTION		1
1.1 Crime & Risk Assessment		1
1.2 Age of the Offender		2
1.3 Psychopathy		2
<i>1.3.1 Measuring Psychopathy</i>		<i>2</i>
<i>1.3.2 Psychopathy and Risk Assessment</i>		<i>3</i>
1.4 Neurobiology of Impulse Control		4
<i>1.4.1 Neural Substrates of Impulsivity, Impulse Control, & Anti-Sociality</i>		<i>4</i>
<i>1.4.2 The Use of Neurobiological Markers for Predicting Impulsivity Related Outcomes</i>		<i>7</i>
<i>1.4.3 The Use of Neurobiological Markers for Predicting Recidivism</i>		<i>7</i>
1.5 Limitations in the Literature		11
1.6 Dissertation Aims		12
2 HEMODYNAMIC MODEL FROM 442 INMATES IMPROVES PREDICTIONS OF REARREST		14

2.1	Abstract	15
2.2	Introduction	15
2.3	Results	20
	2.3.1 <i>Identifying Anatomical Regions of Interest</i>	20
	2.3.2 <i>Does Error-Monitoring Activity in the dACC or Insula Predict Time to Rearrest?</i>	22
	2.3.3 <i>Does the Inclusion of Neurobiological Error-Monitoring Information Increase the Accuracy of Statistical Models in Predicting Recidivism?</i>	23
2.4	Discussion	25
	2.4.1 <i>Limitations and Future Directions</i>	27
2.5	Methods	29
	2.5.1 <i>Participants</i>	29
	2.5.2 <i>Behavioral Task</i>	31
	2.5.3 <i>Experimental Design</i>	31
	2.5.4 <i>Image Acquisition</i>	32
	2.5.5 <i>Preprocessing</i>	33
	2.5.6 <i>Individual and Group Level Analysis</i>	33
	2.5.7 <i>Covariate Risk Assessment</i>	34
	2.5.8 <i>Follow-Up Procedure</i>	35
	2.5.9 <i>Analytic Strategy</i>	35

2.6	Acknowledgements.....	36
2.7	Chapter 2 Supplementary Material	37
2.7.1	<i>Supplementary Cox Model Results</i>	40
2.7.2	<i>Supplementary Discrimination Analysis Results</i>	41
3	FUNCTIONAL BRAIN CONNECTIVITY MEASURES PREDICT REARREST IN MALE OFFENDERS	44
3.1	Abstract.....	45
3.2	Introduction.....	45
3.3	Results	48
3.3.1	<i>Determination of Regions of Interest</i>	48
3.3.2	<i>Resting State Analysis</i>	49
3.3.3	<i>Does Resting State Functional Connectivity between the dACC and Insula Predict Time to Rearrest?</i>	49
3.3.4	<i>Does the Inclusion of Functional Connectivity Information Increase the Accuracy of Statistical Models in Predicting Recidivism?</i>	51
3.4	Discussion.....	54
3.4.1	<i>Limitations and Future Directions</i>	55
3.5	Methods.....	57
3.5.1	<i>Participants</i>	57
3.5.2	<i>Imaging Parameters</i>	57

3.5.3	<i>Preprocessing</i>	58
3.5.4	<i>Seed to ROI Functional Connectivity Analysis</i>	59
3.5.5	<i>Individual and Group Level Error-Monitoring Analysis</i>	59
3.5.6	<i>Covariate Risk Assessment</i>	60
3.5.7	<i>Follow-Up Procedure</i>	61
3.5.8	<i>Analytic Strategy</i>	61
3.6	Acknowledgements	62
3.7	Chapter 3 Supplementary Materials	63
3.7.1	<i>Supplemental Multimodal Analyses</i>	66
4	LIMBIC ACTIVITY PREDICTS REOFFENDING: A PARTIAL VALIDATION AND EXTENSION	70
4.1	Abstract	71
4.2	Introduction	71
4.3	Results	73
4.3.1	<i>Group Level Neuroimaging Analysis</i>	73
4.3.2	<i>Survival Analysis</i>	74
4.3.3	<i>Does the Inclusion of Neurobiological Error-Monitoring Information Increase the Accuracy of Statistical Models in Predicting Rearrest in Women?</i>	78
4.4	Discussion	78
4.4.1	<i>Limitations and Future Directions</i>	80

4.5	Methods.....	82
4.5.1	<i>Participants.....</i>	82
4.5.2	<i>Behavioral Task.....</i>	83
4.5.3	<i>Experimental Design.....</i>	84
4.5.4	<i>Image Acquisition.....</i>	85
4.5.5	<i>Preprocessing.....</i>	85
4.5.6	<i>Individual and Group Level Analysis.....</i>	86
4.5.7	<i>Covariate Risk Assessment.....</i>	86
4.5.8	<i>Follow-Up Procedure.....</i>	88
4.5.9	<i>Analytic Strategy.....</i>	88
4.6	Acknowledgements.....	89
4.7	Chapter 4 Supplementary Materials.....	89
4.7.1	<i>Neurobiologically Informed Risk Assessment of Felony Rearrest: Long-Term Risk.....</i>	94
4.7.2	<i>Neurobiologically Informed Risk Assessment of Non-Violent Rearrest: Long-Term Risk.....</i>	94
4.7.3	<i>Neurobiologically Informed Risk Assessment of Violent Rearrest: Long-Term.....</i>	95
5	GENERAL DISCUSSION.....	98
5.1	Summary.....	98

5.2	Improving the Understanding of Task-Based and Resting State Neurobiological Correlates to Impulsivity	99
5.2.1	<i>The Replicability of Neurobiological Error-Monitoring Activity.....</i>	<i>99</i>
5.2.2	<i>Task-Based Neurobiological Correlates to Impulsivity</i>	<i>100</i>
5.2.3	<i>Resting State Neurobiological Correlates to Impulsivity.....</i>	<i>101</i>
5.3	Testing the Incremental Utility of Neurobiological Data for Predictions of Recidivism.....	102
5.4	The Broader Significance of Antisocial Risk Factor Research.....	104
5.4.1	<i>Implications for Risk Assessment: Considering Accuracy.....</i>	<i>104</i>
5.4.2	<i>Implications for Therapeutic Applications.....</i>	<i>106</i>
5.5	Future Directions	108
	REFERENCES.....	110
	APPENDICES	126
	Appendix A: CV	126

LIST OF TABLES

Table 2.1 Effect of Individual Predictors on Rearrest	23
Table 2.2 Regions Significantly Activated in Error-Monitoring	38
Table 2.3 Cox Model Statistics.....	39
Table 2.4 Effect of Individual Predictors on Rearrest	40
Table 3.1 Effect of Individual Predictors on Rearrest	50
Table 3.2 Regions with Significant rsFCs from the dACC Seed.....	63
Table 3.3 Effect of Individual Predictors on Rearrest	66
Table 3.4 Two-Tailed Correlations Analyses (n = 91)	69
Table 4.1 Effect of Individual Predictors on Rearrest	75
Table 4.2 Areas of Error-Monitoring Activation in Men: Replication of Steele et al., 2014.....	89
Table 4.3 Areas of Error-Monitoring Activation in Women: Replication of Steele et al., 2014..	91
Table 4.4 Effect of Individual Predictors on Rearrest	93
Table 4.5 Two-Tailed Correlation Analyses in Men (n = 290)	96
Table 4.6 Two-Tailed Correlation Analyses in Women (n = 248).....	97

LIST OF FIGURES

Figure 1.1 Regions of Interest and Offender Sample Error-Monitoring Activity	10
Figure 1.2 Rearrest Survival Functions by High & Low Error-Monitoring Activity.....	10
Figure 2.1 Error-Monitoring Activity in Reference Sample and Regions of Interest.	21
Figure 2.2 ROC curves and AUC statistics for predictive models.	24
Figure 2.3 Validation Sample Error-Monitoring Activity	37
Figure 2.4 ROC Analyses	43
Figure 3.1 Regions of Interest.....	48
Figure 3.2 ROC Analyses	53
Figure 3.3 Visualization of Significant rsFCs from the dACC Seed.....	65
Figure 3.4 ROC Analyses	68
Figure 4.1 dACC Region of Interest and Group Level Error-Monitoring Activity.....	74

LIST OF ABBREVIATIONS

AAL: Automated Anatomical Labeling
AUC: area under the curve
AUD: Alcohol Use Disorder
BA: Brodmann area
BIS-11: Barratt Impulsiveness Scale
BOLD: blood oxygenation level dependent
dACC: dorsal anterior cingulate cortex
EEG: electroencephalography
EPI: echo planar
ERP: event related potential
FDR: false discovery rate
fMRI: functional magnetic resonance imaging
FWE: family-wise error rate
ICC: intraclass correlation coefficient
MAO-C: Mind Adult Offender Cohort
M.M.: multimodal model
PCL-R: Psychopathy Checklist-Revised
PCL-YV: Psychopathy Checklist-Youth Version
ROC: receiver operating characteristic
ROI: region of interest
rsFC: resting state functional connectivity
SPECT: single-photon emission computed tomography
STAI: State-Trait Anxiety Inventory
tDCS: transcranial direct-current stimulation

1 INTRODUCTION

1.1 Crime & Risk Assessment

As a country, the US spends over 250 billion dollars each year incarcerating around 1% of its population, only to have over half of the released criminal offenders return to prison within a three-year span (Durose, Cooper, & Snyder, 2014; Kaeble & Cowhig, 2016; Vera Institute of Justice, 2012). It is in both government and community interests to minimize two types of errors: premature release of dangerous offenders and lengthy terms of supervision for non-dangerous ones.

One way to address these interests is better prediction. A criminal justice system that is better able to predict who will abscond, reoffend, relapse, or recover would improve behavioral outcomes and public safety. The ability to distinguish between high- and low-risk offenders is a prerequisite to tailoring interventions to offender's unique needs—a practice found to decrease an offender's likelihood of reoffense (Latessa, Lovins, & Smith, 2010). But not all forms of risk assessment are created equally. Traditionally, one approach to assess an individual's risk of reoffense is through clinical interviews. However, the accuracy of this approach in predicting rearrest is little better than chance (Lidz, Mulvey, & Gardner, 1993).

Alternatively, evidence-based risk assessment has shown promise by utilizing static factors such as age, gender, and criminal history, as well as dynamic factors such as substance abuse, impulsivity, and social support. Perhaps unsurprisingly, evidence-based risk assessment has improved such predictions of reoffense, yet individual assessments still vary drastically in their respective accuracies. Indeed, a recent survey of various evidence-based risk assessment techniques indicates that the highest accuracies of the most commonly used assessments for general recidivism vary from 63% to 74% (Desmarais et al., 2016; Haarsma et al., 2019; Singh et

al., 2011). Below I provide a brief overview of risk factors of recidivism that will subsequently be tested for their predictive utility in the studies that form this dissertation—the offender’s age at release, traits related to psychopathy, and impulsivity related neurobiological activity—with a primary focus on the neurobiological correlates to impulsive phenotypes.

1.2 Age of the Offender

One of the most robustly demonstrated risk factors of recidivism is the offender’s age at release (Gendreau et al., 1996). The younger an offender is at the time of their release, the more likely they are to be rearrested. More specifically, all else being equal, a 25-year-old offender is approximately 25% more likely to be reincarcerated than a 35-year-old offender within 5 years of release (Durose et al., 2014; Kiehl et al., 2018). The heightened risk associated with a lower age at release only becomes more evident as older age groups are considered. For instance, a 2017 United State Sentencing Commission report finds that across an eight-year follow-up period, 67.6% of offenders aged 21 or lower at time of release were rearrested, compared to a mere 13.4% of offenders aged 65 or older (Hunt & Easley, 2017).

1.3 Psychopathy

1.3.1 Measuring Psychopathy

Another common feature of evidence-based risk assessment is the measurement of psychopathy—a personality disorder typified by a lack of empathy, flat emotional response, impulsivity, and increased inclinations towards antisocial behaviors (Hare, 1996). A diagnosis of psychopathy is determined via a semi-structured interview—the most well-validated of which is Hare’s Psychopathy Checklist-Revised (henceforth PCL-R; Hare 1991, 2003).

The PCL-R traditionally consists of 20 items—rated on a 3-point scale (0, 1, 2) by the assessor—which comprise four primary facets (i.e., interpersonal traits, affective traits, lifestyle

traits, and impulsivity traits) and two secondary factors which this chapter will primarily focus on (i.e., Factor 1: interpersonal/affective traits & Factor 2: lifestyle/impulsivity traits) (Hare & Neumann, 2009).¹ Total scores on the PCL-R can range from 0-40, with a clinical cutoff score of 30. Strikingly, individuals with scores breaching this threshold are fifteen to twenty-five times more prevalent in incarcerated populations compared to general populations, suggesting that those with clinical psychopathy are much more likely to commit crimes that land them in prison compared to those without psychopathy (Kiehl & Hoffman, 2011). Importantly though, the scale is intended to be dimensional rather than taxonic (Hare & Neumann, 2009), and accordingly, the most prevalent use of this scale for prediction of antisocial behaviors is dimensional rather than dichotomous.

1.3.2 Psychopathy and Risk Assessment

As a single dimensional construct, the ability of the PCL-R total score to predict recidivism has been well demonstrated in the literature (Anderson, Walsh, & Kosson, 2018; Hemphill, Hare, & Wong, 1998; Kennealy, Skeem, Walters, & Camp, 2010; Leistico, Salekin, DeCoster, & Rogers, 2008; Olver & Wong, 2014; Serin, 1996; Walsh, 2013; Walters, Wilson, & Glover, 2011). Research individually analyzing the factors that make up the PCL-R suggests that Factor 1 & Factor 2 have differential relationships with antisocial behaviors. For instance, some research suggests that Factor 2 scores and individual items have greater utility in predicting general and violent recidivism than Factor 1 scores (Hemphill et al., 1998; Leistico et al., 2008; Kennealy et al., 2010; Ojala, Tiihonen, Repo-Tiihonen, Tikkanen, & Virkkunen, 2015; Olver & Wong, 2014; Walters et al., 2008: though see Serin, 1996). On the other hand, Factor 1 scores

¹ Additionally, diagnoses of psychopathy in youth are determined via the Psychopathy Checklist - Youth Version (henceforth PCL-YV; Forth, Kosson, & Hare, 2003), an assessment that mirrors and approximates all questions, facets, and factors of the PCL-R.

were found to predict negative correctional attitudes (Sohn et al., 2017). Factor 2, therefore, seems to be of greatest relevance when considering recidivism.

Though psychopathy and its underlying traits have been helpful in aiding risk assessments in predicting recidivism, there are reasons to expect limits on the predictive utility of personality factors (and demographic or behavioral factors). The most pertinent limitation is that these measures are relatively distant proxies for underlying neurobiological mechanisms which are more direct proxies to the traits that these measurements attempt to capture, such as impulsivity traits.

1.4 Neurobiology of Impulse Control

1.4.1 Neural Substrates of Impulsivity, Impulse Control, & Anti-Sociality

Trait impulsivity is a strong predictor of whether or not an offender will recidivate (Harris, Rice, & Quinsey, 1993). This construct, sometimes defined as a persistent lack of restraint or consideration of consequences, is measured in a variety of ways, spanning from clinical evaluations all the way to neuropsychological measures. Yet, the impulsive phenotype ultimately arises from the brain's inhibitory and cognitive control systems. Below I will focus on two brain regions involved in these systems—the anterior cingulate cortex (ACC) and the insula—regions that are the primary focus of my subsequent studies.

The regions of the brain that are implicated in impulsivity and impulse control are largely situated within the brain's limbic system, thought to regulate behavioral and emotional responses (Siever, 2008). One of these regions that is commonly implicated as central to impulse control is the ACC. This region is known to be associated with response selection, conflict monitoring, error-monitoring, and avoidance learning (Holroyd & Coles, 2002; Kiehl, Liddle, & Hopfinger, 2000; Kosson et al., 2006; Mathalon, Whitfield, & Ford, 2003; Van Veen & Carter, 2002). More

specifically, the ACC is thought to play the role of a relay, mediating the monitoring of error information about the execution of an action from the inferior frontal cortex and basal ganglia to motor areas, which effectively creates a feedback loop able to update action plans (Holroyd & Coles, 2002). Thus, this ACC relay then serves as a sort of error-monitoring system for the execution of actions. Accordingly, lesioning this region in animal models has been shown to lead to disruptions in the ability to regulate learning behavior (Gabriel, Sparenborg, & Kubota, 1989). Similarly, in healthy human adults, ACC activity during the commission of errors is predictive of a participant's ability to adjust their behavior in subsequent trials (Kerns et al., 2004), though other research suggests the relation of this error-monitoring activity with impulsivity is gender specific—that is, error-monitoring activity has been found to negatively correlate with impulsivity in men yet is positively correlated with the same trait in women (Liu et al., 2013). Finally, damage to a person's ACC results in traits that commonly undergird the diagnosis of “acquired psychopathy”: disinhibition, apathy, and aggression (Devinsky, Morrell, & Vogt, 1995).

Alongside the ACC, much impulse control research also implicates the insular cortex. Rather than serving as a relay, the insula is thought to play a role in a broad range of social, affective, and cognitive tasks, and it seemingly serves to integrate its various inputs into a coherent experience of the world (Kurth, Zilles, Fox, Laird, & Eickhoff, 2010). Though its functions are broad in the literature, a primary focus that has emerged is its role in what's commonly known as the “salience network”—a network integral to the direction of attentional resources to salient events (Menon & Uddin, 2010). Both the insula and the ACC have been shown to be functionally coupled to each other, as well as with further downstream motor areas, suggesting the neural processes that allow salient events to adjust future behaviors (Holroyd &

Coles, 2002). Furthermore, in accordance with the purported roles that these regions play in error-monitoring and salience detection, both regions were found to be highly activated during a simple error-monitoring task in a large sample of healthy adults ($N = 104$) (Steele et al., 2014). Likewise, in patients with borderline personality disorder—a disorder associated with high impulsivity—impulsive decisions made under uncertain circumstances were associated with aberrant activation of both the insula and ACC (Mortensen, Evensmoen, Klensmeden, & Håberg, 2016).

In addition to task-based measures, emerging research suggests that structural differences in functional connectivity between these regions—and more generally, the salience network—are also associated with corresponding differences in impulsivity. For instance, multiple research studies suggest that the volume of and functional connectivity to and from the ACC and insula are associated with trait and task impulsivity—including the Barratt Impulsiveness Scale (BIS-11: Angelides, Gupta, & Vickery, 2017; Hobkirk, Bell, Utevsky, Huettel, & Meade, 2019; Kerr et al., 2015; Li et al., 2013; Matsuo et al., 2009; Philippi et al., 2015; Shannon et al., 2011). Likewise, increased connections to the ACC have been linked to improved response inhibition in an adaptation of the Go/NoGo task—a task designed to capture an individual’s ability to inhibit a prepotent response, one type of impulse control (Mennes et al., 2012). These resting state connections have also been associated with antisocial behavioral phenotypes intrinsically linked to impulsivity, such as reactive aggression (Romero-Martinez et al., 2019). Overall, this research suggests that specific (and measurable) differences in the brain’s structural and functional organization help to explain individual differences in impulsivity, which may be linked to further downstream behavioral—and antisocial—tendencies.

1.4.2 The Use of Neurobiological Markers for Predicting Impulsivity Related Outcomes

Recent research suggests that measurements of brain function can be utilized in predictive models in order to more accurately classify particular behavioral outcomes, many of which have strong links to impulsivity, in humans. For instance, predictive models including functional data from neurobiological markers, have proven useful in classifying whether or not individuals will: complete substance abuse treatment (Steele et al., 2014, 2017), relapse back into substance abuse (Camchong, Stenger, & Fein, 2012; Janes et al., 2010; Paulus, Tapert, & Schuckit, 2005; Sinha & Li, 2007), commit acts of violence (Pardini, Raine, Erickson, & Loeber, 2014), and even, commit suicide (Just et al., 2017). Likewise, recent research suggests that the brain's resting state functional connectivity can also be used to predict outcomes. For example, research by Fede and colleagues (2019) on individuals with Alcohol Use Disorder (AUD) demonstrates that the resting state connectivity of an individual's salience network (alongside other functional networks) is predictive of their severity of AUD. Strikingly, in this case, the predictive utility offered by resting state connectivity was above and beyond that of task-based fMRI measures and other structural measures (i.e., gray and white matter measurements). All of these results raise the possibility that measures of brain activity associated with—and potentially underlying—impulse control may lend incremental utility (i.e., more accurate classification rates) to the prediction of some antisocial behaviors.

1.4.3 The Use of Neurobiological Markers for Predicting Recidivism

The question of whether or not functional data from neurobiological markers (e.g., fMRI and EEG data) can improve predictive models of antisocial behavior formed a set of peer-reviewed studies that ultimately provide support for the hypothesis. For instance, the first study

in this set, an fMRI study conducted by Aharoni and colleagues (2013), found that error-monitoring related activity in the ACC (as assessed by false positive responses during a Go/NoGo task: a fast-paced inhibitory task which asks the participant to respond to certain “Go” stimuli and not respond to other “NoGo” stimuli) predicted later rearrest in a sample of 96 adult offenders. More specifically, the investigators found that offenders with relatively low ACC activity during error-monitoring were roughly two times as likely to be rearrested as those with high activity—while controlling for other known risk factors (see Figure 1.1b for fMRI error-monitoring contrast and Figure 1.2 for reconstruction of results via median split for visualization purposes). These results provide support for the notion that the ACC is integral to error-monitoring, and, perhaps, subsequent behavioral modulation. Upon further analysis and utilization of advanced statistical techniques (i.e., area under the curve, calibration, and discrimination), the investigators demonstrated that models including ACC error-monitoring activity can yield positive predictive accuracy² rates exceeding 75% (Aharoni et al., 2014). Furthermore, convergent validity of these methods, and the importance of the ACC in predictive utility, have subsequently been demonstrated (though see Zijlmans et al., 2021).

Steele and colleagues (2015) conducted a multimodal analysis of error-monitoring activity in the ACC via a combination of electroencephalography (EEG) and fMRI data in a subset of the same sample ($n = 45$). By combining both EEG data and fMRI data, the investigators were able to utilize the temporal acuity afforded by the EEG data, alongside the spatial acuity afforded by the fMRI data within the same predictive models. Using support vector modeling—a type of machine learning technique—the investigators identified and estimated

² Positive predictive accuracy is the ability to correctly discriminate between an individual that will reoffend, and one that will not, when given one of each. Thus, in this case, the model including ACC activity was able to correctly differentiate offender outcomes in randomly drawn pairs over 75% of the time. Excluding ACC activity brought this model’s positive predictive accuracy down to 68%.

which aspects of the collected data are most predictive of later rearrest. The best performing model was a joint fMRI/EEG model that excluded covariates and only included brain measures. This analysis combined the P300, an EEG component of the event-related potential (ERP) following error-commission, and fMRI data from the ACC corresponding to error-monitoring, yielding 83% predictive accuracy in establishing who will be rearrested.

Alongside the use of task-based neuroimaging data in predicting rearrest, I am aware of just one test of the role of resting state measures for the same predictions (Delfin et al., 2019). Delfin and colleagues (2019) used single-photon emission computed tomography (SPECT) to measure cerebral blood flow within predetermined regions of interest during rest in a sample of 44 criminal offenders. Utilizing machine learning techniques to inform model selection, the researchers found that including parietal resting state cerebral blood flow measurements in their models led to increased accuracies of rearrest predictions.

Predictive models utilizing neurocognitive data have also been successful in categorizing behavioral outcomes in other realms relevant to impulsivity and even reoffense. For instance, Pardini and colleagues (2014) have demonstrated the utility of neurocognitive models for the prediction of future violence. Steele and colleagues (2014, 2017) demonstrate that models including ERP data following error-commission and the functional connectivity to the ACC during error-monitoring have both yielded over 80% accuracy rates in predicting substance abuse treatment completion. Altogether, these various research projects lend support to the value of neurocognitive data's inclusion in risk prediction models and also the hypothesis that areas of the brain related to error-monitoring and inhibitory control can serve as candidate neuromarkers for the prediction of antisocial behavior.

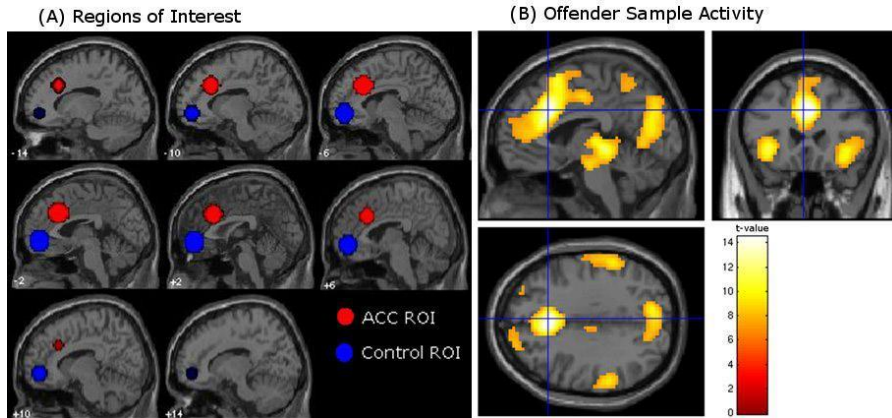


Figure 1.1 Regions of Interest and Offender Sample Error-Monitoring Activity

(A) A priori seed region (red) for BOLD response to commission errors vs. correct hits in anterior cingulate from a GNG task with an independent sample of 102 healthy adult non-offenders; peak voxel $x = -3$, $y = 24$, $z = 33$; radius = 14 mm sphere; $t(94) = 13.38$, $p < 0.0001$, FWE (Steele et al., 2014). A priori control region (blue) embodying anterior portion of the medial prefrontal cortex (peak voxel: $0, 51, -6$; radius = 14 mm sphere). (B) Mean hemodynamic response change in offender sample ($n = 96$) during commission errors vs. correct hits from sagittal (Upper Left), coronal (Right), and axial (Lower Left) orientations. Peak activation located at $x = 3$, $y = 24$, $z = 33$ within the ACC ROI ($p < 0.00001$, FWE) (Aharoni et al., 2013).

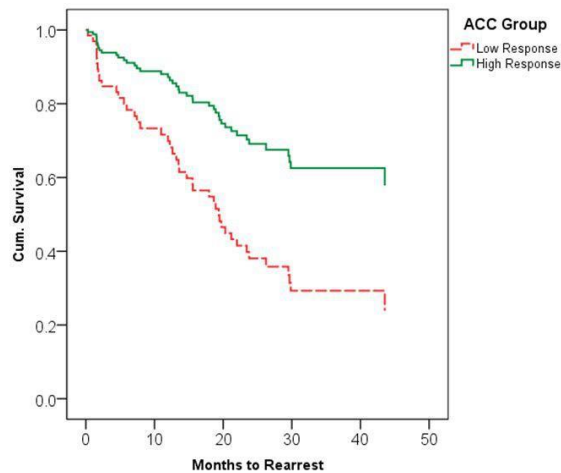


Figure 1.2 Rearrest Survival Functions by High & Low Error-Monitoring Activity

Cox survival function showing proportional rearrest survival rates of high (solid green) vs. low (dashed red) ACC response groups for any crime over a 4-year period. Results of this median split analysis were equivalent to that of the parametric model: bootstrapped $B = 0.96$; $SE = 0.40$; $p < 0.01$; 95% CI, 0.29–1.84. The mean survival times to rearrest for the low and high ACC activity groups were 25.27 (2.80) mo. and 32.42 (2.73) mo., respectively. The overall probabilities of rearrest were 60% for the low ACC group and 46% for the high ACC group (Aharoni et al., 2013).

1.5 Limitations in the Literature

The current scientific research on neuroprediction of antisocial behavior leaves several opportunities for further exploration. There have only been two within-sample attempts at replication for the observed neuroprediction of recidivism (Delfin et al., 2019; Zijlmans et al., 2021). The gold-standard for predictive modeling is a test of out-of-sample utility—indicative of both the sample used to dictate the parameters of interest (the Norm sample), as well as the sample used to validate those parameters (the Validation sample)—because models utilizing in-sample prediction often understate model error when reporting goodness of fit (Poldrack et al., 2018). More descriptively, models will almost certainly reflect the data set used in their development more than any other novel or external data set. Thus far, none of the previous research satisfies this gold-standard; therefore, it is not possible to discern the predictive utility that these models may have in practice were they to be used in a random sample population. Accordingly, both legal and scientific scholars have called for replication and out-of-sample validation of this research (e.g., Meixner, 2015; Poldrack et al., 2018).

Another challenge in this line of research is in obtaining large forensic samples needed to study subtler predictors of behavior, such as resting state neurobiological data. Because of their low signal-to-noise ratio, rsFC measures may have real effects on antisocial behavior that are difficult to detect. Larger samples, though, could help clarify the distinct neurobiological mechanisms that give rise to differences in antisocial outcomes and further increase our understanding, interpretation, and potentially even the accuracy, of predictive models.

Improved risk assessment could help clinical and legal practitioners develop intervention strategies that serve individual risk-needs (e.g., early parole for eligible candidates, treatment diversion, supervision level proportionate to risk). Given the complexity of human behavior, the

most effective approaches are likely to be those that consider a variety of factors, including sociological, psychological, and biological ones.

1.6 Dissertation Aims

Importantly, no previous research has surveyed how the brain's functional organization at a resting state may be associated with error-monitoring nor rearrest within forensic samples, attempted to validate the neurobiological premises underlying the error-monitoring model using an independent sample of criminal offenders, nor tested the out-of-sample utility of this model. Thus, although the neural activity underlying error-monitoring has yielded predictive utility to recidivism risk-models as a proof of concept, *it is unclear whether such models will demonstrate utility in out-of-sample predictions, as well as whether brain activity at resting state is associated with error-monitoring, or even adverse outcomes such as recidivism.*

Currently, a major obstacle in the field is access to an adequate number of criminal offender scans, information regarding rearrest, and the time-lag between scans and rearrest; yet this proposal overcomes this obstacle via unique analyses of previously collected data ($n = 538$) and newly collected behavioral outcomes ($n = 461$).

This dissertation research addresses current gaps in the literature by probing the neurophysiological properties associated with the monitoring of errors in criminal offenders (Chapters 2 & 4), analyzing the, as of yet, unexplored relationships of these properties to the brain at rest and, consequently, recidivism (Chapters 2 & 3), and serving as the first research project in the literature to test the external validity of the error-monitoring model of recidivism (Chapter 4).

The specific aims of this dissertation are to (1) develop novel error-monitoring regions of interest (ROIs) from a large sample of offenders ($n = 442$), (2) analyze the resting state

functional connectivity (rsFC) between these regions of interest, (3) test the utility of the newly established ROIs and rsFC metrics in predicting recidivism in a previously published independent sample ($n = 95$; Aharoni et al., 2013; Aharoni et al., 2014; Steele et al., 2015), and (4) provide an out-of-sample analysis of the original error-monitoring model (Aharoni et al., 2013; Aharoni et al., 2014) in a large sample of female ($n = 248$) and male ($n = 290$) offenders. Broadly, the goal of these specific aims is to improve the basic understanding of the relationships between the various neurobiological components underlying error-monitoring and impulsivity. These empirical analyses will further hone future hypotheses within the neuroprediction of recidivism literature as well as the risk assessment literature more generally, and, if shown to demonstrate utility, will lead to refinements of current models, approaches, and potentially inform future research concerning therapeutic interventions.

2 HEMODYNAMIC MODEL FROM 442 INMATES IMPROVES PREDICTIONS OF REARREST

Corey H. Allen^{1*}, Eyal Aharoni², Carla L. Harenski³, Keith A. Harenski³, & Kent A. Kiehl³

Keywords: impulsivity | recidivism | risk assessment

¹ Neuroscience Institute, Georgia State University, P.O. Box 5030, Atlanta, GA, 30302-5030, USA

² Department of Psychology, Georgia State University, P.O. Box 5010, Atlanta, GA, 30302-5010, USA

³ The Mind Research Network, 1101 Yale Blvd NE, Albuquerque, NM, 87106-4188, USA

In preparation

2.1 Abstract

Despite decades of research examining the brain's contributions to the propensity for antisocial behavior, this process is still poorly understood, owing in part to the highly multivariate relationship between the brain, behavioral phenotypes, and the dynamic environmental contexts in which they operate. An important criterion for evaluating the strength of a given explanation is the degree to which it makes accurate predictions. Using a novel hemodynamic model developed from the largest functional imaging reference sample ($n = 442$) of an inmate population in this body of literature, we show that limbic activity during an error-monitoring task increased the predictive accuracy of a model of reoffense risk developed in a previously published ($n = 95$) inmate sample. Our pattern of results replicates previous research on the dorsal anterior cingulate cortex and is reproduced in another limbic region, the insular cortex. These results validate and extend research on limbic predictors of recurrent, impulsive antisocial behavior. Implications for clinical and forensic risk assessment are discussed.

2.2 Introduction

Understanding the factors that contribute to recurrent antisocial behavior is consequential for clinical and criminal justice procedure as well as public safety and wellbeing. More than one in 50 Americans are under some form of correctional supervision (Kaeble & Cowhig, 2018), contributing to the estimated \$3.2 trillion annual societal cost of crime (Anderson, 2012). Recent policy developments such as the First Step Act (2018) aim to reduce the U.S.'s reliance on incarceration using evidence-based risk assessment technology. Evidence-based risk assessments generate quantitative predictions about individual risk outcomes by comparing their risk factors to those of a large normative sample. Research has shown that the ability to match individuals to risk-appropriate programs leads to a significant decrease in reoffending (Latessa, Lovins, &

Smith, 2010). Thus, an increased understanding of the factors driving persistent antisocial behavior is an important step in the responsible application of risk assessment technology.

There are many contributing factors to repeated antisocial behavior—including social/environmental factors such as socioeconomic status (Barkan & Rocque, 2018; Piotrowska, Stride, Croft, & Rowe, 2015), and psychological factors such as drug addiction (Douglas & Reeves, 2010; Pierce et al., 2017; Yang, Wong, & Coid, 2010) and impulsivity (Harris, Rice, & Quinsey, 1993; Reynolds, Basso, Miller, Whiteside, & Combs, 2019; Thomson et al., 2019). Impulsivity is commonly defined as a persistent lack of restraint or consideration of consequences, and its biological basis has been the subject of increasing investigation (Chamberlain & Sahakian, 2007; Miglin, Bounoua, Goodling, Sheehan, Spielberg, & Sadeh, 2019; Zheng, Chen, Wang, & Zhou, 2019).

Current research suggests the regions of the brain most implicated in impulsivity and impulse control are largely situated within the brain's limbic system, thought to regulate behavioral and emotional response (Siever, 2008). One of these regions is the dorsal anterior cingulate cortex (dACC), which is known to be associated with response selection, error-monitoring, and avoidance learning (Holroyd & Coles, 2002; Kiehl, Liddle, & Hopfinger, 2000; Kosson et al., 2006; Mathalon, Whitfield, & Ford, 2003; Van Veen & Carter, 2002). When an action plan is executed, such as the push of a finger or the pull of a trigger, the dACC helps to monitor goal fulfillment by relaying information between the inferior frontal cortex and basal ganglia—serving as an error-monitoring system (Holroyd & Coles, 2002). Accordingly, in healthy human adults, dACC activity during the commission of errors is predictive of a participant's ability to adjust their behavior in subsequent trials (Kerns et al., 2004; Kiehl, Liddle, & Hopfinger, 2002). Impairment in the dACC has been associated with an increased risk

of violent behavior (Cecil et al., 2008; Liu et al., 2011) and traits that commonly undergird the diagnosis of “acquired psychopathy”: disinhibition, apathy, and aggression (Devinsky, Morrell, & Vogt, 1995). Similarly, disengagement of the dACC has been associated with lower response conflict during dishonest decision-making in incarcerated individuals with psychopathy—a disorder marked by a disruption of moral behavior, impulsivity, and emotional detachment (Abe, Greene, and Kiehl, 2018; Hare & Neumann, 2008).

Despite extant research investigating neurobiological factors contributing to antisocial behavior, this process is still poorly understood, owing in part to the highly multivariate relationship between the brain, behavioral phenotypes, and the dynamic environmental contexts in which they operate. An important criterion for evaluating the strength of a given explanation is the extent to which it makes accurate predictions. In this vein, recent research suggests that measurements of brain function can improve statistical predictions of impulse-related outcomes in humans. For instance, predictive models including functional brain data have demonstrated utility in classifying whether or not individuals will: complete substance abuse treatment (Steele et al., 2014, Fink et al., 2016), relapse back into substance abuse (Camchong, Stenger, & Fein, 2012; Janes et al., 2010; Paulus, Tapert, & Schuckit, 2005; Sinha & Li, 2007), and commit acts of violence (Pardini, Raine, Erickson, & Loeber, 2014). All of these results raise the question of whether measures of brain activity associated with impulse control may increase classification accuracy for statistical predictions of some antisocial behaviors.

Emerging cognitive neuroscientific research informs questions like this one by examining whether models that include functional brain measures can outperform those that contain only conventional psychological and sociological information (Aharoni et al., 2013; Aharoni et al., 2014; Delfin et al., 2019; Steele et al., 2015). For example, longitudinal research with criminal

offenders has shown greater classification accuracy in the prediction of recidivism when a neural signature of error-monitoring and impulse control is included in the risk model (Aharoni et al., 2013; Aharoni et al., 2014; Steele et al., 2015; Zijlmans et al., 2021). Even so, further validation is needed both to demonstrate the robustness of the predictive effects and to understand the causal mechanisms that best explain them, in order to evaluate whether functional brain metrics capture any information that might be useful to researchers, policy makers, or treatment providers.

First, owing in part to the longitudinal nature of the research question, no attempts have yet been made to replicate the original studies, nor have there been attempts to derive new models from new hemodynamic reference samples. Though the hemodynamic reference sample ($N = 102$) used in Aharoni et al. (2013), Aharoni et al. (2014), and Steele et al. (2015) is large by traditional neuroimaging standards, it is modest by risk assessment standards. Likewise, the hemodynamic reference sample for previous neuroprediction studies was selected from the general (non-offender) population, limiting generalizability to the population of interest. General and offender populations may differ in meaningful ways, as suggested by previous research (Ermer, Cope, Nyalakanti, Calhoun, & Kiehl, 2012). A critical test would be to attempt to replicate these predictive effects by using a larger hemodynamic reference sample consisting of criminal offenders—thereby improving the power and generalizability of the hemodynamic model.

Second, the early work on this topic focused on the dACC because this region had been closely implicated in impulse control and error-monitoring, but antisocial behavior represents a heterogeneous category that is undoubtedly shaped by a variety of unique and interacting brain processes. One likely contributor is the insular cortex—a region thought to play a role in a broad

range of social, affective, and cognitive tasks, and integrating its various inputs into a coherent experience of the world (Kurth, Zilles, Fox, Laird, & Eickhoff, 2010). Though the insula's functions are broad in the literature, a primary focus that has emerged is its role in the "salience network"—a network underlying how people allocate attentional resources to salient events, such as the commission of errors (Menon & Uddin, 2010). Indeed, the insulae were found to be highly activated during a simple "Go/No-Go" error-monitoring task in a large sample of healthy adults ($N = 104$) (Steele et al., 2014). Problems within the salience network reduce the likelihood of detecting errors and, in turn, increase the likelihood of making them (Harsay, Spaan, Wijnen, & Ridderinkhof, 2012). Furthermore, in patients with borderline personality disorder—a disorder associated with high impulsivity—impulsive decisions made under uncertain circumstances were associated with aberrant activation of the insula (Mortensen, Evensmoen, Klensmeden, & Håberg, 2016). Thus, existing evidence of the insula's role in impulse control and error-monitoring lends support to the hypothesis that, with relevant task-based activity, the insula may provide incremental predictive utility to risk models for antisocial behavior.

This project provides a validation and extension of Aharoni and colleagues' (2014) error-monitoring model for the prediction of recidivism, which includes an error-monitoring related brain measure, and the following covariates: Hare's revised Psychopathy Checklist (PCL-R) Factor 1, Factor 2, the interaction of Factor 1 and 2, and the offender's release age (Hare & Neumann, 2008). To accomplish this, we constructed two new neurobiological models using the largest hemodynamic reference sample ($n = 442$) of an inmate population in this body of literature, and tested their predictive utility in a separate, previously studied Validation sample ($n = 95$) (see Aharoni et al., 2013; Aharoni et al., 2014; Steele et al., 2015). Our ROIs—coordinates determined from the hemodynamic reference sample—were the dACC and L. Insula. Our task

was a classic Go/NoGo task, meant to test a participant's ability to inhibit prepotent motor responses, and our contrast was commission errors versus correct hits. Our predictions were that error-related activity for commission errors relative to correct hits in the dACC and Insula will 1) be associated with increased time to non-violent rearrest in the Validation sample, and 2) will lend incremental utility to statistical models predicting individual rearrest relative to models excluding these factors.

2.3 Results

2.3.1 Identifying Anatomical Regions of Interest

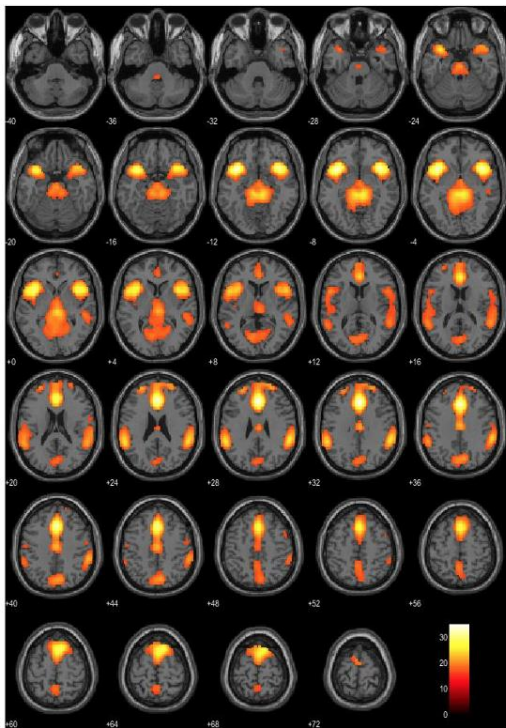
Following a first level analysis contrasting commission errors versus correct hits in the hemodynamic reference sample (see Methods), a group level analysis utilizing a conservative correction ($t > 16.0$) identified 15 areas of activation (Figure 2.1a and Table 2.2).

Within the frontal lobe, increased activation was found for commission errors in the right dACC (BA32), ventral ACC (BA 24), superior and frontal gyri (BA 8 & 10), and precentral gyrus (BA 6), all relative to a smaller positive response for correct hits. A similar pattern was observed for the bilateral insulae (BA13) and right superior temporal gyrus (BA 22) in the temporal lobe, and the right inferior parietal lobule (BA 40), left angular gyrus (BA 39), and the left postcentral gyrus (BA 1) in the parietal lobe. Likewise, engagement of the midbrain and occipital areas such as the cuneus (BA 7) were observed.

Consistent with expectations, the two strongest activations for commission errors versus correct hits were in the right dACC (BA 32; $x = 3, y = 29, z = 28$) and bilateral insulae (BA 13; $x = -36, y = 14, z = -11$ and $x = 39, y = 14, z = -8$) (see Figure 2.1b). These dACC and (Left) Insula peaks formed the basis of separate spherical ROIs defined for analysis of the Validation sample (see Figure 2.1b). Though both insulae were active during error-monitoring, the left

insula was chosen over the right insula for subsequent analyses because it was found to be comparatively more active during the task within the hemodynamic reference sample. For each participant in the validation sample, we computed a mean β -coefficient for each ROI, for commission errors versus correct hit trials, and entered that parameter as an independent factor in our subsequent prediction models.

(A)



(B)

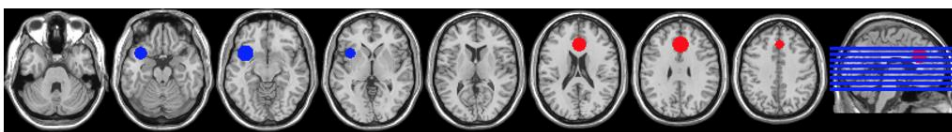


Figure 2.1 Error-Monitoring Activity in Reference Sample and Regions of Interest.

A) Mean hemodynamic response change in the hemodynamic reference sample ($n = 442$) during commission errors vs. correct hits from axial view. Peak activations located at $x = 3, y = 29, z = 28$ and $x = -36, y = 14, z = -11$, within the dACC and Left Insula, respectively (threshold: $t > 16$). See Figure 2.3 for a similar second level analysis in the Validation sample. B) Axial view of ROIs in the Left Insula (blue) and dACC (red) for bold response during commission errors vs. correct hits to be extracted in the Validation sample.

2.3.2 Does Error-Monitoring Activity in the dACC or Insula Predict Time to Rearrest?

To test our primary hypothesis (that error-monitoring activity will be associated with time to non-violent rearrest), we used cox proportional-hazards regression (in a bootstrapping sequence with 9,999 iterations to assess the reliability of the β -coefficients) to test two models including previously defined risk factors in the validation sample: 1) PCL-R Factor 1, PCL-R Factor 2, their interaction, the offender's release age, and the dACC's mean β -values for commission error versus correct hit trials, and 2) PCL-R Factor 1, PCL-R Factor 2, their interaction, the offender's release age, and the Insula's mean β -values for commission error versus correct hit trials.³ These models were regressed onto time to rearrest for a non-violent crime (see Table 2.1; see Table 2.3 for raw cox proportional-hazards regressions), and bootstrapped 9,999 times. A significant overall effect ($p < .05$) was obtained for each model. As expected, age at release and PCL-R Factor 2 were each significantly associated with days to non-violent rearrest ($p = .029$ and $p = .007$, respectively) in the Non-Violent with dACC model. dACC activity exhibited a significant association with rearrest above and beyond these other risk factors. For every one unit increase in dACC activity, there was a 1.71 decrease in the probability of rearrest for a non-violent crime ($p = .006$). In the Non-Violent with Insula model, PCL-R Factor 2 emerged as a significant predictor for days to non-violent recidivism ($p = .008$). Insular activity exhibited a significant association with rearrest above and beyond these other risk factors. There was a significant association such that for every one unit increase in Insular

³ As expected, dACC and L. Insular error-monitoring activity were highly correlated— $r(93) = .724$, $p > .001$ —and thus, not jointly included in the same models.

error-monitoring activity, there was a 1.52 decrease in the probability of rearrest for a non-violent crime ($p = .035$), controlling for the other risk factors.

There was an insufficient number of offenders rearrested for violent crimes ($n = 9$), thus no analysis was conducted for violent rearrests (See Table 2.3 and 2.4 for analyses of violent crimes and non-violent crimes combined—i.e., “Any Crimes” models).

Table 2.1 Effect of Individual Predictors on Rearrest

Model/Predictor	<i>B</i>	SE (<i>B</i>)	Bootstrapped Data				
			<i>B</i>	SE (<i>B</i>)	<i>P</i> value	exp[<i>B</i>] 95% CI for <i>B</i>	
Non-Violent with dACC							
- Age at release	-0.061	0.026	-0.061	0.03	0.029*	0.941	-.127 - -.009
- PCL-R factor 1 score	0.003	0.071	0.003	0.084	0.964	1.003	-.161 - .171
- PCL-R factor 2 score	-3.129	1.067	-3.129	1.308	0.007**	0.044	-6.064 - -.913
- PCL-R factor interaction	0.316	0.301	0.316	0.373	0.317	1.372	-.216 - 1.244
- dACC	-0.539	0.205	-0.539	0.216	0.006**	0.584	-1.000 - -.153
Non-Violent with Insula							
- Age at release	-0.05	0.025	-0.05	0.029	0.061	0.952	-.117 - -.002
- PCL-R factor 1 score	-0.026	0.07	-0.026	0.084	0.728	0.974	-.200 - .134
- PCL-R factor 2 score	-3.164	1.071	-3.164	1.328	0.008**	0.042	-6.311 - -.989
- PCL-R factor interaction	0.348	0.299	0.348	0.386	0.289	1.417	-.207 - 1.306
- Insula	-0.419	0.191	-0.419	0.221	0.035*	0.658	-.901 - -.0927

Results of Cox regression analyses examining the predictive effect of the dACC and Insula on rearrest for a non-violent crime controlling for covariates. In order to normalize the distribution for PCL-R Factor 2 scores, a lg10 reflection transformation was used. Due to this transformation interpretation of Cox proportional-hazards β -coefficients and exp[*B*] are reversed: higher PCL-R Factor 2 scores are associated with a decreased time to rearrest. Table reports unstandardized *B*, bootstrapped *B*, and relative risk ratio (exp[*B*]). * $p < 0.05$, ** $p < 0.01$, and *** $p < 0.001$.

2.3.3 Does the Inclusion of Neurobiological Error-Monitoring Information Increase the Accuracy of Statistical Models in Predicting Recidivism?

The receiver operating characteristic (ROC) curve—an analysis that indicates a model’s true positive and false positive fractions (i.e., sensitivity and 1-specificity)—is a direct way to test a model’s accuracy. An area under the curve (AUC) analysis was conducted in the validation

sample to discriminate between those rearrested and not rearrested as functions of the Non-Violent with dACC and Non-Violent with Insula models. Generally, AUC values exceeding .70 are seen as “good” in terms of ability to discriminate between events (i.e., rearrested vs. not rearrested) (Harrell, 2001).

In order to assess the unique contribution of the dACC and Insula’s error-monitoring activity to our model’s predictive accuracies, we fitted both models with and without ROI data at a twelve-month time point (see Figures 2.2a & 2.2b; See Figures 2.4a-d for time-dependent (6, 12, 24, & 36 months) ROC curve and AUC analyses). In Figure 2.2a, the Non-Violent without dACC model reports an AUC of .676, and an improved AUC of .715 when including the dACC factor. In Figure 2.2b, the Non-Violent without Insula reports an AUC of .676, and an improved AUC of .702 when including the Insula factor. Overall, we find that both models incrementally benefit from the inclusion of brain-based error-monitoring activity.

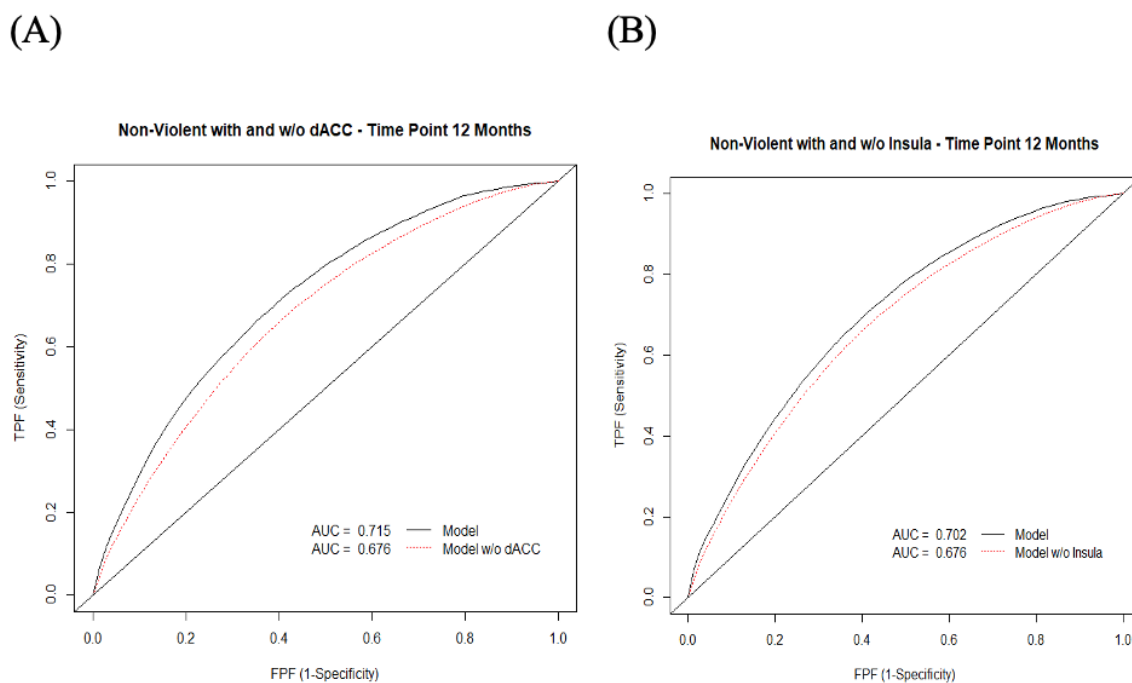


Figure 2.2 ROC curves and AUC statistics for predictive models.

A) ROC curve and AUC statistics for Non-violent model with and without the dACC. B) ROC curve and AUC statistics for Non-violent model with and without the Insula.

2.4 Discussion

The present project represents a validation and extension of the Aharoni et al. (2014) error-monitoring model using an independent hemodynamic reference sample of 442 incarcerated offenders to establish anatomical ROIs. Our results demonstrate improvement in the prediction of later rearrest using an index of functional brain activation in the dACC—a region previously implicated in error-monitoring, inhibition, and impulsivity (Bastin et al., 2016; Orr & Hester, 2012; Spunt, Liberman, Cohen, & Eisenberger, 2012; Steele et al., 2014). A novel predictive association was also observed in the insular cortex. This finding provides convergent evidence that the predictive utility of error-monitoring activity is not constrained to a particular region of the brain, but rather, within a widespread network. The insula has been commonly implicated in salience and error detection, behavioral regulation, bodily self-awareness, and individual sense of agency (Bastin et al., 2016; Craig, 2009; Farrer & Frith, 2002; Harsay, Spaan, Wijnen, & Ridderinkhof, 2012; Kurth, Zilles, Fox, Laird, & Eickhoff, 2010; Mortensen, Evensmoen, Klensmeden, & Håberg, 2016).

Previous efforts to test neuroprediction models in forensic populations have been limited by hemodynamic reference samples that are considered small or modest, and often unrepresentative of the forensic population being tested (Aharoni et al., 2013; Aharoni et al., 2014; Camchong, Stenger, & Fein, 2012; Delfin et al., 2019; Janes et al., 2010; Pardini, Raine, Erickson, & Loeber, 2014; Poldrack et al., 2018; Steele et al., 2014; Steele et al., 2015). The present study addressed this problem by testing, to our knowledge, the largest functional imaging hemodynamic reference sample ($n = 442$) of an inmate population in this body of literature to

date. The use of a large offender hemodynamic reference sample to identify paralimbic anatomical regions of interest reduces the probability of false positives and the influence of confounds relative to smaller, non-offender samples.

Our results provide support to the literature suggesting that theoretically-relevant patterns of functional brain activity may lend incremental utility to risk assessment models designed to predict antisocial outcomes such as rearrest (Aharoni et al., 2013; Aharoni et al., 2014; Camchong, Stenger, & Fein, 2012; Delfin et al., 2019; Janes et al., 2010; Pardini, Raine, Erickson, & Loeber, 2014; Paulus, Tapert, & Schuckit, 2005; Sinha & Li, 2007; Steele et al., 2014; Steele et al., 2015; Fink et al., 2016). This pattern of results is also consistent with theories positing that paralimbic dysfunction acts as a mediator between cognitive control and antisocial behavior (Kiehl, 2006).

Furthermore, our results validate existing evidence demonstrating the dACC and Insula's role in error-monitoring and inhibition (Bastin et al., 2016; Orr & Hester, 2012; Spunt, Liberman, Cohen, & Eisenberger, 2012; Steele et al., 2014). For instance, Bastin and colleagues (2016) demonstrate via intracerebral EEG recordings a feed-forward relationship between the Insula and dACC during error processing, such that the Insula feeds saliency information during error commission to the dACC. Once received by the dACC, this information is then thought to modulate future behavior (see Orr & Hester, 2012; Spunt, Liberman, Cohen, & Eisenberger, 2012). Yet, other research noting the importance of the Insula for conscious consolidation of various inputs complicate this view (Kurth, Zilles, Fox, Laird, & Eickhoff, 2010). Thus, more work is needed to understand the causal mechanisms leading to the predictive utility within these models. For example, it is not clear whether the predictive utility of Insular activity to rearrest is indicative solely of its role as an error-monitoring hub feeding forward priors to the dACC for

behavioral regulation, or rather reflective of the Insula's role in downstream behavioral regulation and consolidation of signals to a coherent world experience (Bastin et al., 2016; Harsay, Spaan, Wijnen, & Ridderinkhof, 2012; Kurth, Zilles, Fox, Laird, & Eickhoff, 2010). Future research utilizing the functional connectivity and Granger causality measures between the dACC and Insula may help to answer this question.

Overall, our results support the interpretation that basic hemodynamic measures associated with error-monitoring may contain unique information that precipitates and possibly contributes to a variety of criminal-type behaviors. Thus, as a statistical matter, the addition of neurobiological markers to traditional risk assessment methods might potentially improve overall performance.

2.4.1 Limitations and Future Directions

Though our results provide statistical support for the predictive utility of the error-monitoring model for rearrest, we caution against overinterpretation. First, our validation sample could potentially have characteristics that do not readily generalize a broader forensic population. Second, larger and more diverse validation samples must be utilized in future studies in order to increase confidence in the external validity of the error-monitoring model. Third, the present project is not intended to suggest that a single brain region can explain the wide variety of criminal motivations. Additional research examining the functional interactions between brain regions, as well as their associations with distinct crime types, could help to address this gap.

There are also legal and ethical reasons for caution. Legally, risk assessment is already an established part of criminal justice procedure, but the prospect of employing such tools for use against the defendant's best interest is highly contentious (Starr, 2014). It is not clear that such uses meet legal standards on due process, self-incrimination, equal protection, or ethical

standards of privacy, autonomy, and beneficence. The addition of information on individuals' brain function should be evaluated with equal skepticism. But the consequences of making such decisions without the aid of the best evidence-based tools should also be subject to the same level of scrutiny (Aharoni, Abdulla, Allen, & Nadelhoffer, in press). At the very least, if the classification accuracy of brain-based risk assessment performs as well or better than traditional methods, this will obviate the need for clear standards defining what level of accuracy should be required to justify different assessment strategies (Aharoni et al., in press).

There are other forensic uses of risk assessment that don't seem to violate defendants' rights, such as decisions to grant early parole or to divert to a treatment court. Indeed, accurately assessing individual offenders' risk-needs has been shown to reduce antisocial behavior and increase treatment program success (Aos, Miller, & Drake, 2006; Andrews, 2006; MacKenzie, 2006; Taxman, 2002). For such uses, legal standards for accuracy are likely to be lower than for punitive uses. This does not necessarily mean that brain measures should be incorporated into such decision protocols. But it does mean that legal authorities need to anticipate how the strengths and weaknesses of the next generation of risk assessment tools compare to existing tools.

Aside from using brain-based risk assessment in criminal procedure, it carries great potential as a research tool. This is because predictive modeling provides an important way of identifying and validating causal relationships between brain and behavior. Understanding these mechanisms at the population level can aid in the development of pharmacological treatments and behavioral interventions for certain types of clinical conditions—such as the use of brain stimulation technology to reduce aggressive criminal intentions and self-reported aggression (Molero-Chamizo et al., 2019; Choy, Raine, & Hamilton, 2018). Though the use of brain

stimulation meant to reduce antisocial behavior shows encouraging results, as with any treatment, these approaches must meet high standards of reliability and validity (Large & Neilssen, 2017).

The present study provides a critical validation and extension of previous research on the neuroprediction of rearrest (Aharoni et al., 2013; Aharoni et al., 2014; Steele et al., 2014; Steele et al., 2015). Much work remains to be done to discern the most robust and appropriate uses of neurobiologically informed risk assessment technology. Follow up research should employ an independent validation sample to account for the possibility of data overfitting and other limitations raised in this literature (Poldrack et al., 2018). Until then, neuroprediction research remains a promising candidate for uncovering the causal mechanisms likely to underlie persistent antisocial behavior.

2.5 Methods

2.5.1 Participants

2.5.1.1 Hemodynamic Reference Sample

Participants were 442 adult offenders (64.9% female)⁴ ranging in age from 20 to 61 y (Mean, 34.6; SD, 8.43). Approximately 10% were left-hand-dominant. Based on National Institutes of Health racial and ethnic classification, 78.5% of the sample self-identified as white, 9.3% as black/African American, 6.6% as American Indian, 1.7% as mixed/OTHER, 55.9% as Hispanic, and 2.5% chose not to respond.

⁴ As in Aharoni et al. (2013), the hemodynamic reference sample used to establish the anatomical ROIs consisted of both men and women, as the location of error-monitoring activity across genders is seen to largely overlap (Liu, Zubieta, Hietzeg, 2012).

2.5.1.2 Validation Sample

Participants were 95 adult male offenders ranging in age from 18 to 49 y (Mean, 32.1; SD, 7.70). Six of them did not complete the PCL-R assessment and one participant was removed from the original sample (Aharoni et al., 2013) due to incomplete task data. Approximately 9% were left-hand-dominant. 37.9% of the sample self-identified as white, 9.5% as black/African American, 9.5% as American Indian, 29.5% as mixed/OTHER, 44.2% as Hispanic, and 13.7% chose not to respond.

All 537 participants were selected based on their being determined to have minimal or no history of traumatic brain injury (as defined by a loss of consciousness for longer than 30 minutes), no lifetime history of a psychotic disorder, and had an IQ greater than 65 (as estimated by the vocabulary and matrix reasoning subscales of the Wechsler Adult Intelligence Scale; see Ryan & Ward, 1999). Participants reported having normal hearing, and visual acuity was normal or corrected to normal with the use of contact lenses or MRI compatible glasses. Participants were paid an hourly rate commensurate with standard pay for work assignments at their facility. Participants completed a number of psychological and behavioral assessment measures and an fMRI-based inhibition task using the Mind Research Network's Mobile MRI system before release from one of two New Mexico state correctional facilities. After being released, the participants in the Validation sample were tracked from 2007 to 2010, and the average follow-up period was 34.5 mo. Participants provided written informed consent in protocols approved by the institutional review board of the University of New Mexico and Ethical and by the Independent Review (E&I) Services for the Mind Research Network.

2.5.2 Behavioral Task

Behavioral impulsivity was measured during fMRI using the Go/NoGo task. The task, modeled after the work of Kiehl et al. (2000), presents participants with a frequently occurring target (the letter “X”; occurrence probability, 0.84) interleaved with a less-frequent distracter (the letter “K”; occurrence probability, 0.16) on a computer screen. Participants were instructed to depress a button with their right index finger as quickly and accurately as possible whenever they saw the target (the “go” stimulus) and not when they saw the distracter (the “no-go” stimulus). Because targets are more frequent than distracters in this task, a prepotent response toward the targets is elicited. When a distracter is presented, participants are required to inhibit their button response, which increases the rate of commission errors. Successful performance on this task requires the ability to monitor error-related conflicts and to selectively inhibit the prepotent go response on cue. Before scanning, participants completed a brief practice session of ~10 trials.

2.5.3 Experimental Design

The present fMRI study comprised a hemodynamic reference sample second level analysis to establish anatomical ROIs, and a Validation sample second level ROI constrained analysis. All extracted imaging data used for the ROI constrained analysis within the Validation sample are included in Dataset S1 in the form of an average β -value for each subject per ROI. Dataset S1 also includes PCL-R scores, factor 1 scores, factor 2 scores, the two factors’ interaction term, and the offender’s age at release.

The experimental design used on all participants was adopted from Kiehl et al. (2000) and is identical to that of Aharoni et al.’s (2013). Two scanning runs, each composed of 246 visual stimuli, were presented to participants using Presentation, a computer-controlled visual and auditory software (Neurobehavioral Systems). Stimuli were displayed on a rear-projection

screen mounted at the rear entrance to the magnet bore and subtended a visual angle of $\sim 3 \times 3.5^\circ$. Each stimulus appeared for 250 ms in white text within a continuously displayed rectangular fixation box. Participants viewed the screen by means of a mirror system attached to the head coil.

The stimulus onset asynchrony (SOA) between go stimuli varied pseudorandomly among 1,000, 2,000, and 3,000 ms, subject to the constraint that three go stimuli were presented within each consecutive 6-s period. The no-go stimuli were interspersed among the go stimuli in a pseudorandom manner subject to three constraints: the minimum SOA between a go and a no-go stimulus was 1,000 ms; the SOA between successive no-go stimuli was in the range of 10 ± 15 s; and no-go stimuli had an equal likelihood of occurring at 0, 500, or 1,000 ms after the beginning of a 1.5-s acquisition period. By jittering stimulus presentation relative to the acquisition time, the hemodynamic response to the stimuli of interest was sampled effectively at 500-ms intervals.

Behavioral responses were recorded by using a MRI-compatible fiberoptic response device—created by Lightwave Medical—that is commercially available. Correct hits were defined as go (ie, X-stimuli) events that were followed by a button press within 1,000 ms of stimulus onset. Correct rejections were defined by an absence of a motor response within 1,000 ms of the no-go stimulus. Commission errors were defined as the presence of a response within 1,000 ms of the onset of a no-go stimulus.

2.5.4 Image Acquisition

MRI acquisition parameters were identical to those discussed in Aharoni et al. (2013), thus will only briefly be described here. Images were collected with a mobile Siemens 1.5-T Avanto system with advanced SQ gradients (max slew rate, 200T/m/s; 346 T/m/s vector summation, rise time 200 μ s) equipped with a 12-element head coil. The echoplanar image

gradient-echo pulse sequence (repetition/echo times, 2,000/39 ms; flip angle, 75°; field of view, 24 × 24 cm; 64 × 64 matrix; 3.4 × 3.4-mm in-plane resolution; 5-mm slice thickness; 30 slices) effectively covers the entire brain (150 mm) in 2,000 ms. Head motion was limited by using padding and restraint.

2.5.5 Preprocessing

Functional images were reconstructed offline at 16-bit resolution and manually reoriented to approximately the anterior commissure/posterior commissure plane. Functional images were spatially normalized to the Montreal Neurological Institute template via EPI norm (an affine transform followed by a nonlinear registration of the EPI image to an EPI template in standard space) and spatially smoothed (12mm full-width half maximum) in SPM12. High frequency noise was removed by using a low-pass filter (cutoff, 128s). The functional images were despiked using ArtRepair and motion corrected using InRialign—a motion correction procedure unbiased by local signal change (Freire, Roche, & Mangin, 2002).

2.5.6 Individual and Group Level Analysis

As in Aharoni et al. (2013), response types (correct hits and commission errors) were modeled as separate events. Event-related responses were modeled using a synthetic hemodynamic response function composed of two gamma functions. The first gamma function modeled the hemodynamic response using a peak latency of 6 s. A term proportional to the derivative of this gamma function was included to allow for small variations in peak latency. The second gamma function and associated derivative was used to model the small “overshoot” of the hemodynamic response on recovery. A latency variation amplitude-correction method was used to provide a more accurate estimate of hemodynamic response for each condition that

controlled for differences between slices in timing and variation across regions in the latency of the hemodynamic response (Calhoun et al., 2004).

Individual runs were modeled together at first level of analysis, and functional images were computed for each participant that represented hemodynamic responses associated with commission errors and correct hits. General linear models included regressors to model motion (six parameters).

Activation differences between commission errors and correct hits were extracted from 14 mm radius spheres centered around the seed coordinates in the ACC and Insula ($x = 3, y = 29, z = 28$ and $x = -36, y = 14, z = -11$, respectively; Figure 2.1b) in the form of a mean β -value for each participant via the MarsBaRs plugin for SPM (Brett, Anton, Valabregue, & Poline, 2002).

2.5.7 Covariate Risk Assessment

Data from additional risk factors (Hare's PCL-R and the offender's age at release) were obtained to examine the incremental predictive validity provided by the established ROIs. These additional variables have been previously found to predict antisocial behavior in offender populations (Aharoni et al., 2014; Olver & Wong, 2015). Scores from the Hare PCL-R—a semistructured interview and archival analysis which assesses psychopathy in incarcerated, forensic, psychiatric, and normal populations—were included as primary risk factors. These assessments were conducted by trained raters with high interrater reliability (ICC: .93). Nineteen percent of the Validation sample with PCL-R scores ($n = 89$; Mean, 23.58; SD, 6.97) met the pre-established criteria for a diagnosis of psychopathy (score of ≥ 30). The PCL-R further splits into two separate clusters of traits: factor 1 includes interpersonal/affective traits (such as glibness and lack of empathy) and factor 2 includes antisocial behavioral traits (such as impulsivity and early behavioral problems). As in Aharoni et al. (2014), these factors are entered

individually into the overall predictive models sans a total PCL-R score (due to issues of collinearity).

2.5.8 Follow-Up Procedure

As per Aharoni et al. (2013), rearrest data, including arrest date and offense type, were obtained by a professional criminal background check service (SSC), which conducted national, state, and county criminal searches following each participant's release date. Approximately 53% of the sample was rearrested at least once between their release date (ranging from 2007 to 2010) and their follow-up date during July to September 2011. In line with previous predictive modeling, minor parole and probation violations were excluded from analysis, and the remaining offenses were further classified as violent or nonviolent when warranted. A larger portion of the sample was rearrested for nonviolent offenses (42.1%) than for violent offenses (9.5%).

2.5.9 Analytic Strategy

The primary hypothesis was evaluated in the validation sample by using Cox proportional-hazards regression. A Cox regression is a semiparametric test that investigates the effect of variables of interest on the time it takes for an event to happen—in this case, rearrest—while also estimating time courses of those that have yet to reach that event (censored cases). The dependent variable is the proportion of cases surviving the event (the cumulative survival function). In order to interpret the effect of individual variables on the cumulative survival function, hazard ratios (i.e., $\exp[B]$) are computed. These hazard ratios characterize an individual's relative odds of reaching the event for every one unit change in the risk factor (e.g., error-monitoring brain activity), while controlling for other covariates.

The secondary hypothesis was evaluated in the validation sample by using receiver operating characteristic (ROC) curves which describe the differences between those who were

and were not rearrested as a function of the predictors in the model (i.e., discrimination). While most assessments of ROC curves are time independent, our analyses of AUC characteristics are evaluated per model at a variety of time points (6, 12, 24, & 36 months) by utilizing Heagerty and Zheng's time-dependent ROC curve function as found in the *risksetROC* package in *R*, version 3.60 (Heagerty & Zheng, 2005). This analysis yields an AUC per time point in order to evaluate each model's ability to discriminate those who were and were not re-arrested across a series of time scales.

2.6 Acknowledgements

This material is based upon work supported by the National Science Foundation under Grant No. (1829495), the National Institute of Health under Grant Nos. (R01MH080539, R01DA020870, R01DA026964, and R01HD092331), and the Center for Science & Law. The contents of this manuscript are solely the responsibility of the authors and do not necessarily represent the views of the National Science Foundation, the National Institute of Health, or the Center for Science & Law.

2.7 Chapter 2 Supplementary Material

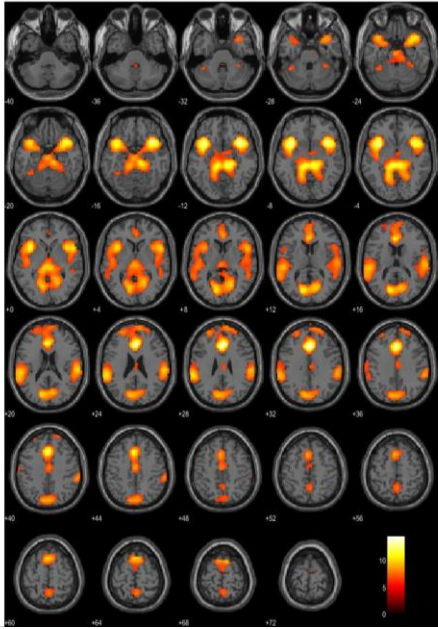


Figure 2.3 Validation Sample Error-Monitoring Activity
Mean Hemodynamic Response Change in Validation Sample ($n = 95$) During Commission Errors vs. Correct Hits from Axial View.

Table 2.2 Regions Significantly Activated in Error-Monitoring

Location	<i>t</i>-score	<i>X</i>	<i>y</i>	<i>z</i>	BA	Effect Size
Frontal Lobe						
R Dorsal Anterior Cingulate Cortex	34.93*****	3	29	28	32	3.33
R Precentral Gyrus	29.65*****	6	17	61	6	2.82
R Anterior Cingulate Cortex	22.61*****	0	-16	40	24	2.15
L Superior Frontal Gyrus	21.41*****	-27	50	25	10	2.04
R Superior Frontal Gyrus	16.56*****	48	8	49	8	1.58
Temporal Lobe						
L Insula	34.46*****	-36	14	-11	13	3.28
R Insula	33.05*****	39	14	-8	13	3.15
R Superior Temporal Gyrus	18.88*****	51	-31	1	22	1.80
Parietal Lobe						
R Inferior Parietal Lobule	25.60*****	57	-40	28	40	2.44
L Angular Gyrus	25.14*****	-57	-43	28	39	2.39
L Postcentral Gyrus	16.36*****	-54	-13	40	1	1.56
Occipital Lobe						
Cuneus	20.98*****	6	-73	40	7	2.00
Subcortical						
R Midbrain (Brainstem)	25.97*****	6	-31	-5	NA	2.47
L Midbrain (Brainstem)	25.40*****	-3	-31	-5	NA	2.42
Midbrain	17.97*****	0	-37	-38	NA	1.71

Summary of the *t*-scores extracted from a traditional hemodynamic response analysis of false alarms vs. Hits for the total sample ($n = 442$) (threshold: $t > 16$). ***** $p < .0001$ corrected for multiple comparisons. Effect size is reported in the form of Cohen's *D*.

Table 2.3 Cox Model Statistics

Model	-2 Log Likelihood	Overall			Change from Previous		
		χ^2	df	P value	$\Delta \chi^2$	df	P value
Non-Violent Zero Order dACC	335.151	2.636	1	0.104	2.675	1	0.102
Any Crime Zero Order dACC	414.262	2.216	1	0.137	2.246	1	0.134
Non-Violent with dACC	284.99	20.118	5	0.001***	22.266	5	<.001***
Any Crime with dACC	367.355	11.87	5	0.037*	12.567	5	0.028*
Non-Violent Zero Order Insula	334.378	3.324	1	0.068	3.447	1	0.063
Any Crime Zero Order Insula	414.845	1.621	1	0.203	1.664	1	0.197
Non-Violent with Insula	286.965	18.339	5	.003**	20.291	5	.001***
Any Crime with Insula	369.733	9.558	5	0.089	10.189	5	0.07

Omnibus test of Cox regression model with χ^2 statistics showing the zero-order effect of dACC activity and Insula activity on days to rearrest for non-violent crimes and any crimes. Additionally shown, the shared and unique influence of the dACC/Insula and other potential risk factors on days to rearrest for non-violent crimes and any crimes. * $p < 0.05$, ** $p < 0.01$, and *** $p < 0.001$

Table 2.4 Effect of Individual Predictors on Rearrest

Model/Predictor	B	SE (B)	Bootstrapped Data				
			B	SE (B)	P value	exp[B]	95% CI for B
Non-Violent Zero Order dACC							
- dACC	-0.285	0.176	-0.285	0.165	0.073	0.752	-.618 - .033
Any Crime Zero Order dACC							
- dACC	-0.234	0.157	-0.234	0.142	0.089	0.791	-.518 - .042
Any Crime with dACC							
- Age at release	-0.042	0.021	-0.042	0.025	0.069	0.959	-.099 - .000
- PCL-R factor 1 score	-0.04	0.061	-0.04	0.071	0.545	0.961	-.183 - .099
- PCL-R factor 2 score	-1.872	0.909	-1.872	1.099	0.063	0.154	-4.066 - .1256
- PCL-R factor interaction	0.039	0.226	0.039	0.269	0.864	1.04	-.355 - .711
- dACC	-0.425	0.179	-0.425	0.192	0.017*	0.653	-.836 - -.082
Non-Violent Zero Order Insula							
- Insula	-0.309	0.17	-0.309	0.161	0.045*	0.734	-.630 - .006
Any Crime Zero Order Insula							
- Insula	-0.186	0.146	-0.186	0.137	0.157	0.83	-.454 - .092
Any Crimes with Insula							
- Age at release	-0.034	0.02	-0.034	0.023	0.115	0.966	-.088 - .005
- PCL-R factor 1 score	-0.056	0.061	-0.056	0.072	0.4	0.946	-.203 - .084
- PCL-R factor 2 score	-1.845	0.923	-1.845	1.105	0.073	0.158	-4.166 - .197
- PCL-R factor interaction	0.086	0.227	0.086	0.28	0.737	1.09	-.355 - .756
- Insula	-0.299	0.166	-0.299	0.177	0.067	0.741	-.663 - .036

Results of Cox regression analyses examining the zero order predictive effect of the dACC and Insula on rearrest for Non-Violent crimes and Any Crimes, and Any Crimes controlling for covariates. Table reports unstandardized B, bootstrapped B, and relative risk ratio (exp[B]). * $p < 0.05$, ** $p < 0.01$, and *** $p < 0.001$.

2.7.1 Supplementary Cox Model Results

Cox models Non-Violent Zero-Order dACC/Insula, and Any Crime Zero Order dACC/Insula examined the zero order effect of error related activity in the dACC and Insula, respectively, on days to a non-violent felony and days to any felony, before entering any other

risk factors into the model (see Tables 2.3 and 2.4). All non-bootstrapped zero order analyses of error-monitoring activity in the ACC and Insula for non-violent/any crimes were insignificant (all p -values $> .05$) (see Table 2.3). Once bootstrapped, there was a significant association such that for every one unit increase in Insular activity, there was a 1.36 (i.e., $1/\exp[B]$) decrease in the probability of rearrest for a non-violent crime (see Table 2.3; bootstrapped model Non-Violent Zero Order Insula). All other bootstrapped zero order analyses were marginally significant (Non-Violent Zero-Order dACC: $B = -0.285$, $p = .073$, and Any Crime Zero Order dACC: $B = -0.234$, $p = .089$) or statistically insignificant (Any Crime Zero Order Insula: $B = -0.186$, $p = .157$).

In model Any Crimes with dACC, the dACC error-monitoring factor was the only risk factor to survive bootstrapping, such that there was a 1.53 decrease in the probability of rearrest for any crime for every one unit increase in error-monitoring activity ($p = .017$) (See Table 2.4). The overall model Any Crimes with Insula was marginally significant ($p = .089$), but none of the individual factors were significant.

2.7.2 Supplementary Discrimination Analysis Results

An area under the curve (AUC) analysis was conducted to discriminate between those rearrested and not rearrested as functions of models Non-Violent with dACC, Any Crimes with dACC, and Non-Violent with Insula at four different time periods (6, 12, 24, and 36 months)—see Figures 2.4a, 2.4c, and 2.4d, respectively. Model Any Crime with Insula was excluded for further analysis, due to previous null results (see Tables 2.3 and 2.4).

In Figure 2.4a, model Non-Violent with dACC reports an AUC of .713 at six months, which remains relatively stable (ranging from .703 to .715) until $t = 36$ months, where the model's discriminatory ability declines (AUC = 0.661). These results indicate that the model

provides a good accuracy in discriminating between those rearrested for a non-violent crime and not rearrested as a function of its covariates. In Figure 2.4b, model Any Crimes with dACC reports an AUC of .643 at six months, which remains relatively stable (ranging from .641 to .644) until $t = 36$ months, where the model's discriminatory ability declines (AUC = .612). These results demonstrate a modest ability of the model to discriminate between those rearrested for any crime from those not rearrested. Still yet, in Figure 2.4c, we see that the dACC offers incremental utility to the Any Crimes with dACC, for the model excluding the dACC factor (AUC = .608) is less predictive than the model including the dACC factor (AUC = .643).

In Figure 2.4d, model Non-Violent with Insula reports an AUC of .699 at six months, which remains stable (ranging from .680 to .702) through 36 months. These results indicate that the model Non-Violent with Insula provides a good accuracy in discriminating between those rearrested for a non-violent crime and not rearrested as a function of its covariates, and that its discriminative ability is relatively stable through time.

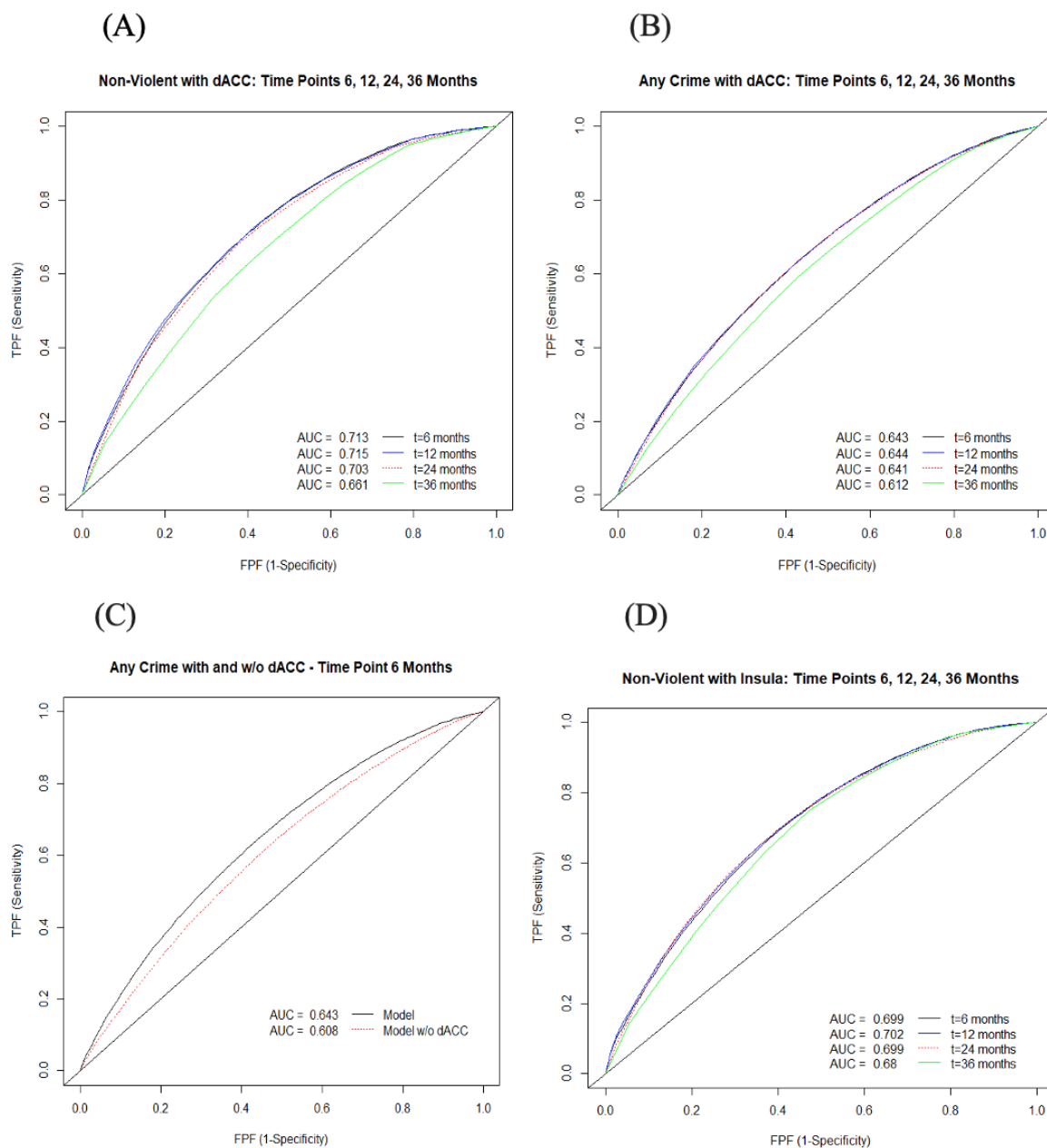


Figure 2.4 ROC Analyses

a) ROC curve and AUC statistics for Non-Violent with dACC model across four time periods. b) ROC curve and AUC statistics for Any Crime with dACC model across four time periods. c) ROC curve and AUC statistics for model Any Crime model with and without the ACC. d) ROC curve and AUC statistics for Non-Violent with Insula model across four time periods.

3 FUNCTIONAL BRAIN CONNECTIVITY MEASURES PREDICT REARREST IN MALE OFFENDERS

Corey H. Allen^{1*}, Eyal Aharoni², Carla L. Harenski³, Keith A. Harenski³, & Kent A.
Kiehl³

Keywords: impulsivity | recidivism | risk assessment | resting state functional connectivity

¹ Neuroscience Institute, Georgia State University, P.O. Box 5030, Atlanta, GA, 30302-5030, USA

² Department of Psychology, Georgia State University, P.O. Box 5010, Atlanta, GA, 30302-5010, USA

³ The Mind Research Network, 1101 Yale Blvd NE, Albuquerque, NM, 87106-4188, USA

In preparation

3.1 Abstract

Recent research has demonstrated that error-monitoring related hemodynamic activity in the dorsal anterior cingulate cortex (dACC) (Aharoni et al., 2013, 2014) and insula (Allen et al., in prep) improved predictions of rearrest in a sample of criminal offenders. Related research has shown that the resting state functional connectivity (rsFC) between dACC and insula is associated with various impulsivity related outcomes and traits, such as risky decision making and psychopathy (Philippi et al., 2015; Wei et al., 2016). The present project tested whether predictions of rearrest can be improved by modeling resting state functional connectivity between these regions within the Mind Adult Offender Cohort (MAO-C). As predicted, the rsFC between the dACC and insula improved predictions of rearrest relative to other clinically relevant predictors (age and psychopathy score). Our pattern of results aligns with previous task-based research on the dACC and insula (Aharoni et al., 2013, 2014; Allen et al., in prep; Steele et al., 2015) as well as resting state functional connectivity analyses on the same nodes (Philippi et al., 2015; Wei et al., 2016). These results reinforce and extend research on limbic predictors of recurrent, impulsive antisocial behavior. Implications for clinical and forensic risk assessment are discussed.

3.2 Introduction

Previous research utilizing functional magnetic resonance imaging (fMRI) has demonstrated that individual differences in impulsivity task-related hemodynamic activity improved predictions of rearrest within a sample of 96 adult male criminal offenders (Aharoni et al., 2013, 2014). The dACC and insula were selected as regions of interest (ROIs) due to their known involvement in impulsivity, error-monitoring, inhibition, and response selection (Holroyd & Coles, 2002; Kiehl et al., 2000; Kosson et al., 2006; Mathalon et al., 2003; Menon, 2015; Van

Veen & Carter, 2002). However, no work to date has examined the predictive value of measures of functional connectivity on re-arrest outcomes.

Resting state functional connectivity analysis (rsFC) is a task-free imaging paradigm requiring only that the participant lie still during their scan session (with eyes open). rsFC data is indicative of the brain's functional activity while at "rest" and can be used to gather information about regional functional connectivity—that is, how brain regions' functional activities coordinate with each other. Task-free designs reduce the likelihood of confounding task-related activity (Soares et al., 2016). Finally, research suggests that the majority of variance in brain activity (at rest & during tasks) can be accounted for by connections between brain regions, whereas task related activity is relatively small in comparison (Fu et al., 2017). Accordingly, the resulting signal-to-noise ratio may be nearly three times higher for resting state scans (Fox & Greicius, 2010).

rsFC has also proven to be a useful tool in investigating impulsive behavior. While rsFC studies focusing on impulsivity are broad in terms of behavioral outcome measures, the majority of them focus on the "salience network"—a network undergirding the ability to allocate attentional resources to salient events (Janes et al., 2015; Li et al., 2013; Menon & Uddin, 2010; Philippi et al., 2015; Stoeckel et al., 2016; Wei et al., 2016). Two nodes within the salience network are pertinent to impulsive antisocial outcomes: the dACC and insula. The functional connectivity, or coupling, between these regions has been shown to be associated with multiple impulsivity related outcomes such as: a preference for immediate rewards compared to long term goals (Li et al., 2013), enhanced smoking cue-reactivity in patients with nicotine dependence (Janes et al., 2015), risky decision making (Wei et al., 2016), and even psychopathy (Philippi et al., 2015). Many of these results implicate a positive relationship between dACC-insula

functional connectivity and impulsivity measures—that is, increased functional connectivity between these nodes of the salience network is associated with increased impulsive outcomes. Despite important work on the coupling of the insula and dACC in regard to impulsivity, there is a gap in the literature as to whether these functional, and in turn, impulsivity effects precipitate differences in antisocial behaviors outside of the lab—such as criminal reoffense.

To date, we are aware of just one test of the role of resting state measures in predictions of arrest (Delfin et al., 2019). Delfin and colleagues (2019) used single-photon emission computed tomography (SPECT) to measure regional cerebral blood flow during rest in a sample of 44 criminal offenders. Utilizing machine learning techniques for model selection, the researchers found that including the resting state cerebral blood flow measurements in their models led to increased accuracies of rearrest predictions, consistent with task-based studies (Aharoni et al., 2013, 2014).

One advantage of fMRI over SPECT is its superior spatial and temporal acuity (Lystad & Pollard, 2009). For instance, while SPECT analyses focus on broad activity differences within and across anatomical lobes in the brain, fMRI studies can focus on more refined points of analysis, such as the temporal coordination between spatially relevant nodes in a functionally defined network of interest—allowing direct testing of more temporally and spatially specific hypotheses.

This project intends to fill this gap in the literature by testing whether predictions of rearrest in a subset of the Mind Adult Offender Cohort (MAO-C) can be independently improved by the resting state functional connectivity (rsFC) between nodes in the salience network (the dACC and Insula) alongside other clinically-relevant predictors (age and psychopathy score; (Hare & Neumann, 2008)). To accomplish this, we utilized ROI coordinates generated from a

large subset of the MAO-C ($n = 442$) (Allen et al., in prep), and tested the predictive utility of the rsFCs of those ROIs in a separate, previously studied subset ($n = 91$) from the same cohort who underwent a resting state fMRI procedure. By testing our rsFC model on a previously studied subset of the MAO-C, we could also test the convergent validity of our methods. Because the theorized mechanisms behind various crime types (e.g., violent vs. non-violent) may be different (Ling et al., 2019), we conducted separate analyses by crime type. Our predictions were that for non-violent crimes and any crimes, (1) the rsFC between the dACC and Insula will exert an incremental effect above and beyond other established risk factors, and (2) a model including rsFC will exhibit greater classification accuracy than a model excluding it.⁵

3.3 Results

3.3.1 Determination of Regions of Interest

Regions of interest were defined a priori as the right dACC (BA 32; $x = 3, y = 29, z = 28$) and Left Insula (BA 13; $x = -36, y = 14, z = -11$) in a large subset of the MAO-C ($n = 442$; see Figure 3.1; see (Allen et al., in prep). These dACC and left insula coordinates formed the basis of separate spherical ROIs defined for resting state functional connectivity analysis in our sample ($n = 91$).

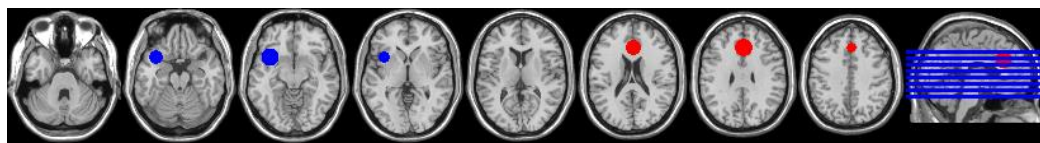


Figure 3.1 Regions of Interest

Axial view of ROIs in the Left Insula (blue) and dACC (red).

⁵ Additionally, supplementary analyses were performed to analyze multimodal predictive models for rearrest, including previously established task-based error-monitoring neurobiological risk factors (See Table 3.3).

3.3.2 *Resting State Analysis*

In order to test whether there was significant functional connectivity between our ROIs, we conducted a seed-based functional connectivity analysis with the dACC coordinates ($x = 3, y = 29, z = 28$) (see Methods). The functional connectivity between the dACC seed and 133 other ROIs (including the left insula ROI) were then analyzed for significant connectivity.⁶ At an FDR threshold of $p < .01$, this analysis identified 58 regions of the brain whose activity were significantly associated with that of the dACC during resting state (see Table 3.2). Out of the 58 regions, 15 were within the frontal lobe, 17 were within the temporal lobe, 7 were within the parietal lobe, 4 were within the occipital lobe, and 15 were within the cerebellum (see Figure 3.3 for visualization).

Consistent with expectation, the L. Insula coordinate ($x = -36, y = 14, z = -11$) was found to be one of the areas with significant functional connectivity to the dACC ROI, $t(90) = -3.04, p = .007$. For each participant, we computed a functional connectivity parameter (Fisher's transformed correlation coefficients) between the dACC and (Left) Insula ROIs and entered that parameter as an independent factor in our subsequent prediction models.

3.3.3 *Does Resting State Functional Connectivity between the dACC and Insula Predict Time to Rearrest?*

Cox proportional-hazards regression was used to examine the shared and unique influence of the functional connectivity between the dACC and Insula among other risk factors (release age, PCL-R factor 1, PCL-R factor 2, PCL-R factor interaction, & dACC error-

⁶ ROIs included were a combination of the Harvard-Oxford atlas cortical and subcortical areas, and the AAL atlas cerebellar areas.

monitoring activity) on days to rearrest for non-violent crimes and any crimes (see Table 3.1).⁷

To assess the reliability of the β -coefficients, each Cox distribution was resampled in a bootstrapping sequence with 9,999 iterations (see Table 3.1).

Table 3.1 Effect of Individual Predictors on Rearrest

Model	<i>B</i>	SE (<i>B</i>)	Bootstrapped Data			exp[<i>B</i>]	95% CI for exp[<i>B</i>]
			<i>B</i>	SE (<i>B</i>)	<i>p</i> value		
Non-Violent Crimes							
- Age at release	-0.044	0.026	-0.044	.029	0.089	0.957	0.910 - 1.007
- PCL-R factor 1 score	-0.05	0.071	-0.05	.082	0.482	0.952	0.829 - 1.093
- PCL-R factor 2 score	-4.26	1.196	-4.26	1.493	0.001***	0.014	0.001 - 0.147
- PCL-R factor interaction	0.296	0.314	0.296	.398	0.345	1.345	0.727 - 2.489
- dACC-Insula Conn.	-2.574	1.054	-2.574	1.174	0.015*	0.076	0.010 - 0.602
Any Crimes							
- Age at release	-0.035	0.021	-0.035	0.023	0.100	0.966	0.926 - 1.007
- PCL-R factor 1 score	-0.067	0.063	-0.067	0.072	0.303	0.935	0.826 - 1.058
- PCL-R factor 2 score	-2.7	0.992	-2.7	1.174	0.012*	0.067	0.010 - 0.469
- PCL-R factor interaction	0.114	0.246	0.114	0.315	0.688	1.121	0.693 - 1.814
- dACC-Insula Conn.	-2.104	0.919	-2.104	1.066	0.028*	0.122	0.020 - 0.739

Results of Cox regression multivariate analyses examining the predictive effect of the dACC-Insula functional connectivity and dACC error-monitoring activity (multimodal model: M.M.) on rearrest for non-violent crimes and any crimes controlling for covariates in a sample of 91 offenders. Table reports unstandardized *B*, bootstrapped *B*, and relative risk ratio (exp[*B*]). All variables are mean centered. **p* < 0.05, ***p* < 0.01, and ****p* < 0.001.

To test our primary hypothesis (that the rsFC between the dACC and Insula will exert an incremental effect above and beyond other established risk factors), we tested a model including previously defined risk factors: the offender's release age, PCL-R Factor 1, PCL-R Factor 2, their interaction, and the functional connectivity value between the dACC and L. Insula (see Table 3.3 for multimodal models including previously established task-based neurobiological

⁷ There was an insufficient number of offenders rearrested for violent crimes (*n* = 9), thus no analysis was conducted for violent rearrests.

risk factors). This model was regressed onto time to rearrest for a non-violent crime. A significant overall effect ($p < .05$) was obtained for the model. The PCL-R Factor 2 was significantly associated with days to non-violent rearrest ($p < .001$),⁸ as expected. The functional connectivity between the dACC-Insula exhibited a significant association with rearrest above and beyond these other risk factors. For every one unit decrease in dACC-Insula functional connectivity, there was a 13.16 decrease in the probability of rearrest for a non-violent crime ($p = .015$). That is, the more anticorrelated the two regions were with each other, the more likely an offender was to be rearrested for a non-violent crime.

The same model was then regressed onto time to rearrest for any crime. A significant overall effect ($p < .05$) was obtained for the model. The PCL-R Factor 2 was significantly associated with days to rearrest ($p = .012$), as expected. The functional connectivity value between the dACC-Insula exhibited a significant association with rearrest above and beyond the other risk factors in the model. For every one unit decrease in dACC-Insula functional connectivity, there was a 8.20 decrease in the probability of rearrest for any crime ($p = .028$).

3.3.4 Does the Inclusion of Functional Connectivity Information Increase the Accuracy of Statistical Models in Predicting Recidivism?

The receiver operating characteristic (ROC) curve is an analysis that indicates a model's true positive and false positive fractions (i.e., sensitivity and 1-specificity). Thus, it is a direct way to test a model's accuracy. In order to discriminate between those rearrested and not rearrested as functions of the Non-Violent with rsFC and Any Crime with rsFC, an area under the curve (AUC) analysis was conducted for each within the validation sample. A model's ability

⁸ In order to normalize the distribution for PCL-R Factor 2 scores, a lg10 reflection transformation was used. Due to this transformation interpretation of Cox proportional-hazards beta-values and $\exp[B]$ are reversed: higher PCL-R Factor 2 scores are associated with a decreased time to rearrest.

to discriminate between events (i.e., rearrested vs. not rearrested) is interpreted as “good” when its AUC values exceed .70.

In order to assess our final hypothesis (that the model that includes the rsFC will exhibit greater classification accuracy than the reduced model), we fitted the two models at a twelve-month time frame (see Figure 3.2a-b). In Figure 3.2a, the Non-Violent without functional connectivity model yields a baseline AUC of .683, and an improved AUC of .714 when including the dACC-Insula functional connectivity factor. In Figure 3.2b, the Any Crime without functional connectivity model yields a baseline AUC of .619, and an improved AUC of .645 when including the dACC-Insula functional connectivity factor. Overall, we find that both models incrementally benefit from the inclusion of theoretically relevant functional connectivity data.

In Figure 3.2c, the Non-Violent model including dACC-Insula functional connectivity factor yields a stable AUC for predictions within 6 to 24 months (ranging from .704 to .713), and an AUC of .684 for predictions within 36 months. In Figure 3.2d, the Any Crime model including dACC-Insula functional connectivity data also demonstrates a stable, though lower, AUC for predictions within 6 to 24 months (ranging from .634 - .646), and an AUC of .610 for predictions within 36 months. These results indicate that the Non-Violent model containing the dACC-Insula functional connectivity factor provides a good accuracy in discriminating between those rearrested for a non-violent crime and not rearrested as a function of its covariates, while the Any Crime model with the dACC-Insula functional connectivity factor yields more modest effects. Both models report discriminative abilities that are relatively stable through time.

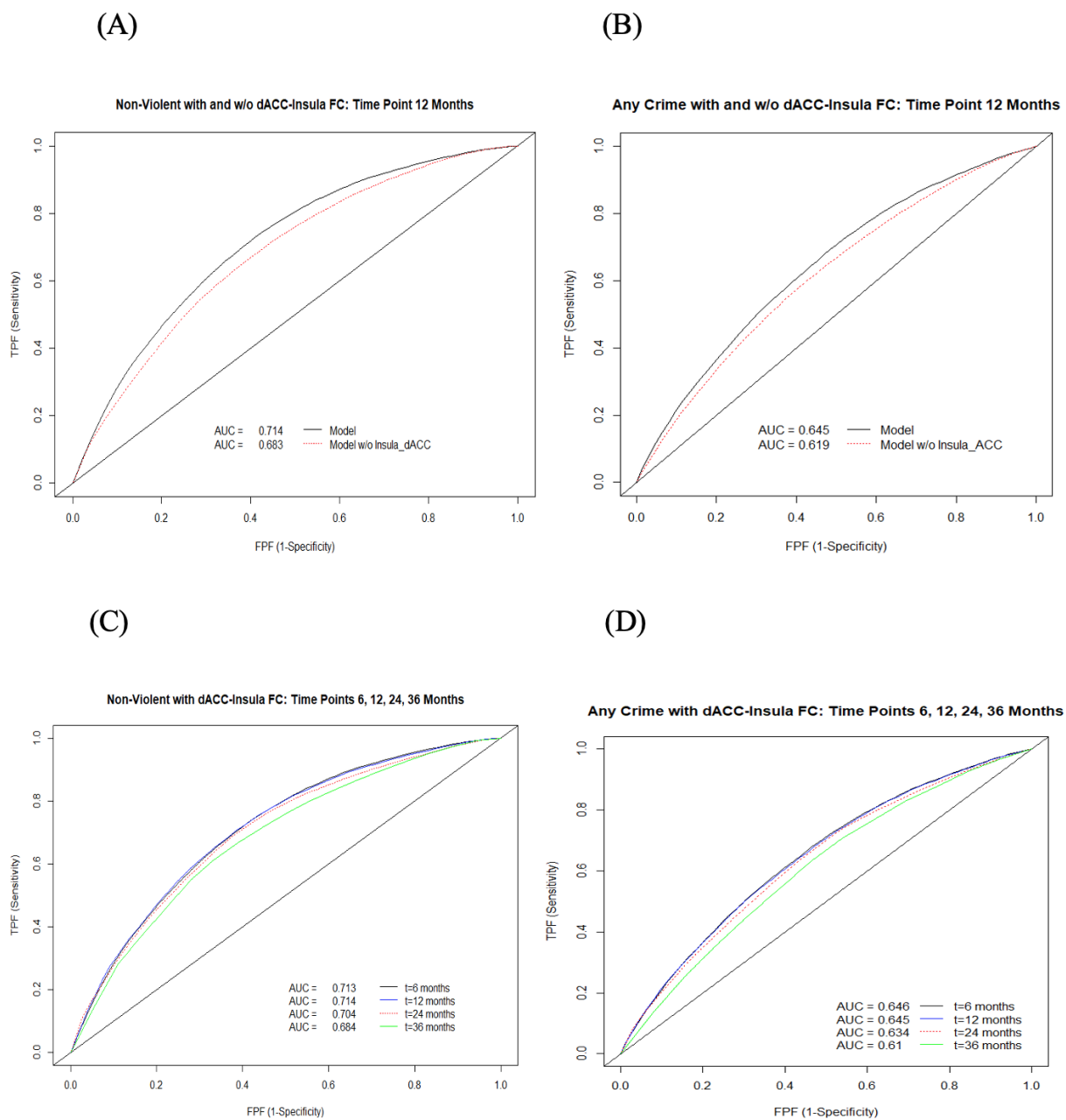


Figure 3.2 ROC Analyses

a) ROC curve and AUC statistics for Non-violent model with and without the dACC-Insula functional connectivity factor. b) ROC curve and AUC statistics for Any Crime model with and without the dACC-Insula functional connectivity factor. c) ROC curve and AUC statistics for Non-violent model with dACC-Insula functional connectivity factor across four time periods. d) ROC curve and AUC statistics for Any Crime model with dACC-Insula functional connectivity factor across four time periods.

3.4 Discussion

The present project represents an extension of recent work (Aharoni et al., 2013, 2014; Delfin et al., 2019), by combining resting state functional connectivity measures with previously established covariates (Aharoni et al., 2014) to predict rearrest in a target sample of incarcerated offenders ($n = 91$). Our results demonstrate improvement in the prediction of later rearrest using an index of resting state functional connectivity between the dACC and insula—a metric previously linked with multiple impulsivity related outcomes such as: a preference for immediate rewards compared to long term goals, enhanced smoking cue-reactivity in nicotine dependents, risky decision making, and psychopathy (Janes et al., 2015; Li et al., 2013; Philippi et al., 2015; Stoeckel et al., 2016; Wei et al., 2016). Specifically, the inclusion of resting state functional connectivity between the dACC and insula increased the accuracy of predictions of non-violent rearrest from 68.3% to 71.4%.

To our knowledge, there has only been one other attempt to test a neuropredictive model of rearrest based on neurobiological activity at rest (Delfin et al., 2019). Delfin and colleagues (2019) found that including resting state regional cerebral blood flow measurements in their predictive models led to increased accuracies of rearrest predictions. The present study validates and extends this research by producing similar effects using a larger sample size, a higher-resolution imaging method (fMRI), and a hypothesis-driven approach, which reduces concerns about model overfitting (see (Poldrack et al., 2020)).

Overall, our results corroborate and extend previous literature demonstrating that theoretically-relevant measurements of resting state functional brain activity may improve accuracy of risk models designed to predict antisocial outcomes, providing convergent validity of the methods previously utilized (Aharoni et al., 2013, 2014; Allen et al., in prep; Camchong et

al., 2012; Delfin et al., 2019; Janes et al., 2010; Pardini et al., 2014; Paulus et al., 2005; Sinha & Li, 2007; Steele et al., 2015; Zijlmans et al., 2021). Likewise, our results provide support to previous research suggesting the importance of paralimbic functional connectivity and dysfunction as a mediator between cognitive control and antisocial behavior (Janes et al., 2015; Kiehl, 2006; Li et al., 2013; Philippi et al., 2015; Stoeckel et al., 2016; Wei et al., 2016).

3.4.1 Limitations and Future Directions

While the ROIs used as hubs for our resting state connectivity measures have been previously implicated in impulsivity relevant outcomes such as error-monitoring, inhibition, impulsivity, salience, an individual sense of agency, and behavioral regulation (Bastin et al., 2017; Craig, 2009; Farrer & Frith, 2002; Harsay et al., 2012; Kurth et al., 2010; Mortensen et al., 2016; Orr & Hester, 2012; Spunt et al., 2012; Steele et al., 2014), the direction of the relationship between their functional connectivity and antisocial outcomes is not always consistent in the literature. For instance, though we show that an increased coupling between the dACC and Insula is shown to be positively associated with subsequent antisocial behavior, previous projects have reported a negative association (Hu et al., 2015). Thus, further research is necessary to tease apart the role of intra-limbic coupling in antisocial outcomes.

Furthermore, testing the convergent validity of our methods necessitated the use of a previously studied subset of the MAO-C (Aharoni et al., 2013, 2014; Allen et al., in prep). A drawback of this decision is that there could be unique features of that sample that limit its generalizability to broader offender populations. And, though our sample is large compared to traditional neuroimaging standards, it is relatively modest from a predictive modeling perspective (Poldrack et al., 2020). Future analyses aimed at modeling the predictive utility of resting state functional connectivity measures for antisocial behavior should strive for even

larger validation samples to test the generalizability, as well as the specificity of the observed effect (Poldrack et al., 2020).

The legal and ethical concerns raised by neurobiologically informed risk assessments are also reasons for caution (Aharoni et al., in press; Baum & Savulescu, 2013; Campbell & Eastman, N, 2014; Meynen, 2018). Although evidence-based risk assessment has shown promise in treatment-program success and reducing antisocial behavior (Andrews, 2006; Aos et al., 2006; MacKenzie, 2006; Taxman, 2002), the use of these techniques in opposition to a defendant's interests remains highly controversial (Starr, 2014). Though there is no clear consensus in the literature regarding the unique legal and ethical concerns posed by neurobiologically informed risk assessment, existing scholarship consistently cautions against the hasty utilization of these methods in legal decision making, and stresses the importance of a continued dialogue about the standards required for the various uses of said risk assessments (Aharoni et al., in press; Focquaert, 2018; Jurjako et al., 2018; Nadelhoffer & Sinnott-Armstrong, 2012).

These limitations notwithstanding, discerning the functional networks underlying repeated antisocial behavior represents an important step in evaluating the convergent validity of existing risk models and helps to illuminate some of the potential causes of repeated antisocial behavior (Allen & Aharoni, 2021). The present study provides an important extension of previous research on the neuroprediction of rearrest, further validating the association of theoretically relevant limbic activity to antisocial outcomes for basic research purposes (Aharoni et al., 2013, 2014; Delfin et al., 2019; Steele et al., 2015).

3.5 Methods

3.5.1 Participants

Participants were 91 adult male offenders ranging in age from 20 to 52 y ($M = 32.8$, $SD = 7.71$). Six of them did not complete the PCL-R assessment. Approximately 9% were left-hand-dominant. 38.5% of the sample self-identified as white, 8.8% as black/African American, 8.8% as American Indian, 28.6% as mixed/other, 41.8% as Hispanic, and 15.4% chose not to respond.

All participants were part of the MAO-C and were determined to have minimal or no history of traumatic brain injury (as defined by a loss of consciousness for longer than 30 minutes), no lifetime history of a psychotic disorder, and had an IQ greater than 65 (as estimated by the vocabulary and matrix reasoning subscales of the Wechsler Adult Intelligence Scale; see Ryan & Ward, 1999). Participants reported having normal hearing, and visual acuity was normal or corrected to normal with the use of contact lenses or MRI compatible glasses. Participants were paid an hourly rate commensurate with standard pay for work assignments at their facility. Participants completed a number of psychological and behavioral assessment measures and an fMRI-based inhibition task using the Mind Research Network's Mobile MRI system before release from one of two New Mexico state correctional facilities. After being released, the participants in the Validation sample were tracked from 2007 to 2010, and the average follow-up period was 34.5 mo. Participants provided written informed consent in protocols approved by the institutional review board of the University of New Mexico and Ethical and by the Independent Review (E&I) Services for the Mind Research Network.

3.5.2 Imaging Parameters

Resting state fMRI images were collected on prison grounds using a mobile Siemens 1.5 T Avanto with advanced SQ gradients (max slew rate 200 T/m/s, 346 T/m/s vector

summation, rise time 200 us) equipped with a 12-element head coil. The EPI gradient-echo pulse sequence (TR = 2000 ms, TE = 39 ms, flip angle 90°, FOV 24 × 24 cm, 64 × 64 matrix, 3.4 × 3.4 mm in-plane resolution, 4 mm slice thickness, 1 mm gap, 30 slices) effectively covered the entire brain (150 mm) in 2.0 s. Head motion was minimized using padding and restraint. The participants were asked to lay still, look at the fixation cross and keep eyes open during the five-minute resting state fMRI scanning. Compliance with instructions was monitored by eye tracking.

3.5.3 Preprocessing

Data were pre-processed using statistical parametric mapping (Friston et al., 1994) (<http://www.fil.ion.ucl.ac.uk/spm>) including slice-timing correction, realignment (INRIalign), co-registration, and spatial normalization, and then transformed to the Montreal Neurological Institute standard space at a resolution of a 3 × 3 × 3 mm³. Despiking consisted of the orthogonalization with respect to spike regressors. Each spike is represented by an independent regressor valued one at the spike time point and zero everywhere else. The DVARS method (Power et al., 2013) was used to find spike regressors where the root mean square exceeded three standard deviations. Time-courses were also orthogonalized with respect to the following: (1) linear, quadratic, and cubic trends; (2) the six realignment parameters; (3) realignment parameters derivatives; and (4) spike regressors. A full width half maximum Gaussian kernel of 6 mm was then used for spatial smoothing. An anatomical component-based noise correction procedure (aCompCor: (Behzadi et al., 2007) regressed additional noise components including cerebral white matter and cerebrospinal noise (see Behzadi et al. 2007 & Chai et al. 2012), and session effects (see Whitfield-Gabrieli & Nieto-Castanon, 2012).

Temporal filtering was conducted below 0.008 Hz or above 0.09 Hz for each participants' BOLD signals in order to further minimize the influence of head motion and other noise sources. Implemented via a discrete cosine transform windowing operation, this temporal filtering was intended to minimize border effects and was performed after additional regressions to avoid any frequency mismatch in the nuisance regression procedure (Hallquist et al., 2013).

3.5.4 Seed to ROI Functional Connectivity Analysis

Resting state functional connectivity analyses were conducted using the CONN Functional Connectivity Toolbox (Whitfield-Gabrieli & Nieto-Castanon, 2012) (<http://www.nitrc.org/projects/conn>). To compute the rsFC value from the dACC to the L. Insula, a seed-to-ROI analysis was conducted following preprocessing of the data. This analysis computes the Fisher-transformed bivariate correlation coefficient between the predetermined seed's BOLD time series and each individual ROI's BOLD time series, which was then extracted to be analyzed alongside other variables of interest.

3.5.5 Individual and Group Level Error-Monitoring Analysis

For supplementary multimodal analyses, error-monitoring activity from the dACC was quantified as described in Aharoni et al. (2013) & Allen et al. (in prep), response types (correct hits and commission errors) were modeled as separate events (see Aharoni et al., 2013 & Allen et al., in prep, for more information on Go/NoGo task procedures). Event-related responses were modeled using a synthetic hemodynamic response function composed of two gamma functions. The first gamma function modeled the hemodynamic response using a peak latency of 6 s. A term proportional to the derivative of this gamma function was included to allow for small variations in peak latency. The second gamma function and associated derivative was used to model the small "overshoot" of the hemodynamic response on recovery. A latency variation

amplitude-correction method was used to provide a more accurate estimate of hemodynamic response for each condition that controlled for differences between slices in timing and variation across regions in the latency of the hemodynamic response (Calhoun et al., 2004).

Individual runs were modeled together at first level of analysis, and functional images were computed for each participant that represented hemodynamic responses associated with commission errors and correct hits. General linear models included regressors to model motion (six parameters).

Activation differences between commission errors and correct hits were extracted from 14 mm radius spheres centered around the seed coordinate in the ACC ($x = 3, y = 29, z = 28$) in the form of a mean β -value for each participant via the MarsBaRs plugin for SPM (Brett, Anton, Valabregue, & Poline, 2002).

3.5.6 Covariate Risk Assessment

Data from additional risk factors (Hare's PCL-R and the offender's age at release) were obtained to examine the incremental predictive validity provided by the established ROIs. These additional variables have been previously found to predict antisocial behavior in offender populations (Aharoni et al., 2014; Olver & Wong, 2015). Scores from the Hare PCL-R—a semistructured interview and archival analysis which assesses psychopathy in incarcerated, forensic, psychiatric, and normal populations—were included as primary risk factors. These assessments were conducted by trained raters with high interrater reliability (ICC: .93). Twenty-one percent of the Validation sample with PCL-R scores ($n = 80$; Mean, 23.28; SD, 7.03) met the pre-established criteria for a diagnosis of psychopathy (score of ≥ 30). The PCL-R further splits into two separate clusters of traits: factor 1 includes interpersonal/affective traits (such as glibness and lack of empathy) and factor 2 includes antisocial behavioral traits (such as

impulsivity and early behavioral problems). As in Aharoni et al. (2014), these factors were entered individually into the overall predictive models excluding total PCL-R score (due to issues of collinearity).

Additional exploratory correlational analyses were also conducted with the following variables (see Table 3.4): the offender's estimated IQ, their alcohol/drug dependency (as assessed from the Structured Clinical Interview for the DSM (SCID) via determinations of lifetime abuse or dependence (scoring: 0 = no lifetime abuse/dependence, 1 = lifetime abuse, and 2 = lifetime dependence),⁹ their State-Trait Anxiety Inventory score (STAI: Spielberger et al., 1983), and The Barratt Impulsiveness Scale (BIS-11; Patton et al., 1995).

3.5.7 Follow-Up Procedure

As per Aharoni et al. (2013), rearrest data, including arrest date and offense type, were obtained by a professional criminal background check service (SSC), which conducted national, state, and county criminal searches following each participant's release date. Approximately 55% of the sample was rearrested at least once between their release date (ranging from 2007 to 2010) and their follow-up date during July to September 2011. In line with previous predictive modeling, minor parole and probation violations were excluded from analysis, and the remaining offenses were further classified as violent or nonviolent when warranted. A larger portion of the sample was rearrested for nonviolent offenses (42.9%) than for violent offenses (9.9%).

3.5.8 Analytic Strategy

The primary hypothesis was evaluated by using Cox proportional-hazards regression. A Cox regression is a semiparametric test that investigates the effect of variables of interest on the

⁹ Scoring for drug abuse/dependence is computed via an averaging across abuse/dependence in the following individual drug classes: sedatives, cannabis, stimulants, opioids, cocaine, and hallucinogens.

time it takes for an event to happen—in this case, rearrest—while also estimating time courses of those that have yet to reach that event (censored cases). The dependent variable is the proportion of cases surviving the event (the cumulative survival function). In order to interpret the effect of individual variables on the cumulative survival function, hazard ratios (i.e., $\exp[B]$) are computed. These hazard ratios characterize an individual's relative odds of reaching the event for every one unit change in the risk factor (e.g., resting state functional connectivity), while controlling for other covariates.

The secondary hypothesis was evaluated by using receiver operating characteristic (ROC) curves which describe the differences between those who were and were not rearrested as a function of the predictors in the model (i.e., discrimination). While most assessments of ROC curves are time independent, our analyses of AUC characteristics are evaluated per model at a variety of time points (6, 12, 24, & 36 months) by utilizing Heagerty and Zheng's time-dependent ROC curve function as found in the *risksetROC* package in *R*, version 3.60 (Heagerty & Zheng, 2005). This analysis yields an AUC per time point in order to evaluate each model's ability to discriminate those who were and were not re-arrested across a series of time scales.

3.6 Acknowledgements

This material is based upon work supported by the National Science Foundation under Grant No. (1829495), the National Institute of Health under Grant Nos. (R01MH080539, R01DA020870, R01DA026964, and R01HD092331), and the Center for Science & Law. The contents of this manuscript are solely the responsibility of the authors and do not necessarily represent the views of the National Science Foundation, the National Institute of Health, or the Center for Science & Law.

3.7 Chapter 3 Supplementary Materials

Table 3.2 Regions with Significant rsFCs from the dACC Seed

Location	X	y	z	t-score	Effect Size
Frontal Lobe					
R Paracingulate Gyrus	7	37	23	24.94****	5.26
L Paracingulate Gyrus	-6	37	21	11.80****	2.49
Frontal Medial Cortex	0	43	-19	-7.69****	-1.62
L Central Opercular Cortex	-48	-9	12	-6.80****	-1.43
Subcallosal Cortex	0	21	-15	-5.59****	-1.18
R Central Opercular Cortex	49	-6	11	-5.25****	-1.11
L Frontal Orbital Cortex	-30	24	-17	-5.03****	-1.06
L Supplementary Motor Cortex	-5	-3	56	-4.88****	-1.03
R Superior Frontal Gyrus	15	18	57	4.86****	1.02
L Precentral Gyrus	-34	-12	49	-4.79****	-1.01
R Frontal Operculum Cortex	41	19	5	4.61***	0.97
L Inferior Frontal Gyrus	-50	28	9	-3.80**	-0.8
R Middle Frontal Gyrus	39	19	43	3.52**	0.74
R Supplementary Motor Cortex	6	-3	58	-3.33**	-0.7
R Inferior Frontal Gyrus	52	28	8	2.94**	0.62
Temporal Lobe					
L Anterior Middle Temporal Gyrus	-57	-4	-22	-8.65****	-1.82
L Posterior Middle Temporal Gyrus	-61	-27	-11	-6.36****	-1.34
L Anterior Superior Temporal Gyrus	-56	-4	-8	-5.76****	-1.21
L Temporal Pole	-41	11	-30	-5.66****	-1.19
L Posterior Superior Temporal Gyrus	-62	-30	4	-5.31****	-1.12
L Temporoccipital Middle Temporal Gyrus	-58	-53	1	-4.81****	-1.01
L Heschl's Gyrus	-45	-20	7	-4.80****	-1.01
L Planum Polare	-47	-6	-7	-4.54***	-0.96
R Temporal Pole	41	13	-30	-4.37***	-0.92
L Planum Temporale	-53	-30	11	-4.34***	-0.91
R Heschl's Gyrus	46	-17	7	-4.32***	-0.91
R Anterior Middle Temporal Gyrus	58	-2	-25	-4.05***	-0.85
R Planum Temporale	55	-25	12	-3.92***	-0.83

R Anterior Superior Temporal Gyrus	58	-1	-10	-3.70**	-0.78
R Planum Polare	48	-4	-7	-3.40**	-0.72
L Insular Cortex	-36	14	-11	-3.04**	-0.64
L Amygdala	-23	-5	-18	-3.00**	-0.63
Parietal Lobe					
L Postcentral Gyrus	-38	-28	52	-6.01****	-1.27
L Angular Gyrus	-50	-56	30	-4.62****	-0.97
R Postcentral Gyrus	38	-26	53	-4.47****	-0.94
L Parietal Operculum Cortex	-48	-32	20	-4.52****	-0.95
R Parietal Operculum Cortex	49	-28	22	-4.31***	-0.91
Precuneus	1	-59	38	-3.85***	-0.81
R Posterior Supramarginal Gyrus	55	-40	34	3.64**	0.77
Occipital Lobe					
L Superior Lateral Occipital Cortex	-32	-73	38	-4.78****	-1.01
R Inferior Lateral Occipital Cortex	46	-74	-2	-4.14****	-0.87
L Inferior Lateral Occipital Cortex	-45	-76	-2	-3.39**	-0.71
R Superior Lateral Occipital Cortex	33	-71	39	-3.07**	-0.65
Cerebellar					
R Cerebellum 10	26	-34	-41	-4.30****	-0.91
R Cerebellum Crus 2	32	-69	-40	-4.10****	-0.86
R Cerebellum Crus 1	38	-67	-30	-3.74**	-0.79
L Cerebellum 9	-11	-49	-46	-3.71**	-0.78
R Cerebellum 8	25	-56	-50	-3.62**	-0.76
L Cerebellum 10	-23	-34	-42	-3.47**	-0.73
L Cerebellum Crus 2	-29	-73	-38	-3.45**	-0.73
Vermis 8	1	-64	-34	-3.36**	-0.71
L Cerebellum Crus 1	-36	-66	-30	-3.35**	-0.71
R Cerebellum 6	24	-58	-25	-3.31**	-0.7
Vermis 10	0	-46	-32	-3.05**	-0.64
Vermis 6	1	-67	-16	-3.04**	-0.64
Vermis 9	1	-55	-35	-3.04**	-0.64
R Cerebellum 9	9	-50	-46	-3.02**	-0.64
Vermis 4 5	1	-52	-7	-2.93**	-0.62

Summary of the t -scores extracted from resting state functional connectivity analysis for the total sample ($n = 91$) (FDR threshold: $p < .01$). **** p .00001, *** p .0001, ** p .001, * p .01, FDR > .01. Effect size is reported in the form of Cohen's D . $t(90)$. Regions are extracted from the Harvard-Oxford Atlas and the AAL Atlas.

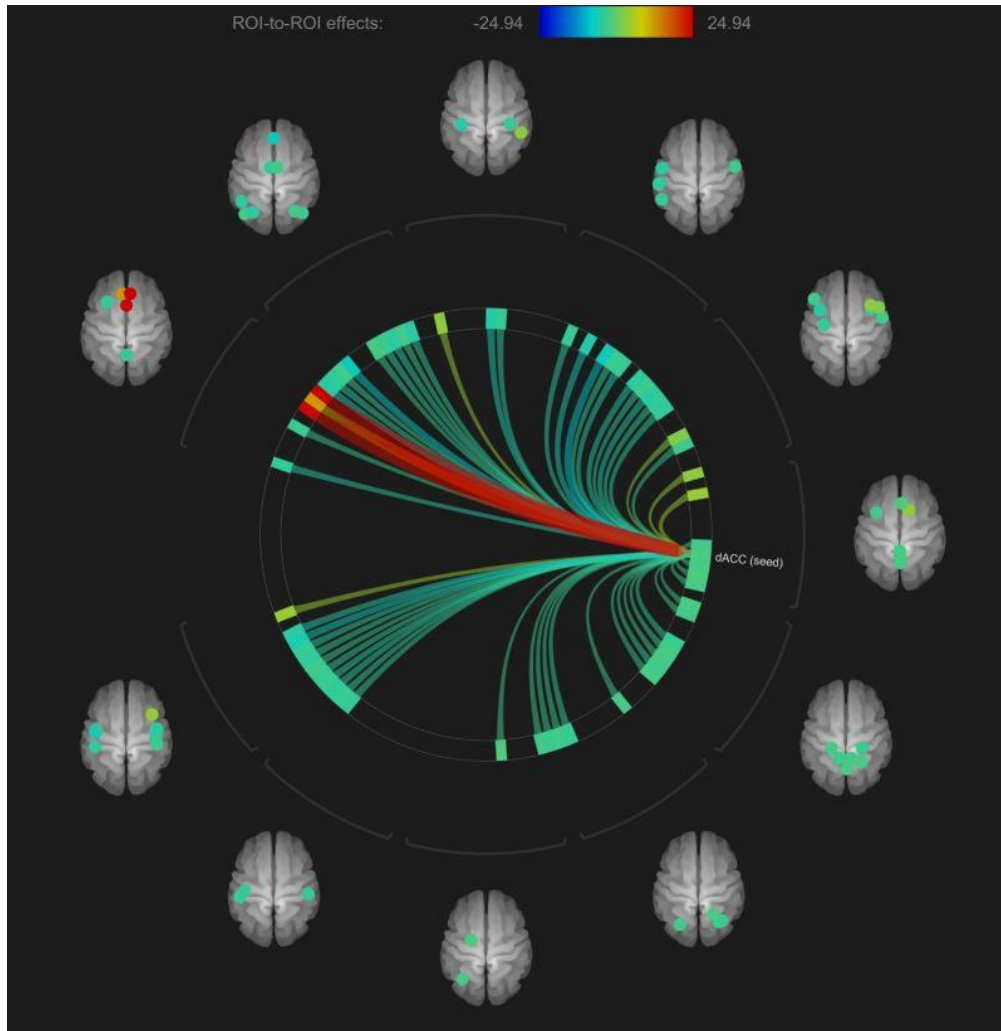


Figure 3.3 Visualization of Significant rsFCs from the dACC Seed

Significant rsFCs from the dACC seed region ($x = 3$, $y = 29$, $z = 28$) tested at FDR threshold of $< .01$. Spheres indicate significantly functionally connected regions to the dACC seed, and colors and line breadth indicate strength of that rsFC.

Table 3.3 Effect of Individual Predictors on Rearrest

Model	<i>B</i>	SE (<i>B</i>)	Bootstrapped Data			exp[<i>B</i>]	95% CI for exp[<i>B</i>]
			<i>B</i>	SE (<i>B</i>)	<i>P</i> value		
Non-Violent Crimes M. M.							
- Age at release	-0.063	0.028	-0.063	0.031	.020*	0.939	0.888 - 0.992
- PCL-R factor 1 score	-0.015	0.075	-0.015	0.091	.842	0.985	0.850 - 1.141
- PCL-R factor 2 score	-4.023	1.165	-4.023	1.504	.002**	0.018	0.002 - 0.175
- PCL-R factor interaction	0.295	0.322	0.295	0.388	.370	1.343	0.714 - 2.526
- dACC Error Monit.	-0.559	0.206	-0.559	0.216	.003**	0.572	0.382 - 0.856
- dACC-Insula Conn.	-2.194	1.085	-2.194	1.307	.054	0.112	0.013 - 0.935
Any Crimes M. M.							
- Age at release	-0.047	0.022	-0.047	0.025	.039*	0.954	0.913 - 0.997
- PCL-R factor 1 score	-0.052	0.066	-0.052	0.083	.489	0.949	0.834 - 1.081
- PCL-R factor 2 score	-2.650	0.970	-2.650	1.218	.017*	0.071	0.011 - 0.473
- PCL-R factor interaction	0.074	0.245	0.074	0.308	.778	1.077	0.666 - 1.742
- dACC Error Monit.	-0.471	0.183	-0.471	0.192	.007**	0.624	0.436 - 0.893
- dACC-Insula Conn.	-1.828	0.971	-1.828	1.257	.103	0.161	0.024 - 1.078

Results of Cox regression multivariate analyses examining the predictive effect of the dACC-Insula functional connectivity and dACC error-monitoring activity (multimodal model: M.M.) on rearrest for non-violent crimes and any crimes controlling for covariates. Table reports unstandardized *B*, bootstrapped *B*, and relative risk ratio (exp[*B*]). All variables are mean centered. * $p < 0.05$, ** $p < 0.01$, and *** $p < 0.001$.

3.7.1 Supplemental Multimodal Analyses

Additional analyses were conducted to test whether the rsFC between the dACC and Insula will exert an incremental effect above and beyond other previously examined neurobiological risk factors (i.e., task-based dACC error-monitoring activity) while controlling for clinical risk factors (Aharoni et al., 2013; Aharoni et al., 2014; Steele et al., 2015). Thus, we tested a multimodal model including: the offender's release age, PCL-R Factor 1, PCL-R Factor 2, their interaction, dACC error-monitoring activity, and the functional connectivity value between the dACC and L. Insula (see Table 3.3). This model was regressed onto time to rearrest

for a non-violent crime. A significant overall effect ($p < .05$) was obtained for the model. A younger age at release and a higher PCL-R Factor 2¹⁰ were each significantly associated with days to non-violent rearrest ($p = .020$ & $p = .002$), as expected. Likewise, low dACC error-monitoring activity was also associated with days to non-violent rearrest ($p = .003$), as previously shown (Aharoni et al., 2013; Aharoni et al., 2014; Steele et al., 2015). The functional connectivity between the dACC-Insula exhibited a marginal association with rearrest while controlling for these other risk factors ($p = .054$).

The same model was then regressed onto time to rearrest for any crime. A significant overall effect ($p < .05$) was obtained for the model. As expected, age at release and the PCL-R Factor 2 were significantly associated with days to rearrest ($p < .05$). Low dACC error-monitoring activity was also associated with days to rearrest ($p = .007$). The effect of the functional connectivity value between the dACC-Insula did not survive bootstrapping.

¹⁰ In order to normalize the distribution for PCL-R Factor 2 scores, a lg10 reflection transformation was used. Due to this transformation interpretation of Cox proportional-hazards beta-values and $\exp[B]$ are reversed: higher PCL-R Factor 2 scores are associated with a decreased time to rearrest.

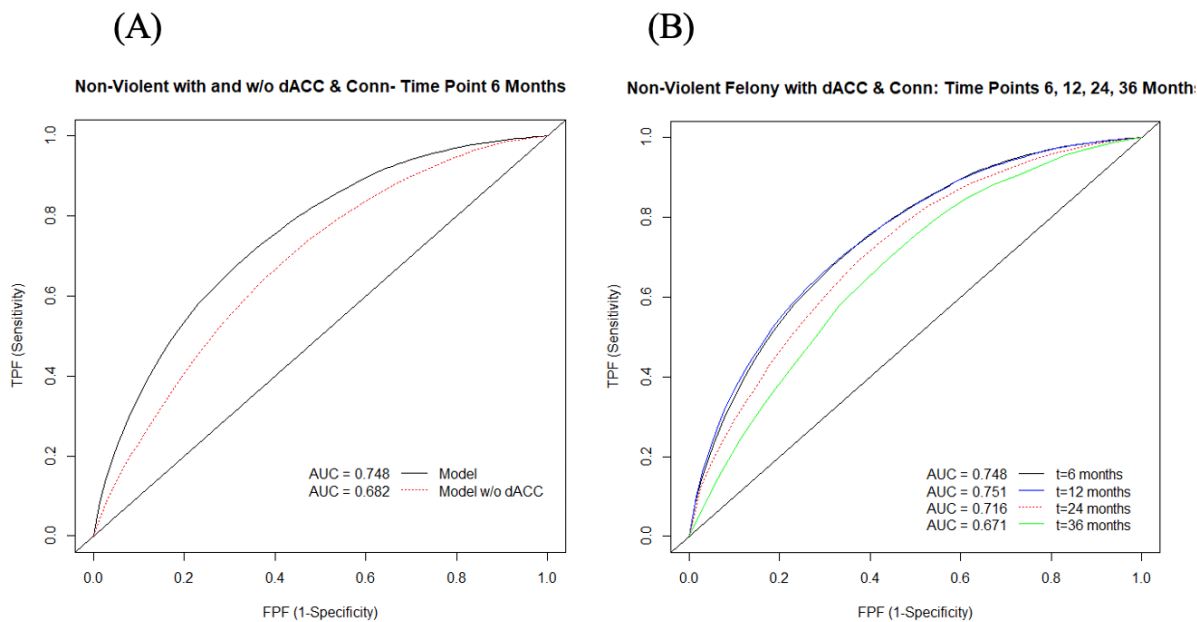


Figure 3.4 ROC Analyses

a) ROC curve and AUC statistics for Non-violent model with and without the dACC-Insula functional connectivity factor. b) ROC curve and AUC statistics for Non-violent model with dACC-Insula functional connectivity factor across four time periods.

In order to assess the incremental utility offered by both neurobiological factors (dACC-Insula rsFC & dACC error-monitoring activity) we analyzed the model's area under the curve with and without the neurobiological variables for non-violent rearrest within a six-month time frame (see Figure 3.4a).¹¹ In Figure 3.4a, the Non-Violent without rsFC and error-monitoring model yields a baseline AUC of .682, and an improved AUC of .748 when including the dACC-Insula functional connectivity factor and error-monitoring activity. In Figure 3.4b, the Non-Violent model including dACC-Insula functional connectivity factor and error-monitoring activity yields a relatively stable AUC for predictions within 6 to 24 months (ranging from .716 to .751), and an AUC of .671 for predictions within 36 months. Overall, we find that models

¹¹ Rearrest for any crimes was unanalyzed, due to null cox-regression results for rsFC within the multimodal model.

predicting non-violent rearrest incrementally benefit from the inclusion of theoretically relevant multimodal neurobiological data.

Table 3.4 Two-Tailed Correlations Analyses (n = 91)

	1	2	3	4	5	6	7	8	9	10	11	12	13	14
1 Release Age														
2 PCLR	-.12													
3 Factor 1	-.07	.83**												
4 Factor 2	-.19	.90**	.57**											
5 Lifetime Drug	.08	.13	.04	.22										
6 Lifetime Alc	.05	.00	-.03	.03	.23*									
7 State Anxiety	.13	-.01	.00	-.02	.21	.09								
8 Trait Anxiety	.10	-.10	-.07	-.08	.08	.11	.61**							
9 Barratt's Impulsivity	.09	.39**	.29*	.37**	.30*	.03	.21	.10						
10 False Alarm Rate	-.20	.18	.06	.20	.02	-.03	-.07	-.20	.08					
11 Wais IQ	.05	.10	.12	.04	-.03	.03	-.04	-.06	-.07	-.08				
12 Insula	-.14	.07	.13	.05	-.22*	.05	-.18	.12	-.07	-.10	-.01			
13 dACC	-.20	.09	.11	.07	-.21*	.13	-.05	.06	-.02	-.16	.13	.65**		
14 dACC-Insula Conn	-.07	.29**	.18	.31**	.17	.08	-.13	-.14	.32**	.05	.06	.03	.11	

Note: STAI state and trait measures are presented separately for analysis. False alarm rate entails the offender's rate of error commission during the Go/NoGo task presented in the M.M. analyses, and Insula & dACC measures represent the error monitoring activity within these ROIs. * $p < 0.05$, ** $p < 0.01$, and *** $p < 0.001$.

4 LIMBIC ACTIVITY PREDICTS REOFFENDING: A PARTIAL VALIDATION AND EXTENSION

Corey H. Allen¹, Eyal Aharoni^{2*}, Gullapalli, A.³, Carla L. Harenski³, Keith A. Harenski³, & Kent
A. Kiehl³

Keywords: impulsivity | recidivism | risk assessment

¹ Neuroscience Institute, Georgia State University, P.O. Box 5030, Atlanta, GA, 30302-5030, USA

² Department of Psychology, Georgia State University, P.O. Box 5010, Atlanta, GA, 30302-5010, USA

³ The Mind Research Network, 1101 Yale Blvd NE, Albuquerque, NM, 87106-4188, USA

In preparation

4.1 Abstract

Published studies (Aharoni et al., 2013; Aharoni et al., 2014; Steele et al., 2015) reported evidence that error-monitoring activity in the dorsal anterior cingulate cortex (dACC) significantly improved predictions of subsequent rearrest for a non-violent felony among male offenders ($n = 96$) from the Mind Adult Offender Cohort (MAO-C). This chapter reports an out-of-sample replication and extension of the Aharoni et al. (2014) model in a large subset of male and female violent and non-violent offenders ($n = 538$) from the same longitudinal cohort. Modest support for the predictive utility of error-monitoring activity in the dACC was found for predictions of rearrest for felonies in women and violent felonies in men, replicating aspects of the previous studies. The dACC's utility in predictions of non-violent rearrest in men were not successfully replicated. Implications for future research and clinical and forensic risk assessment are discussed.

4.2 Introduction

Understanding the factors driving repeated, impulsive antisocial behavior is essential for the effective treatment of such behavior. One criterion for evaluating the strength of a given explanation is the extent to which it predicts outcomes. Previously published functional magnetic resonance imaging (fMRI) studies found that individual differences in limbic function improved predictions of rearrest in a sample of 96 male criminal offenders (Aharoni et al., 2013; Aharoni et al., 2014; Steele et al., 2015). The gold standard for evaluating the external validity of any prediction model is to test the model in an independent sample, known as out-of-sample validation (Poldrack, Huckins, & Varoquaux, 2020). Here we extend previous research (Aharoni et al., 2013; Aharoni et al., 2014; Steele et al., 2015) by testing the incremental predictive effect

of the dACC's error-monitoring activity in a large independent validation sample a large subset of male and female offenders ($n = 538$) from the Mind Adult Offender Cohort (MAO-C).

A large sample affords the opportunity to conduct fine-grained analyses, including prediction of violent crime and gender differences. Previous studies focused on a region of the brain known as the dorsal anterior cingulate cortex (dACC)—an area associated with inhibition, error-monitoring, and response selection (Holroyd & Coles, 2002; Kiehl, Liddle, & Hopfinger, 2000; Kosson et al., 2006; Mathalon, Whitfield, & Ford, 2003; Van Veen & Carter, 2002). Although this region of interest was originally developed from a mixed sample of males and females (Steele et al., 2014), existing tests of the predictive utility of that model have only been reported in men (Aharoni et al., 2013; Aharoni et al., 2014; Steele et al., 2015). Testing potential gender differences is important because functional differences in this brain region have been observed for the same behavioral outcome (see Weafer, 2020 for a comprehensive review on the matter). For example, Liu and colleagues (2012) found that scores on particular trait impulsivity measures were associated with different brain activation profiles for men and women, and they even found gender differences in brain activation for the same behavioral task accuracy, suggesting that different neural mechanisms may underlie impulse control behavior in men and women.

This study marks the first attempt to test such effects in an out-of-sample replication and extension of the Aharoni et al. error-monitoring model (2014), based on a dataset from 102 healthy adults (though see Zijlmans et al., 2021 for null univariate tests of dACC error-monitoring on rearrest). As in previous studies, error-monitoring activity was captured via a classic Go/NoGo designed to test one's ability to inhibit prepotent motor responses—and was defined as the contrast between commission errors versus correct hits. Our predictions were that

for non-violent and violent crimes in both men and women, (1) the dACC will exert an incremental predictive effect above and beyond other established risk factors¹², and (2) a multivariate model that includes the dACC will predict better than models without the dACC.

4.3 Results

4.3.1 Group Level Neuroimaging Analysis

Activation differences between commission errors and correct hits were extracted from an a priori defined 14 mm radius sphere (Steele et al., 2014) centered around the seed coordinate in the ACC ($x = -3$, $y = 24$, $z = 33$: See Figure 4.1a for seed coordinate and Figure 4.1b for group level activation map) in the form of a mean β -values for each participant via the MarsBaRs plugin for SPM (Brett, Anton, Valabregue, & Poline, 2002). Likewise, a group level analysis of 32 ROIs was conducted in order to assess the reliability of error-monitoring activation compared to previous literature (Steele et al., 2014: see Tables 4.2, 4.3 for full replication of regional activations in men and women, separated).

¹² Established risk factors include Hare's revised Psychopathy Checklist (PCL-R) Factor 1, PCL-R Factor 2, the interaction of Factor 1 and 2, and release age (Aharoni et al., 2014; Hare & Neumann, 2008). See Covariate Risk Assessment section for more information.

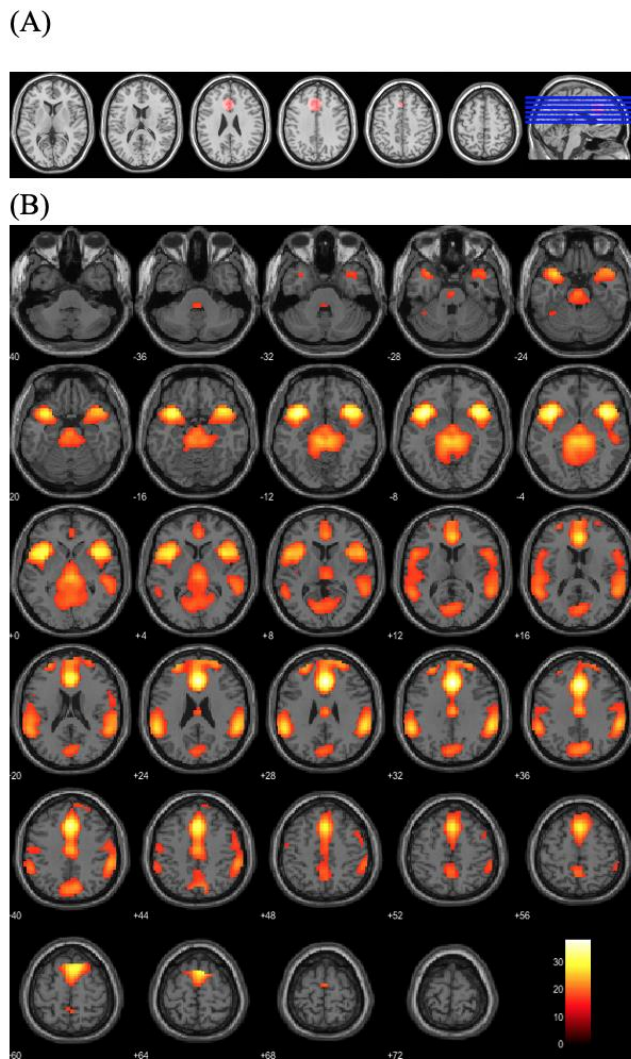


Figure 4.1 dACC Region of Interest and Group Level Error-Monitoring Activity

A) A priori region of interest (red) for hemodynamic response to commission errors vs. correct hits in the dACC from a Go/NoGo task with an independent sample of 102 healthy adult nonoffenders; peak voxel $x = -3$, $y = 24$, $z = 33$ (Steele et al., 2014). B) Mean hemodynamic response change in offender sample ($n = 538$) during commission errors vs. correct hits from axial view. Peak activation located at $x = 3$, $y = 26$, $z = 31$, within the ACC (threshold: $t > 16$).

4.3.2 Survival Analysis

A multivariate Cox proportional-hazards regression was used to examine the shared and unique influence of the dACC among other predefined risk factors (release age, PCL-R factor 1, PCL-R factor 2, and PCL-R factor interaction) on days to rearrest for general felony, non-violent felony, and violent felonies in men and women within a 4-year follow-up window (see Table

4.1). Predefined risk factors were entered into the regression in the first step, to assess whether the dACC exerted significant influence on the model after controlling for the other variables of interest.¹³

Table 4.1 Effect of Individual Predictors on Rearrest

Model/Predictor	Unadjusted Hazards			Adjusted Hazards		
	<i>B (SE)</i>	<i>P value</i>	exp[B] (CI)	<i>B (SE)</i>	<i>P value</i>	exp[B] (CI)
Felony Rearrest in Men (n = 213, 93 rearrests)						
- Age at release	-0.027 (0.010)	.007**	0.973 (0.954 - 0.993)	-0.025 (0.011)	.024*	0.975 (0.954 - 0.997)
- PCL-R factor 1 score	0.077 (0.030)	.010*	1.080 (1.019 - 1.145)	0.339 (0.151)	.025*	1.404 (1.044 - 1.889)
- PCL-R factor 2 score	0.097 (0.030)	.001**	1.102 (1.038 - 1.170)	0.170 (0.070)	.015*	1.186 (1.033 - 1.361)
- PCL-R factor interaction	0.005 (0.002)	.004**	1.005 (1.002 - 1.008)	-0.020 (0.010)	.052	0.980 (0.960 - 1.000)
- dACC	-0.034 (0.118)	.772	.966 (0.766 - 1.218)	-0.137 (0.122)	.262	0.872 (0.687 - 1.108)
Non-Violent Felony Rearrest in Men (n = 183, 63 rearrests)						
- Age at release	-0.022 (0.012)	.067	0.979 (0.956 - 1.002)	-0.024 (0.013)	.072	0.977 (0.952 - 1.002)
- PCL-R factor 1 score	0.075 (0.036)	.037*	1.077 (1.004 - 1.156)	0.303 (0.177)	.086	1.354 (0.958 - 1.914)
- PCL-R factor 2 score	0.073 (0.035)	.039*	1.076 (1.004 - 1.153)	0.118 (0.079)	.136	1.125 (0.963 - 1.315)
- PCL-R factor interaction	0.004 (0.002)	.038*	1.004 (1.000 - 1.008)	-0.017 (0.012)	.173	0.984 (0.960 - 1.007)
- dACC	-0.100 (0.149)	.503	0.905 (0.676 - 1.212)	-0.215 (0.153)	.161	0.807 (0.598 - 1.089)
Violent Felony Rearrest in Men (n = 201, 42 rearrests)						
- Age at release	-0.048 (0.017)	.007**	0.954 (0.921 - 0.987)	-0.045 (0.019)	.021*	0.956 (0.921 - 0.983)
- PCL-R factor 1 score	0.097 (0.042)	.022*	1.101 (1.014 - 1.196)	0.607 (0.243)	.012*	1.835 (1.140 - 2.954)
- PCL-R factor 2 score	0.174 (0.049)	<.001***	1.191 (1.081 - 1.311)	0.390 (0.130)	.003**	1.477 (1.145 - 1.905)
- PCL-R factor interaction	0.006 (0.002)	.005**	1.006 (1.002 - 1.011)	-0.039 (0.016)	.018*	0.962 (0.932 - 0.993)
- dACC	0.051 (0.169)	.761	1.053 (0.756 - 1.465)	-.101 (0.173)	.566	0.904 (0.641 - 1.276)
Felony Rearrest in Women (n = 248, 75 rearrests)						
- Age at release	-0.049 (0.016)	.003**	0.952 (0.922 - 0.983)	-0.041 (0.017)	.016*	0.960 (0.928 - 0.992)
- PCL-R factor 1 score	-0.016 (0.046)	.727	0.984 (0.900 - 1.077)	0.000 (0.218)	.998	1.000 (0.653 - 1.533)
- PCL-R factor 2 score	0.125 (0.034)	<.001***	1.113 (1.060 - 1.211)	0.190 (0.069)	.006**	1.209 (1.055 - 1.385)
- PCL-R factor interaction	0.002 (0.003)	.413	1.002 (0.997 - 1.007)	-0.009 (0.015)	.533	0.991 (0.962 - 1.020)
- dACC	0.190 (0.140)	.173	1.210 (0.920 - 1.590)	0.193 (0.146)	.184	1.213 (0.912 - 1.614)
Non-Violent Felony Rearrest in Women (n = 236, 63 rearrests)						
- Age at release	-0.057 (0.018)	.002**	0.944 (0.912 - 0.979)	-0.051 (0.019)	.007**	0.950 (0.915 - 0.986)
- PCL-R factor 1 score	-0.027 (0.050)	.588	0.973 (0.882 - 1.074)	0.033 (0.247)	.894	1.033 (0.637 - 1.676)
- PCL-R factor 2 score	0.132 (0.037)	<.001***	1.141 (1.061 - 1.228)	0.213 (0.078)	.007**	1.237 (1.061 - 1.442)
- PCL-R factor interaction	0.002 (0.003)	.548	1.002 (0.996 - 1.007)	-0.013 (0.017)	.454	0.987 (0.955 - 1.021)
- dACC	0.293 (0.150)	.051	1.340 (0.999 - 1.799)	0.213 (0.157)	.046*	1.367 (1.005 - 1.858)
Violent Felony Rearrest in Women (n = 185, 12 rearrests)						

Results of Cox regression analyses examining the predictive effect of the dACC on felony rearrest, non-violent felony rearrest, and violent felony rearrest within a four-year window (due to low power, analyses regarding violent

¹³ Due to our primary interest in the full multivariate model reported results focus on multivariate metrics.

rearrest in women are excluded). Unadjusted hazard values reflect univariate analyses, and adjusted hazard values reflect multivariate analyses including all variables of interest. All variables are mean centered, and reported effects are one-tailed. Table reports unstandardized B and relative risk ratio (exp[B]). * $p < 0.05$, ** $p < 0.01$, and *** $p < 0.001$.

4.3.2.1 Neurobiologically Informed Risk Assessment of Felony Rearrest

To test our primary hypothesis (that the dACC will exert an incremental effect above and beyond other established risk factors in the prediction of general felony rearrest), we tested the Aharoni et al. (2014) model—henceforth referred to as the error-monitoring model—including previously defined risk factors: 1) the offender’s release age, PCL-R factor 1, PCL-R factor 2, their interaction, and the dACC’s mean β -values for commission error versus correct hit trials in the male sample, $n = 213$. A significant overall effect ($p < .05$) was obtained for the model.

Within the model, as expected, age at release, PCL-R Factor 1, and PCL-R factor 2 were each significantly associated with days to general felony rearrest ($ps < .05$), with lower age at release and higher PCL-R scores associated with felony rearrest. Additionally, the PCL-R Factor 1 & 2 interaction was marginally significant in its association with rearrest ($p = .052$). However, dACC activity did not exhibit a significant association with felony rearrest above and beyond the other factors in the model, contrary to expectation (see Table 4.1).

The same methods were applied to a female sample, $n = 248$. A significant overall effect ($p < .05$) was obtained, driven by age at release and PCL-R Factor 2 ($ps < .05$), as expected. As in the male sample, dACC activity did not exhibit a significant association with felony rearrest (see Table 4.1: though see Table 4.4 for marginal effects of the dACC on long-term risk of felony rearrest).

4.3.2.2 Neurobiologically Informed Risk Assessment of Non-Violent Rearrest

To test our primary hypothesis (that the dACC will exert an incremental effect above and beyond other established risk factors in the prediction of non-violent rearrest), we regressed the

error-monitoring model on non-violent rearrest in the male sample ($n = 183$). A significant overall effect ($p < .05$) was obtained, driven by marginal effects of age at release and PCL-R Factor 1 ($ps < .1$). dACC activity, again, did not exhibit a significant association with non-violent rearrest (see Table 4.1).

For the same analysis within the female sample, $n = 236$, a significant overall effect ($p < .05$) was obtained for the model. Within the model, as expected, age at release and PCL-R factor 2 were each significantly associated with days to non-violent rearrest ($ps = .007$). In women, dACC activity exhibited a significant association with non-violent felony rearrest above and beyond these other risk factors. For every one unit increase in dACC activity, there was a 0.72 increase in the probability of rearrest for a non-violent crime ($p = .046$) (see Table 4.1; see Table 4.4 for significant effects of the dACC on long-term risk of non-violent felony rearrest).

4.3.2.3 Neurobiologically Informed Risk Assessment of Violent Rearrest

To test our primary hypothesis (that the dACC will exert an incremental effect above and beyond other established risk factors in the prediction of violent rearrest), we regressed the error-monitoring model onto time to rearrest for a violent crime in the male sample, $n = 201$.¹⁴ A significant overall effect ($p < .05$) was obtained for the model. Within the model, age at release, PCL-R Factor 1, Factor 2, and their interaction were each significantly associated with days to violent rearrest ($ps < .05$). Contrary to our prediction, dACC activity did not exhibit association with violent rearrest above and beyond the other factors in the model (see Table 4.1: though see Table 4.4 for marginal effects of the dACC on long-term risk of violent rearrest).

¹⁴ Due to insufficient power, analyses on violent rearrest in women are not explored.

4.3.3 Does the Inclusion of Neurobiological Error-Monitoring Information Increase the Accuracy of Statistical Models in Predicting Rearrest in Women?

The receiver operating characteristic (ROC) curve is a direct way to test a model's accuracy—indicating the true positive (sensitivity) and false positive (1 - specificity) ratio of a model. An area under the curve (AUC) analysis was conducted to discriminate between those women and men rearrested and not rearrested as functions of the error-monitoring model with and without inclusion of neurobiological error-monitoring activity.

In order to test our secondary hypothesis (that a multivariate model that includes the dACC will outperform one that doesn't), we fitted the error-monitoring model with and without dACC ROI data at a six-month time point for non-violent felony rearrest in women. The Non-Violent (Women) without dACC model reports an AUC of .681, and an improved AUC of .695 when including the dACC factor. The accuracy of the model was found to be relatively stable over a span of 6 months to three years (with values ranging from .695 - .699).

Overall, we find that the Non-Violent (Women) model incrementally benefits from the inclusion of brain-based error-monitoring activity.¹⁵

4.4 Discussion

The present project represents an out-of-sample validation and extension of the Aharoni et al. (2014) error-monitoring model using a large subset of the MAO-C. Our results demonstrate modest improvement in the prediction of later rearrest for felony offenses in women, and long-term risks of violent rearrests in men, using a predefined index of functional brain activation in the dACC—a region previously implicated in error-monitoring, inhibition, and impulsivity

¹⁵ Modest long-term effects of error-monitoring activity for felony rearrest in women and violent felony rearrest in men are excluded from ROC analyses.

(Bastin et al., 2017; Kiehl, Liddle, & Hopfinger, 2000; Orr & Hester, 2012; Spunt, Liberman, Cohen, & Eisenberger, 2012; Steele et al., 2014). Likewise, our results uphold previous findings in the literature, underscoring the importance of an offender's age at release and antisocial lifestyle score (PCL-R Factor 2) for predicting subsequent rearrest (Eisenbarth, Osterheider, Nedopil, & Stadtland, 2012; Huebner, DeJong, & Cobbina, 2010).

Previous attempts to test neurobiologically informed risk models for rearrest have been limited by the use of relatively small samples (by actuarial standards) leaving them unable to test the out-of-sample utility of the models more generally (Aharoni et al., 2013; Aharoni et al., 2014; Delfin et al., 2019; Steele et al., 2015; Zijlmans et al., 2021). Likewise, these same samples have been comprised of all (Aharoni et al., 2013 & Aharoni et al., 2014: $n = 96$; Zijlmans et al., 2021: $n = 127$) or mostly (Delfin et al., 2019: $n = 44$, 39 males) male subjects, leaving the generalizability of these models in women an open question. The present study addressed these problems, by conducting the largest ($n = 538$), to our knowledge, out-of-sample test of the error-monitoring model in independent samples of both women and men, and for non-violent and violent offenses. To our knowledge, the present study is the first in the literature to demonstrate the value of impulsivity related neurobiological activity for the prediction of non-violent rearrest in women, and for long-term risk of violent rearrest in men.

Overall, our positive results corroborate previous literature demonstrating that theoretically-relevant measurements of functional brain activity may improve accuracy of risk models designed to predict antisocial outcomes (Aharoni et al., 2013; Aharoni et al., 2014; Camchong, Stenger, & Fein, 2012; Delfin et al., 2019; Janes et al., 2010; Pardini, Raine, Erickson, & Loeber, 2014; Paulus, Tapert, & Schuckit, 2005; Sinha & Li, 2007; Steele et al., 2014; Steele et al., 2015; Steele et al., 2016; Zijlmans et al., 2021).

Our results also reinforce previous research suggesting the importance of paralimbic dysfunction as a mediator between cognitive control and antisocial behavior (Kiehl, 2006), as well as gender differences in the relationship between these paralimbic substrates and behavioral outcomes (Liu et al., 2012).

4.4.1 Limitations and Future Directions

Though our results provide modest support for the predictive utility of limbic activity for antisocial behaviors, we caution against overinterpretation due to the presence of null effects and directional sex differences. Criminal behavior is the result of a complex interaction of factors, including innumerable environmental and psychological variables (Aharoni et al., 2019; Allen & Aharoni, 2021). For this reason, it is striking that this study observed incremental predictive utility of the dACC in an independent sample. Still, the observed effects were modest, raising a demand to examine more complex models that better capture the variety of factors expected to contribute to different types of persistent antisocial behavior

Similarly, though prior research has suggested that increased engagement of error-monitoring processes has a protective effect for non-violent rearrest in men (Aharoni et al., 2013; Aharoni et al., 2014), our results suggest the inverse for women: *lower* error-monitoring neural activity had a protective effect for non-violent rearrest. Notably, previous research utilizing the same Go/NoGo task has demonstrated not only sex differences in limbic activations during error-monitoring, but also sex differences in the relationship between those activations and other impulsivity measures (Liu, Zubieta, & Heitzeg, 2012). Thus, more work is needed to understand sex-specific risk factors for antisocial behavior (Greiner, Law, & Brown, 2014; Olson, Stalans, & Escobar, 2015; Poels, 2007).

Caution is also warranted from a legal and ethical standpoint. Using evidence-based risk assessment techniques for “lower stake” decisions, such as treatment and early grant parole, has shown relative success in increasing treatment-program success and reducing antisocial behavior (Aos, Miller, & Drake, 2006; Andrews, 2006; MacKenzie, 2006; Taxman, 2002). However, using risk assessment techniques in ways that may conflict with a criminal offender’s own interests is controversial (Starr, 2014). Whether the use of neurobiological information presents any unique concerns above and beyond traditional behavioral risk factors is the subject of a small but important body of literature (see Aharoni, Abdulla, Allen, & Nadelhoffer, in press; Focquaert, 2019; Jurjako, Malatesti, & Brazil, 2019; Nadelhoffer et al., 2012). Ultimately, even if brain-based risk assessments demonstrably improve upon traditional risk assessment techniques, this does not necessarily mean that they ought to be utilized in legal decision making. Instead, the potential success of brain-based models for risk assessment should highlight the importance of continued discussion about the ethical and legal standards required for their various uses (Aharoni et al., in press).

Outside of the legal domain, research regarding neurobiologically informed risk assessment serves a critical basic research function by providing a way of testing causal relationships between brain and behavior. These causal mechanisms could prove useful in identifying potential behavioral interventions that may be beneficial in curbing antisocial behavior. Indeed, previous research has suggested that technologies such as transcranial direct current stimulation (tDCS) can be utilized to reduce self-reported aggression and even aggressive criminal intentions (Molero-Chamizo et al., 2019; Choy, Raine, & Hamilton, 2018). While these tDCS studies report encouraging results, clinical interventions such as these must meet high

standards of reliability and validity, and often warrant caution from ethical and legal standpoints as well (Large & Neilssen, 2017).

The present study provides an important out-of-sample validation and extension of previous research on the neuroprediction of rearrest (Aharoni et al., 2013; Aharoni et al., 2014; Steele et al., 2014; Steele et al., 2015). Still, much work remains to be done to determine whether the predictive utility of limbic activity for antisocial behavior will ever reach high enough standards to warrant the use of neurobiologically informed risk assessment technology. Follow up research should employ machine learning techniques in order to uncover other potential neurobiologically based metrics that may be helpful in the prediction of antisocial behavior, including, but not limited to sex-specific and crime-specific models. Until then, hypothesis-based neuropredictive modeling remains a helpful tool for testing potential causal mechanisms thought to mediate antisocial tendencies (Allen & Aharoni, in press).

4.5 Methods

4.5.1 Participants

Participants were 538 offenders (46% female) ranging in age from 15 to 63 y ($M = 32.95$, $SD = 9.68$). Approximately 8% were left-hand-dominant. Based on National Institutes of Health racial and ethnic classification, 80.3% of the sample self-identified as white, 7.6% as black/African American, 7.6% as American Indian, 3.3% as mixed/other, 58.9% as Hispanic, and 3% chose not to respond.

All 538 participants were part of the MAO-C and were determined to have minimal or no history of traumatic brain injury (as defined by a loss of consciousness for longer than 30 minutes), no lifetime history of a psychotic disorder, and had an estimated general IQ of greater than 65 (as estimated by the vocabulary and matrix reasoning subscales of the Wechsler Adult

Intelligence Scale; see Ryan & Ward, 1999). Participants reported having normal hearing, and visual acuity was normal or corrected to normal with the use of contact lenses or MRI compatible glasses. Participants were paid an hourly rate commensurate with standard pay for work assignments at their facility. Participants completed a number of psychological and behavioral assessment measures and an fMRI-based inhibition task using the Mind Research Network's Mobile MRI system before release from one of two New Mexico state correctional facilities. After being released, the participants in the validation sample were tracked from 2007 to 2017, and the average follow-up period was 60.6 mo. Participants provided written informed consent in protocols approved by the institutional review board of the University of New Mexico and by the Independent Review (E&I) Services for the Mind Research Network.

4.5.2 Behavioral Task

Behavioral impulsivity was measured during fMRI using the Go/NoGo task. The task, modeled after the work of Kiehl et al. (2000), presents participants with a frequently occurring target (the letter "X"; occurrence probability, 0.84) interleaved with a less-frequent distracter (the letter "K"; occurrence probability, 0.16) on a computer screen. Participants were instructed to depress a button with their right index finger as quickly and accurately as possible whenever they saw the target (the "go" stimulus) and not when they saw the distracter (the "no-go" stimulus). Because targets are more frequent than distracters in this task, a prepotent response toward the targets is elicited. When a distracter is presented, participants are required to inhibit their button response, which increases the rate of commission errors. Successful performance on this task requires the ability to monitor error-related conflicts and to selectively inhibit the prepotent go response on cue. Before scanning, participants completed a brief practice session of ~10 trials.

4.5.3 *Experimental Design*

The present fMRI study relied on a previously established set of coordinates to constrain the second level analysis within the present sample (Steele et al., 2014). All extracted imaging data used for the ROI constrained analysis within the sample are included in Dataset S1 in the form of an average β -values for each subject. Dataset S1 also includes PCL-R scores, their interaction term, and the offender's age at release.

The experimental design used on all participants was adopted from Kiehl et al. (2000) and is identical to that of Aharoni et al.'s (2013). Two scanning runs, each composed of 246 visual stimuli, were presented to participants using Presentation, a computer-controlled visual and auditory software (Neurobehavioral Systems). Stimuli were displayed on a rear-projection screen mounted at the rear entrance to the magnet bore and subtended a visual angle of $\sim 3 \times 3.5^\circ$. Each stimulus appeared for 250 ms in white text within a continuously displayed rectangular fixation box. Participants viewed the screen by means of a mirror system attached to the head coil.

The stimulus onset asynchrony (SOA) between go stimuli varied pseudorandomly among 1,000, 2,000, and 3,000 ms, subject to the constraint that three go stimuli were presented within each consecutive 6-s period. The no-go stimuli were interspersed among the go stimuli in a pseudorandom manner subject to three constraints: the minimum SOA between a go and a no-go stimulus was 1,000 ms; the SOA between successive no-go stimuli was in the range of 10 ± 15 s; and no-go stimuli had an equal likelihood of occurring at 0, 500, or 1,000 ms after the beginning of a 1.5-s acquisition period. By jittering stimulus presentation relative to the acquisition time, the hemodynamic response to the stimuli of interest was sampled effectively at 500-ms intervals.

Behavioral responses were recorded by using a MRI-compatible fiberoptic response device—created by Lightwave Medical—that is commercially available. Correct hits were defined as go (i.e., X-stimuli) events that were followed by a button press within 1,000 ms of stimulus onset. Correct rejections were defined by an absence of a motor response within 1,000 ms of the no-go stimulus. Commission errors were defined as the presence of a response within 1,000 ms of the onset of a no-go stimulus.

4.5.4 Image Acquisition

MRI acquisition parameters were identical to those discussed in Aharoni et al. (2013) and will only briefly be described here. Images were collected with a mobile Siemens 1.5-T Avanto system with advanced SQ gradients (max slew rate, 200T/m/s; 346 T/m/s vector summation, rise time 200 μ s) equipped with a 12-element head coil. The echoplanar image gradient-echo pulse sequence (repetition/echo times, 2,000/39 ms; flip angle, 75°; field of view, 24 \times 24 cm; 64 \times 64 matrix; 3.4 \times 3.4-mm in-plane resolution; 5-mm slice thickness; 30 slices) effectively covers the entire brain (150 mm) in 2,000 ms. Head motion was limited by using padding and restraint.

4.5.5 Preprocessing

Functional images were reconstructed offline at 16-bit resolution and manually reoriented to approximately the anterior commissure/posterior commissure plane. Functional images were spatially normalized to the Montreal Neurological Institute template via EPInorm (an affine transform followed by a nonlinear registration of the EPI image to an EPI template in standard space) and spatially smoothed (12mm full-width half maximum) in SPM12. High frequency noise was removed by using a low-pass filter (cutoff, 128s). The functional images were despiked using ArtRepair and motion corrected using InRialign—a motion correction procedure unbiased by local signal change (Freire, Roche, & Mangin, 2002).

4.5.6 Individual and Group Level Analysis

As in Aharoni et al. (2013), response types (correct hits and commission errors) were modeled as separate events. Event-related responses were modeled using a synthetic hemodynamic response function composed of two gamma functions. The first gamma function modeled the hemodynamic response using a peak latency of 6 s. A term proportional to the derivative of this gamma function was included to allow for small variations in peak latency. The second gamma function and associated derivative was used to model the small “overshoot” of the hemodynamic response on recovery. A latency variation amplitude-correction method was used to provide a more accurate estimate of hemodynamic response for each condition that controlled for differences between slices in timing and variation across regions in the latency of the hemodynamic response (Calhoun et al., 2004).

Individual runs were modeled together at first level of analysis, and functional images were computed for each participant that represented hemodynamic responses associated with commission errors and correct hits. General linear models included regressors to model motion (six parameters).

Activation differences between commission errors and correct hits were extracted from an a priori defined 14 mm radius sphere (Steele et al., 2014) centered around the seed coordinate in the ACC ($x = -3$, $y = 24$, $z = 33$: See Figure 4.1a for seed coordinate and Figure 4.1b for group level activation map) in the form of a mean β -values for each participant via the MarsBaRs plugin for SPM (Brett, Anton, Valabregue, & Poline, 2002).

4.5.7 Covariate Risk Assessment

Data from additional risk factors (Hare’s PCL-R and the offender’s age at release) were obtained to examine the incremental predictive validity provided by the established ROIs. These

additional variables have been previously found to predict antisocial behavior in offender populations (Aharoni et al., 2014; Olver & Wong, 2015). Scores from the Hare PCL-R—a semistructured interview and archival analysis which assesses psychopathy in incarcerated, forensic, psychiatric, and normal populations—were included as primary risk factors. These assessments were conducted by trained raters with high interrater reliability (ICC: .93). Eight percent (1% Female) of the sample ($n = 538$; Mean, 20.24; SD, 6.70) met the pre-established criteria for a diagnosis of psychopathy (score of ≥ 30). The PCL-R further splits into two separate clusters of traits: factor 1 includes interpersonal/affective traits (such as glibness and lack of empathy) and factor 2 includes antisocial behavioral traits (such as impulsivity and early behavioral problems). In cases where appropriate, PCL-R Factor scores were substituted with PCL-YV scores (the corresponding youth version of the PCL-R, with all individual items and their corresponding factors mirroring those of the PCL-R).¹⁶ As in Aharoni et al. (2014), these factors are entered individually into the overall predictive models sans a total PCL-R score (due to issues of collinearity).

Additional exploratory correlational analyses were also conducted with the following variables (see Tables 4.5, 4.6): the offender's estimated IQ, their alcohol/drug dependency (as assessed from the Structured Clinical Interview for the DSM (SCID) via determinations of lifetime abuse or dependence (scoring: 0 = no lifetime abuse/dependence, 1 = lifetime abuse, and 2 = lifetime dependence),¹⁷ their State-Trait Anxiety Inventory score (STAI: Spielberger et al., 1983), and The Barratt Impulsiveness Scale with three subscales measuring attentional impulsivity, motor impulsivity, and non-planning impulsivity (BIS-11; Patton et al., 1995).

¹⁶ PCL-YV scores were used for 70 of the men in our sample. Results excluding PCL-YV scores did not differ in results and trends.

¹⁷ Scoring for drug abuse/dependence is computed via an averaging across abuse/dependence in the following individual drug classes: sedatives, cannabis, stimulants, opioids, cocaine, and hallucinogens.

4.5.8 Follow-Up Procedure

Rearrest data, including arrest date and offense type, were obtained by the Center for Science & Law, which conducted state and county criminal searches following each participant's release date. Approximately 47.2% of the sample was rearrested at least once for a felony between their release date (ranging from 2007 to 2017) and their follow-up date (August, 2019). In line with previous predictive modeling, minor parole and probation violations were excluded from analysis, and the remaining offenses were further classified as violent or nonviolent when warranted. A larger portion of the sample was rearrested for nonviolent offenses (38.1%; 43.0% of males and 34.3% of females) than for violent offenses (20.1%; 27.1% of males and 11.7% of females). For primary cox-hazard analyses (Table 4.1) those first arrested for violent offenses were excluded from nonviolent rearrest analyses and those first rearrested for non-violent rearrest were excluded from violent rearrest analyses. Supplementary analyses (Table 4.4) for long term risk analyses without a four-year follow-up window did not utilize further group exclusions in order to maximize power. New violent rearrest data from the previously studied subset of the MAO-C (Aharoni et al., 2013; Aharoni et al., 2014; Steele et al., 2015) were also included in analyses.

4.5.9 Analytic Strategy

The primary hypothesis was evaluated by using Cox proportional-hazards regression. A Cox regression is a semiparametric test that investigates the effect of variables of interest on the time it takes for an event to happen—in this case, rearrest—while also estimating time courses of those that have yet to reach that event (censored cases). The dependent variable is the proportion of cases surviving the event (the cumulative survival function). In order to interpret the effect of individual variables on the cumulative survival function, hazard ratios (i.e., $\exp[B]$) are

computed. These hazard ratios characterize an individual's relative odds of reaching the event for every one unit change in the risk factor (e.g., error-monitoring brain activity), while controlling for other covariates.

The secondary hypothesis was evaluated by using receiver operating characteristic (ROC) curves which describe the differences between those who were and were not rearrested as a function of the predictors in the model (i.e., discrimination). While most assessments of ROC curves are time independent, our analyses of AUC characteristics are evaluated per model at a variety of time points (6, 12, 24, & 36 months) by utilizing Heagerty and Zheng's time-dependent ROC curve function as found in the *risksetROC* package in *R*, version 3.60 (Heagerty & Zheng, 2005). This analysis yields an AUC per time point in order to evaluate each model's ability to discriminate those who were and were not re-arrested across a series of time scales.

4.6 Acknowledgements

This material is based upon work supported by the National Science Foundation under Grant No. (1829495), the Center for Science & Law, and the National Institute of Health under Grant Nos. (R01MH080539, R01DA020870, R01DA026964, and R01HD092331). The contents of this manuscript are solely the responsibility of the authors and do not necessarily represent the views of the National Science Foundation, the Center for Science & Law, or the National Institute of Health.

4.7 Chapter 4 Supplementary Materials

Table 4.2 Areas of Error-Monitoring Activation in Men: Replication of Steele et al., 2014

Location	<i>t</i>-score	<i>x</i>	<i>y</i>	<i>z</i>	BA
Frontal Lobe					
1 R Superior Frontal Gyrus	19.78****	9	18	66	6

2	R Superior Frontal Gyrus	15.99****	24	54	30	10
3	L Superior Frontal Gyrus	17.17****	-27	54	30	10
4	R Inferior Frontal Gyrus	26.19****	36	18	-15	47
5	L Inferior Frontal Gyrus	25.89****	-36	15	-12	47
6	R Precentral Gyrus	11.28****	48	-9	36	6
7	L Precentral Gyrus	12.44****	-51	-12	33	4
8	L Anterior Cingulate Cortex	26.33****	-3	24	33	24
9	L Anterior Cingulate Cortex	16.16****	0	-12	42	24
10	R Anterior Cingulate Cortex	24.38****	6	33	12	24
11	Bi Anterior Frontal Cortex	26.19/25.89****	±36	15	0	11

Temporal Lobe

12	L Superior Temporal Gyrus	17.96****	-63	-51	18	22
13	R Middle Temporal Gyrus	14.23****	54	-33	-6	21
14	L Middle Temporal Gyrus	11.05****	-54	-30	-9	21

Parietal Lobe

15	L Inferior Parietal Lobule	19.10****	-63	-45	30	40
16	R Inferior Parietal Lobule	18.73****	63	-42	30	40

Occipital Lobe

17	L Middle Occipital Gyrus	5.82***	-42	-87	-12	18
18	L Middle Occipital Gyrus	6.95****	-45	-81	-12	18
19	L Inferior Occipital Gyrus	5.04**	-36	-93	-9	18
20	L Inferior Occipital Gyrus	4.40*	-33	-96	-6	18
21	R Fusiform	8.13****	45	-75	-18	18
22	R Precuneus	15.76****	6	-75	42	19
23	L Cuneus	14.78****	-12	-72	6	7
24	R Inferior Occipital Gyrus	5.26**	42	-87	-9	30
25	R Cuneus/Lingual Gyrus	15.21****	15	-66	3	18
26	Intrahemishperic	14.08****	0	-54	60	18

Subcortical

27	Midbrain (Pons)	17.77****	0	-21	-21	NA
28	L Midbrain (Brainstem)	20.13****	-3	-30	-3	NA
29	R Subthalamic Nucleus (Midbrain)	15.70****	3	-9	-3	NA

Cerebellum

30	L Cerebellum (Declive)	11.75****	-42	-63	-21	NA
----	------------------------	-----------	-----	-----	-----	----

31 R Cerebellum (Culmen)	11.18****	36	-51	-27	NA
32 R Cerebellum (Declive)	10.85****	39	-57	-24	NA

Note: ROI radii of 12mm. * $p < .05$, ** $p < .01$, *** $p < .001$, **** $p < .0001$ corrected for multiple comparisons.

Table 4.3 Areas of Error-Monitoring Activation in Women: Replication of Steele et al., 2014

Location	t-score	x	y	z	BA
Frontal Lobe					
1 R Superior Frontal Gyrus	22.27****	9	18	66	6
2 R Superior Frontal Gyrus	16.04****	24	54	30	10
3 L Superior Frontal Gyrus	15.28****	-27	54	30	10
4 R Inferior Frontal Gyrus	24.92****	36	18	-15	47
5 L Inferior Frontal Gyrus	25.16****	-36	15	-12	47
6 R Precentral Gyrus	13.48****	48	-9	36	6
7 L Precentral Gyrus	12.87****	-51	-12	33	4
8 L Anterior Cingulate Cortex	27.49****	-3	24	33	24
9 L Anterior Cingulate Cortex	18.09****	0	-12	42	24
10 R Anterior Cingulate Cortex	25.09****	6	33	12	24
11 Bi Anterior Frontal Cortex	24.92/25.16****	±36	15	0	11
Temporal Lobe					
12 L Superior Temporal Gyrus	19.50****	-63	-51	18	22
13 R Middle Temporal Gyrus	16.18****	54	-33	-6	21
14 L Middle Temporal Gyrus	10.62****	-54	-30	-9	21
Parietal Lobe					
15 L Inferior Parietal Lobule	20.38****	-63	-45	30	40
16 R Inferior Parietal Lobule	19.96****	63	-42	30	40
Occipital Lobe					
17 L Middle Occipital Gyrus	5.24**	-42	-87	-12	18
18 L Middle Occipital Gyrus	6.07***	-45	-81	-12	18
19 L Inferior Occipital Gyrus	5.09**	-36	-93	-9	18
20 L Inferior Occipital Gyrus	4.80**	-33	-96	-6	18
21 R Fusiform	6.10***	45	-75	-18	18
22 R Precuneus	16.22****	6	-75	42	19

23 L Cuneus	15.40****	-12 -72 6 7
24 R Inferior Occipital Gyrus	4.95**	42 -87 -9 30
25 R Cuneus/Lingual Gyrus	14.14****	15 -66 3 18
26 Intrahemispheric	14.25****	0 -54 60 18
Subcortical		
27 Midbrain (Pons)	17.50****	0 -21 -21 NA
28 L Midbrain (Brainstem)	20.33****	-3 -30 -3 NA
29 R Subthalamic Nucleus (Midbrain)	17.17****	3 -9 -3 NA
Cerebellum		
30 L Cerebellum (Declive)	11.70****	-42 -63 -21 NA
31 R Cerebellum (Culmen)	12.20****	36 -51 -27 NA
32 R Cerebellum (Declive)	13.83****	39 -57 -24 NA

Note: ROI radii of 12mm. * $p < .05$, ** $p < .01$, *** $p < .001$, **** $p < .0001$ corrected for multiple comparisons.

Table 4.4 Effect of Individual Predictors on Rearrest

Model/Predictor	Unadjusted Hazards			Adjusted Hazards		
	B (SE)	P value	exp[B] (CI)	B (SE)	P value	exp[B] (CI)
Felony Rearrest in Men (n = 213, 111 rearrests)						
- Age at release	-0.028 (0.009)	.003**	0.972 (0.955 - 0.991)	-0.025 (0.010)	0.016*	0.976 (0.956 - 0.995)
- PCL-R factor 1 score	0.063 (0.027)	.018*	1.066 (1.011 - 1.123)	0.228 (0.133)	.086	1.256 (0.968 - 1.630)
- PCL-R factor 2 score	0.094 (0.028)	.001**	1.099 (1.041 - 1.160)	0.134 (0.059)	0.024*	1.143 (1.017 - 1.285)
- PCL-R factor interaction	0.004 (0.001)	.004**	1.004 (1.001 - 1.007)	-0.013 (0.009)	.136	0.987 (0.969 - 1.004)
- dACC	-0.005 (0.107)	.964	.995 (0.807 - 1.227)	-0.104 (0.111)	.350	0.901 (0.725 - 1.121)
Non-Violent Felony Rearrest in Men (n = 213, 77 rearrests)						
- Age at release	-0.018 (0.011)	.088	0.982 (0.961 - 1.003)	-0.019 (0.012)	.113	0.981 (0.959 - 1.004)
- PCL-R factor 1 score	0.058 (0.032)	.075	1.059 (0.994 - 1.129)	0.191 (0.151)	.207	1.210 (0.900 - 1.627)
- PCL-R factor 2 score	0.062 (0.032)	.050	1.064 (1.000 - 1.133)	0.086 (0.068)	.203	1.090 (0.954 - 1.245)
- PCL-R factor interaction	0.003 (0.002)	.053	1.003 (1.000 - 1.007)	-0.010 (0.010)	.332	0.990 (0.970 - 1.010)
- dACC	-0.120 (0.133)	.369	0.887 (0.683 - 1.152)	-0.207 (0.139)	.136	0.813 (0.620 - 1.067)
Violent Felony Rearrest in Men (n = 290, 79 rearrests)						
- Age at release	-0.040 (0.012)	.001**	0.961 (0.938 - 0.984)	-0.031 (0.013)	0.016*	0.969 (0.941 - 0.994)
- PCL-R factor 1 score	0.044 (0.033)	.175	1.045 (0.981 - 1.114)	0.154 (0.176)	.383	1.166 (0.826 - 1.646)
- PCL-R factor 2 score	0.150 (0.035)	<.001***	1.162 (1.085 - 1.245)	0.214 (0.079)	0.007**	1.239 (1.061 - 1.447)
- PCL-R factor interaction	0.004 (0.002)	.017*	1.004 (1.001 - 1.007)	-0.011 (0.011)	.304	0.989 (0.967 - 1.010)
- dACC	-0.132 (0.132)	.312	0.876 (0.676 - 1.135)	-0.241 (0.138)	.082	0.786 (0.559 - 1.030)
Felony Rearrest in Women (n = 248, 97 rearrests)						
- Age at release	-0.050 (0.014)	<.001***	0.951 (0.925 - 0.978)	-0.044 (0.015)	0.003**	0.957 (0.930 - 0.986)
- PCL-R factor 1 score	-0.017 (0.040)	.677	0.983 (0.909 - 1.064)	-0.012 (0.118)	.949	0.988 (0.684 - 1.427)
- PCL-R factor 2 score	0.126 (0.029)	<.001***	1.135 (1.071 - 1.202)	0.197 (0.060)	0.001**	1.218 (1.084 - 1.369)
- PCL-R factor interaction	0.002 (0.002)	.324	1.002 (0.998 - 1.007)	-0.009 (0.013)	.464	0.991 (0.966 - 1.016)
- dACC	0.216 (0.124)	.082	1.241 (0.973 - 1.582)	0.220 (0.129)	.088	1.246 (0.968 - 1.604)
Non-Violent Felony Rearrest in Women (n = 248, 79 rearrests)						
- Age at release	-0.057 (0.016)	<.001***	0.945 (0.915 - 0.975)	-0.052 (0.017)	0.002**	0.949 (0.918 - 0.981)
- PCL-R factor 1 score	0.025 (0.045)	.570	0.975 (0.893 - 1.064)	0.077 (0.217)	.721	1.081 (0.707 - 1.652)
- PCL-R factor 2 score	0.126 (0.033)	<.001***	1.135 (1.064 - 1.210)	0.244 (0.070)	0.001**	1.251 (1.091 - 1.434)
- PCL-R factor interaction	0.002 (0.003)	.517	1.002 (0.997 - 1.007)	-0.016 (0.015)	.275	0.984 (0.955 - 1.013)
- dACC	0.310 (0.136)	.023*	1.364 (1.045 - 1.781)	0.334 (0.141)	0.018*	1.396 (1.058 - 1.842)
Violent Felony Rearrest in Women (n = 248, 29 rearrests)						
- Age at release	-0.069 (0.028)	.034*	0.942 (0.892 - 0.995)	-0.050 (0.030)	.096	0.951 (0.896 - 1.009)
- PCL-R factor 1 score	0.052 (0.071)	.469	1.053 (0.916 - 1.211)	-0.057 (0.382)	.881	0.944 (0.447 - 1.998)
- PCL-R factor 2 score	0.198 (0.062)	.001**	1.219 (1.079 - 1.377)	0.228 (0.125)	.068	1.256 (0.983 - 1.603)
- PCL-R factor interaction	0.006 (0.004)	.098	1.006 (0.999 - 1.014)	-0.002 (0.025)	.939	0.998 (0.951 - 1.048)
- dACC	0.078 (0.223)	.727	1.081 (0.698 - 1.674)	0.036 (0.234)	.878	1.037 (0.656 - 1.639)

Results of Cox regression analyses examining the predictive effect of the dACC on felony rearrest, non-violent felony, and violent felony rearrest. Unadjusted hazard values reflect univariate analyses, and adjusted hazard values reflect multivariate analyses including all variables of interest. All variables are mean centered, and reported effects are one-tailed. Table reports unstandardized B and relative risk ratio (exp[B]). * $p < 0.05$, ** $p < 0.01$, and *** $p < 0.001$.

4.7.1 Neurobiologically Informed Risk Assessment of Felony Rearrest: Long-Term Risk

To test the hypothesis (that the dACC will exert an incremental effect above and beyond other established risk factors in the assessment of long-term general felony rearrest risk), we regressed the error-monitoring model on general felony rearrest in the male sample ($n = 213$). A significant overall effect ($p < .05$) was obtained, driven by significant effects of age at release and PCL-R Factor 2 ($ps < .05$), as well as a marginal effect of PCL-R Factor 1 ($p = .086$). dACC activity did not exhibit a significant association with long term risk for felony rearrest (see Table 4.4).

For the same analysis within the female sample, $n = 248$, a significant overall effect ($p < .05$) was obtained for the model. Within the model, as expected, age at release and PCL-R factor 2 were each significantly associated with days to felony rearrest ($ps < .05$). In women, dACC activity exhibited a marginal association with general felony rearrest ($p = .088$).

4.7.2 Neurobiologically Informed Risk Assessment of Non-Violent Rearrest: Long-Term Risk

To test the hypothesis (that the dACC will exert an incremental effect above and beyond other established risk factors in the assessment of long-term non-violent felony rearrest risk), we regressed the error-monitoring model on general felony rearrest in the male sample ($n = 213$). A significant overall effect ($p < .05$) was obtained, but no individual predictors were significant.

For the same analysis within the female sample, $n = 248$, a significant overall effect ($p < .05$) was obtained for the model. Within the model, as expected, age at release and PCL-R factor 2 were each significantly associated with days to felony rearrest ($ps < .05$). In women, dACC

activity exhibited a significant association with long-term non-violent felony rearrest risk ($p = .018$).

4.7.3 Neurobiologically Informed Risk Assessment of Violent Rearrest: Long-Term

To test the hypothesis (that the dACC will exert an incremental effect above and beyond other established risk factors in the assessment of long-term violent rearrest risk), we regressed the error-monitoring model onto time to rearrest for a violent crime in the male sample ($n = 290$). A significant overall effect of the model ($p < .05$) was obtained. Age at release and PCL-R Factor 2 ($ps < .05$), were significantly associated with days to violent rearrest. As expected, dACC activity was marginally associated ($p = .082$) with long term risk for violent rearrest (see Table 4.4), such that those with low dACC activity were 1.27 times more likely to be rearrested for a violent felony than those with high dACC activity.

For the same analysis within the female sample, $n = 248$, a significant overall effect ($p < .05$) was obtained, driven by marginal effects of age at release and PCL-R Factor 2 ($ps < .10$). dACC activity was not significantly associated with long-term risk of violent rearrest in women.

Table 4.5 Two-Tailed Correlation Analyses in Men ($n = 290$)

Variable	1	2	3	4	5	6	7	8	9	10	11	12	13
1. Age at Release													
2. PCL-R Factor 1	-.04												
3. PCL-R Factor 2	-.32***	.48***											
4. PCL-R F1xF2	-.16**	.93***	.72***										
5. PCL-R Total	-.19**	.83***	.86***	.94***									
6. dACC	-.14*	.11	.14*	.14*	.15*								
7. IQ	.09	.05	-.03	.02	.01	.03							
8. Alcohol (Lifetime)	-.06	-.11	.11	-.03	.01	.1	-.01						
9. Drug (Lifetime)	-.19*	.09	.25**	.16	.19*	.08	.03	.23**					
10. Anxiety	.00	-.02	.26**	.10	.12	.08	-.13	.14	.13				
11. BIS-11 Factor 1	-.24***	.04	.26***	.14*	.18**	.04	-.16*	.17	.27**	.41***			
12. BIS-11 Factor 2	-.07	.12	.21**	.18**	.20**	-.02	-.06	.06	.31**	.09	.44***		
13. BIS-11 Factor 3	-.14*	.05	.28***	.14*	.18**	.00	-.17**	.06	.20*	.21*	.53***	.43***	
14. BIS-11 Total	-.18**	.09	.32***	.19**	.24***	.00	-.18**	.12	.31**	.30**	.79***	.76***	.85***

* $p < 0.05$, ** $p < 0.01$, and *** $p < 0.001$.

Table 4.6 Two-Tailed Correlation Analyses in Women (n = 248)

Variable	1	2	3	4	5	6	7	8	9	10	11	12	13
1. Age at Release													
2. PCL-R Factor 1	-.08												
3. PCL-R Factor 2	-.23**	.48**											
4. PCL-R F1xF2	-.13*	.93**	.69***										
5. PCL-R Total	-.18**	.76**	.91***	.88***									
6. dACC	.03	-.01	.08	.03	.06								
7. IQ	-.03	-.01	.07	.02	.08	.05							
8. Alcohol (Lifetime)	.13	.03	.12	.07	.12	-.12	.05						
9. Drug (Lifetime)	-.02	.22**	.37***	.30***	.41***	.01	.07	.23**					
10. Anxiety	-.12	.02	.06	.02	.04	.01	-.02	.13	.06				
11. BIS-11 Factor 1	-.12	.05	.32***	.12	.23**	.06	-.05	.11	.17*	.39***			
12. BIS-11 Factor 2	-.13	.22**	.44***	.31***	.41***	-.05	.07	.14	.15	.18*	.35***		
13. BIS-11 Factor 3	-.16*	.09	.33***	.15*	.26***	.00	-.17*	-.04	.06	.44***	.51***	.44***	
14. BIS-11 Total	-.18*	.16*	.47***	.26***	.39***	.01	-.08	.08	.13	.43***	.75***	.76***	.85***

* $p < 0.05$, ** $p < 0.01$, and *** $p < 0.001$.

5 GENERAL DISCUSSION

5.1 Summary

My dissertation research combined task-based and resting state fMRI approaches to probe potential candidate neurobiological substrates underlying antisocial outcomes (i.e., recidivism), with a primary focus on validating and extending the error-monitoring model of neurobiological risk assessment (Aharoni et al., 2013; Aharoni et al., 2014; Steele et al., 2015). My findings suggest that the inclusion of impulsivity related neurobiological metrics—error-monitoring activity (Chapters 2, 3, & 4) and resting state functional connectivity (Chapter 3) within the salience network—in risk assessment models may increase the accuracy with which these models are able to predict antisocial outcomes such as recidivism. Likewise, my findings support previous literature suggesting gender-specific relationships between impulsivity related neurobiological activity and subsequent impulsivity related outcomes (Chapter 4) (Liu et al., 2012). My results also provide validation to the utility of both the offender’s age at release and antisocial/impulsivity psychopathy traits for the prediction of subsequent recidivism (Chapters 2, 3, & 4) (Gendreau et al., 1996; Hemphill et al., 1998; Leistico et al., 2008; Kennealy et al., 2010; Ojala, Tiihonen, Repo-Tiihonen, Tikkanen, & Virkkunen, 2015; Olver & Wong, 2014; Walters et al., 2008).

Here I will synthesize my results in relation to my dissertation’s broader goal of improving the basic understanding of the neurobiological components underlying error-monitoring and their association with impulsivity. First, I will review the replicability of the error-monitoring neuroimaging analyses across my various samples (Section 5.2.1) and assess the association of these measures (and related rsFC measures) with various types of impulsivity related metrics (Sections 5.2.2, 5.2.3). Then I will discuss the incremental utility of

neurobiological data in predictive models for rearrest (Section 5.3). Finally, I will end the chapter with a consideration of the importance of this type of research for risk assessment and therapeutic interventions (Sections 5.4.1, 5.4.2) as well as consider future directions necessary to the field (Section 5.5).

5.2 Improving the Understanding of Task-Based and Resting State Neurobiological Correlates to Impulsivity

5.2.1 The Replicability of Neurobiological Error-Monitoring Activity

Here I will briefly synthesize the overall replicability of error-monitoring analyses across samples of male ($n = 95$ & $n = 290$) and female offenders ($n = 248$).

The analyses of error-monitoring activity presented in this dissertation demonstrate a high level of replicability of the brain regions recruited in error-monitoring. The error-monitoring analyses presented in Chapters 2 & 4 (see Tables 2.2, 4.2, 4.3) highlight the dACC and insulae as the primary regions most robustly recruited for this type of contrast. With more rigorous testing protocols, the error-monitoring analyses presented in Chapter 4 (see Tables 4.2, 4.3) represent the largest (to my knowledge) direct replication of the most thorough analysis of error-monitoring activity in the literature, utilizing samples of 290 male and 248 female offenders (Steele et al., 2014). More specifically, analyses in both samples replicated error-monitoring activity across 32 regions of the brain (11 in the Frontal Lobe, 3 in the Temporal Lobe, 2 in the Parietal Lobe, 10 in the Occipital Lobe, 3 Subcortical, and 3 Cerebellar: see Tables 4.2, 4.3 for discrete regions). Overall, these results demonstrate the highly replicable nature of the brain areas recruited in error-monitoring via the Go/NoGo task across large samples of male and female criminal offenders, directly validating what has been demonstrated in non-offender populations (Steele et al., 2014).

5.2.2 *Task-Based Neurobiological Correlates to Impulsivity*

Analyses concerning error-monitoring activity in forensic samples often focus on impulsivity related outcomes due to the heightened significance of these outcomes to both the offenders and society at large (e.g., rearrest or relapse: Aharoni et al., 2013; Aharoni et al., 2014; Chapters 2, 4; Steele et al., 2015a; Steele et al., 2015b). Broadly speaking, these analyses have demonstrated an inverse relationship between error-monitoring and impulsivity related outcomes: that is, higher error-monitoring activity is associated with lower incidence of impulsivity related outcomes (Aharoni et al., 2013; Aharoni et al., 2014; Chapter 2; Steele et al., 2015a; Steele et al., 2015b: but see Chapter 4). These associations with outcomes often detract from simpler, yet nonetheless important, analyses regarding the associations between error-monitoring activity and other impulsivity related measures (e.g., Barratt's Impulsivity Task, offender age, PCL-R Factor 2, and lifetime drug/alcohol abuse metrics). As such, I will briefly highlight significant associations (and lack thereof) between error-monitoring activity and other impulsivity related metrics, while first noting the directionality of error-monitoring activity's relation to rearrest (in order to ground these results directionally within my separate samples).

First, in a sample of male offenders, my Chapter 2 results suggest an association between low error-monitoring activity and likelihood of rearrest ($n = 95$: see Table 2.1), a relationship previously shown in Aharoni et al. (2013).¹⁸ Looking to my larger sample of male offenders ($n = 290$), I find that error-monitoring activity is negatively associated with the offender's age and positively associated with the offender's PCL-R Factor 2 score ($ps < .05$: see Table 4.5), both relationships that are directionally counterintuitive to what one would expect given the previous literature (Aharoni et al., 2013; Aharoni et al., 2014). Notably, error-monitoring activity in men

¹⁸ This relationship was not found to extend to the larger sample of men ($n = 290$: see Table 4.1)

was not significantly associated with their subsequent scoring on Barratt's Impulsivity Task ($p > .05$), nor lifetime alcohol or drug abuse and dependence ($ps > .05$).

In the female sample ($n = 248$), high error-monitoring activity was associated with incidence of rearrest (Chapter 4: see Table 4.1). While previous literature has noted gender-differences in the relation of error-monitoring activity and impulsive traits, there were no significant differences or associations ($ps > .05$) within the female sample between error-monitoring activity and other impulsivity related outcomes (Chapter 4: $n = 248$, see Table 4.6).

Overall, these results form a complicated picture of the relationships between error-monitoring activity and other (non outcomes-based) impulsivity related measures. Indeed, results indicating that high error-monitoring activity in men is associated with high PCL-R Factor 2 scores and lower ages (two positive predictors of impulsive outcomes) complicate the notion of an inverse relationship between error-monitoring activity and impulsivity related metrics/risk factors, as does the positive relationship between error-monitoring activity and rearrest incidence in women. Despite some consistency, much more work is needed to investigate whether there is a reliable relationship between error-monitoring activity and these other impulsivity related risk factors, or whether they all capture different aspects of the same underlying trait, potentially explaining the various directionalities present in the literature.

5.2.3 Resting State Neurobiological Correlates to Impulsivity

Previous work has suggested that the resting state functional connectivity between the dACC and insula is positively related to impulsivity related outcomes, such as risky decision making (Wei et al., 2016). When considering the most ecologically valid impulsivity measurement (rearrest), the results reported in Chapter 3 (see Table 3.1) support the directionality of this relationship—that is, the higher the dACC-Insular rsFC, the more likely an

offender was to be rearrested. However, a more granular analysis of the relationship between dACC-Insular rsFC and other impulsivity measures (e.g., Barratt's Impulsivity Task, offender age, PCL-R Factor 2, and lifetime drug/alcohol abuse metrics) complicate this picture of a simplistic unidirectional relationship. For instance, my results indicate that the dACC-Insular rsFC is negatively associated with PCL-R Factor 2 (antisocial & impulsive psychopathic traits) as well as an offender's total score on the Barratt's Impulsivity Task ($p < .05$: see Table 3.4). As noted previously in Section 5.2.2, the directionality of this relationship is contrary to what one would expect given the positive relationship between dACC-Insular rsFC and rearrest. Likewise, the dACC-Insular rsFC was not found to be significantly associated ($p > .05$) with an offender's dACC error-monitoring activity, further complicating the relation between these two different measures that both prove useful in predicting rearrest in the same offender sample (Chapter 2 & 3).

5.3 Testing the Incremental Utility of Neurobiological Data for Predictions of Recidivism

Measurements of impulsivity within lab environments advance our understanding of impulsivity under idealized conditions, but they often lack ecological validity. One method of addressing this shortcoming is linking lab-based impulsivity measures with outcomes outside of the lab—such as rearrest. Consistent with previous literature (Aharoni et al., 2013; Aharoni et al., 2014; Delfin et al., 2019; Steele et al., 2015), my results suggest that task-based and resting state impulsivity related neurobiological data can add incremental utility to predictions of rearrest (Chapters 2, 3, & 4). First, in Chapter 2, I find that the parameters used to extract the error-monitoring activity (to then be utilized in subsequent rearrest predictions) are fairly robust, as both newly established dACC and insular ROIs demonstrated success in increasing accuracies of non-violent rearrest predictions ($n = 95$; see Table 2.1) by 3.9% and 2.6%, respectively. In

Chapter 3, my results suggest that this incremental utility in risk models for rearrest isn't solely afforded by task-related data, but instead extends to resting state data from the same newly established dACC and insular ROIs ($n = 91$; see Table 3.1) increasing the accuracy of non-violent rearrest predictions by 3.1%. Additionally, a multi-modal model including both task-based and resting state data performs better than either unimodal analyses alone (see Figure 3.4), increasing predictive accuracy by 6.6%.

Chapter 4, on the other hand, demonstrates more modest and mixed effects of error-monitoring data in predictive models for rearrest in a large sample of offenders ($n = 538$). More specifically, with a strict exclusion criteria and truncated follow-up window (meant to directly replicate criteria used in Aharoni et al., 2013),¹⁹ a predictive effect of error-monitoring activity on rearrest in the males of this sample was not found ($n = 290$; see Table 4.1). Supplementary analyses suggest, though, when maximizing power (i.e., using an offender's full follow-up time rather than a 4-year window) and minimizing exclusion criteria (as is common in risk assessment literature analyzing less common outcomes like violent arrests), I observe marginal effects of error-monitoring activity in predictions of violent rearrest in men ($n = 290$; see Table 4.4).

More consistent effects of neurobiological data were found in the women of this sample ($n = 248$), with error-monitoring activity being a significant predictor of non-violent felony rearrest, regardless of the exclusion criteria used (see Tables 4.1, 4.4), providing convergent validity to prior research (Aharoni et al., 2013; Aharoni et al., 2014; Steele et al., 2015). More

¹⁹ More specifically, all individuals that committed a non-violent felony prior to a violent felony were excluded in violent felony analyses. Likewise, individuals that committed a violent felony prior to a non-violent felony were excluded from non-violent felony analyses. These strict exclusion criteria were employed in order to control for potential time-spent in prison for an offense not of interest (i.e., a non-violent felony when analyzing violent felonies).

specifically, the inclusion of error-monitoring activity increased the accuracy of predictions of non-violent rearrest in women by 1.4%.

5.4 The Broader Significance of Antisocial Risk Factor Research

5.4.1 Implications for Risk Assessment: Considering Accuracy

Risk assessment plays a pervasive role in the criminal justice pipeline, informing decisions from bail to release, and many steps in-between. The accuracy of risk assessments varies significantly depending on the mode of delivery and analysis (Desmarais et al., 2016; Haarsma et al., 2019; Monahan & Silver, 2003; Singh et al., 2011), yet risk assessments are now mandated in service of offender sentencing and placements decisions in over 20 states (Starr, 2014). As such, the use of risk assessment in legal settings remains a highly contentious issue due to various ethical concerns associated with them. While a comprehensive consideration of the debates surrounding the use of risk assessment in legal decision making is out of the scope of this chapter (though see Aharoni, Abdulla, Allen & Nadelhoffer, in press for overview), here I will focus on the relative importance of increasing the accuracy of these types of assessments by reviewing what serves to be gained via the use of improved risk assessment in lower-stake legal decisions.

Many criticisms of the use of risk assessment in the criminal justice pipeline focus on sentencing applications, but there has been a recent call for the use of risk assessment in lower-stake decisions that often benefit the offender (Aharoni, Abdulla, Allen & Nadelhoffer, in press; Baum & Savulescu, 2013; Tonry, 2014). Consider an excerpt from a recent chapter titled *Ethical Implications of Neurobiologically Informed Risk Assessment for Criminal Justice Decisions: A Case for Pragmatism* outlining some examples of lower-stake applications of risk assessment, as well as the rationale behind the use in such cases:

These include decisions to reduce a charge; decisions to offer bail, probation, or parole in lieu of jail or prison time; decisions to place an inmate in a lower security level; decisions about early release from civil commitment; diversion from traditional court to drug court; or the provision of benign treatment services. In all of these cases, the default choice (e.g., neglecting to offer treatment) is generally less favorable to the offender, and the offender qualifies for the more favorable choice by demonstrating low risk. Certainly, concerns could still be raised in these cases, but these concerns would likely apply to an even greater extent when such choices are not offered. (Aharoni et al., in press).

Aside from providing multiple examples of lower-conflict criminal justice decisions where risk assessment may be appropriate, Aharoni and colleagues (in press) also make an important observation worth reflecting on: it serves the offender to demonstrate low-risk in all of these decisions, as it will yield favorable outcomes compared to the default. As such, low-risk offenders would directly benefit from more accurate risk assessments, as they would be more likely to be correctly assigned to their true low-risk categorization.

The identification of true low-risk individuals in these types of legal decisions doesn't just benefit the low-risk offender, but also has the capacity to appease a variety of shared interests between the offender and the general public. One example of this is demonstrated in risk-needs-responsivity research, which argues that the most appropriate interventions within incarcerated populations occur when an offender's environment or treatment (that is, the "response" by the institution) is determined by the offender's relative risk. More specifically, work by Latessa, Lovins, and Smith (2010) suggest that low-risk offenders appropriately placed under low supervision are less likely to reoffend than those under high supervision. Inversely, low-risk offenders placed under high supervision (alongside high-risk offenders) are more likely to be rearrested than other low-risk offenders, suggesting a criminogenic effect of misplacement. In this case, the joint interest served by an increased accuracy in risk assessment is fairly straightforward: the appropriately placed low-risk offender benefits from a higher likelihood of

desistance from future rearrest, and the general public similarly benefits from a lower likelihood of being the victim of a crime at the hands of an appropriately placed offender.²⁰

This said, the extent to which *neurobiological data specifically* increased the accuracies of model predictions varied widely across my studies (from increases of 1.4% to 6.6% in traditionally significant models) and was insignificant in other models (see Table 4.1). Thus, it is necessary to caution against overinterpretation of the observed positive effects. Nonetheless, and as argued above, *any* incremental improvement of predictive accuracy in legal decision-making holds value, as it has the potential to provide better outcomes to both criminal offenders and the broader public alike. Thus, research on neurobiological predictors is important in generating further hypotheses to be tested in hopes of increasing the accuracies of these assessments. Likewise, hypothesis-based approaches in identifying candidate neural mechanisms associated with antisocial outcomes remain important for reasons other than risk assessment—such as in aiding progress in the domain of interventional research.

5.4.2 Implications for Therapeutic Applications

The use of neurobiological data to make predictions of antisocial outcomes is not dependent on a comprehensive knowledge regarding the causes of such behaviors. But research advancing such neurobiologically informed predictive models—such as the studies within this dissertation—can often help discriminate potential causal mechanisms, or even elucidate regions of interest, that can guide the design and development of tailored interventions meant to manage those behaviors (see also Barabas et al., 2018; Douglas et al., 2017; Gilligan & Lee, 2005; Latessa et al., 2010; Meynen, 2018). As proof of concept, consider the following recent brain

²⁰ Similar arguments can be made from the perspective of the general public regarding the tax-dollars necessary to apprehend, charge, and house the potential future offender for the entirety of their sentence.

stimulation studies, all of which use transcranial direct-current stimulation (tDCS) to alter the firing rates of large patches of neurons within particular regions of interest in the brain.

First, a study carried out by To and colleagues (2018) suggests that tDCS of the ACC can improve performance on cognitive and affective attentional tasks. Another study from Choy and colleagues (2018) similarly suggests that a single tDCS session targeting the dorsolateral prefrontal cortex (dlPFC: a region implicated in the inhibition of aggression) is sufficient to reduce aggressive criminal intentions surrounding violent & sexual assault. Correspondingly, this stimulation of the dlPFC also induced an increase in the belief that those criminal acts were wrong. Finally, a similar study utilizing a sample of criminal offenders suggests that stimulation of the prefrontal cortex can reduce aggressive behaviors (i.e., anger, and verbal/physical aggression) (Molero-Chamizo et al., 2019). While a group level difference in aggressive behaviors was observed, the largest reductions in hostility-specific aggressions—that is, aggression driven by impulsivity and high affect in the presence of a perceived threat—was also observed in the most violent subset of their sample (i.e., murderers). Consistent with this sub-population specific effect, a recent review of the literature suggests that these types of aggression pertinent interventions are more likely to see success in offender populations (Romero-Martínez, Bressanutti, & Moya-Albiol, 2020). Importantly, these interventionary tDCS studies all rely on prior research suggesting the relevance of specific brain regions in relation to certain behaviors and outcomes. As such, neuroprediction research, like mine, serves to establish candidate regions related to relevant outcomes.

Overall, it is important to consider larger takeaways that we can glean from the results of this dissertation, as well as a point that is echoed above: *one size does not fit all*. For instance, while my results suggest that error-monitoring activity is negatively associated with recidivism

in men, we observe the opposite effect in women, partially consistent with other impulsivity related literature demonstrating gender specific differences in the relationship between impulsivity related neurobiological activity and impulsive traits (Liu et al., 2013). Alongside the sub-population specific effects observed in Molero-Chamizo and colleagues' work (2019), and the differential success rates in general vs. offender populations uncovered by Romero-Martínez and colleagues (2020), my gender specific directional effects underscore the idea above; that is, future therapeutic approaches must utilize tailored interventions that are specific to the individual rather than to a population more generally.

Despite the demand for more effective treatment interventions for impulsive, antisocial behavior, much more research is necessary prior to the implementation of any sorts of neuro-interventions in offender populations. As is the case with any novel type of therapeutic intervention, the relative success of neuro-interventions must meet and demonstrate high standards of reliability and validity (Large & Nielszen, 2017).

5.5 Future Directions

While the work presented in this dissertation represents modest extensions and validations of the current research in the field of neurobiologically informed risk assessment of recidivism, many questions still remain. Here I will briefly address directions that future work in the field should consider.

First, further analyses regarding the utility of error-monitoring activity in predictions of rearrest remain necessary. Though the majority of literature within this young field focuses on this error-monitoring construct (see Aharoni et al., 2013; Aharoni et al., 2014; Steele et al., 2015; Zijlmans et al., 2021; Chapters 2, 3, & 4), work is still needed to further examine the

generalizability of this construct, and the relation of this construct to antisocial outcomes as modulated by individual differences (e.g., gender).

Secondly, if proven to be robust, research regarding the therapeutic modulation of error-monitoring activity and its subsequent implication for antisocial outcomes is necessary. As has been previously demonstrated, basic knowledge regarding which regions of the brain are primary substrates for particular phenotypes (i.e., aggression) can generate hypotheses about interventions intended to alter those phenotypes (Barabas et al., 2018; Douglas et al., 2017; Gilligan & Lee, 2005; Latessa et al., 2010; Meynen, 2018; Molero-Chamizo et al., 2019; Romero-Martínez, Bressanutti, & Moya-Albiol, 2020; To et al., 2018), but those hypotheses must be explicitly tested.

Finally, more broad data-driven approaches (e.g., the implementation of independent component analysis and support vector machines) for extracting and categorizing relevant biological (including both task-based & resting state data), psychological, and sociological measures for the prediction of anti-social behaviors is necessary, as hypothesis-based approaches to such remain narrowly scoped. Ultimately, a combination of multiple methodologies may improve our ability to identify cluster-specific causes and risk factors as well as develop more effective tailored treatments for impulsive and antisocial behaviors.

REFERENCES

- Abe, N., Greene, J. D., & Kiehl, K. A. (2018). Reduced engagement of the anterior cingulate cortex in the dishonest decision-making of incarcerated psychopaths. *Social cognitive and affective neuroscience*, *13*(8), 797-807.
- Aharoni, E., Abdulla, S., Allen, C. H., & Nadelhoffer, T. (in press). Ethical implications of neurobiologically informed risk assessment for criminal justice decisions. *MIT Press*.
- Aharoni, E., Mallett, J., Vincent, G. M., Harenski, C. L., Calhoun, V. D., Sinnott-Armstrong, W., Gazzaniga, M. S., & Kiehl, K. A. (2014). Predictive accuracy in the neuroprediction of rearrest. *Social Neuroscience*, *9*(4), 332–336.
<https://doi.org/10.1080/17470919.2014.907201>
- Aharoni, E., Vincent, G. M., Harenski, C. L., Calhoun, V. D., Sinnott-Armstrong, W., Gazzaniga, M. S., & Kiehl, K. A. (2013). Neuroprediction of future rearrest. *Proceedings of the National Academy of Sciences*, *110*(15), 6223–6228.
<https://doi.org/10.1073/pnas.1219302110>
- Aharoni, E., Anderson, N. E., Barnes, J. C., Allen, C. H., & Kiehl, K. A. (2019). Mind the gap: toward an integrative science of the brain and crime. *BioSocieties*, *14*(3), 463-468.
- Allen, C. H. & Aharoni, E. (2021). Current Trends in Cognitive Neuroscience and Criminal Punishment. In F. Focquaert, E. Shaw, & B. Waller (Eds.) *The Routledge Handbook of the Philosophy and Science of Punishment*. Routledge.
- Anderson, D. A. (2012). The Cost of Crime. *Foundations and Trends® in Microeconomics*, *7*(3), 209–265. <https://doi.org/10.1561/07000000047>

- Anderson, J. R., Walsh, Z., & Kosson, D. S. (2018). Psychopathy, self-identified race/ethnicity, and nonviolent recidivism: A longitudinal study. *Law and Human Behavior*, 42, 531–544. <https://doi.org/10.1037/lhb0000302>
- Andrews, D. A. (2006). Enhancing adherence to risk-need-responsivity: Making quality matter of policy. *Criminology & Public Policy*, 5, 595–602. <https://doi.org/10.1111/j.1745-9133.2006.00394.x>
- Aos, S., Miller, M., & Drake, E. (2006). Evidence-based public policy options to reduce future prison construction, criminal justice costs, and crime rates. *Federal Sentencing Reporter*, 19, 275–290.
- Barabas, C., Virza, M., Dinakar, K., Ito, J., & Zittrain, J. (2018, January). Interventions over predictions: Reframing the ethical debate for actuarial risk assessment. In Conference on Fairness, Accountability and Transparency (pp. 62-76). PMLR.
- Barkan, S. E., & Rocque, M. (2018). Socioeconomic Status and Racism as Fundamental Causes of Street Criminality. *Critical Criminology*, 26(2), 211–231. <https://doi.org/10.1007/s10612-018-9387-x>
- Bastin, J., Deman, P., David, O., Gueguen, M., Benis, D., Minotti, L., Hoffman, D., Combrisson, E., Kujala, J., Perrone-Bertolotti, M., Kahane, P., Lachaux, J., & Jerbi, K. (2016). Direct recordings from human anterior insula reveal its leading role within the error-monitoring network. *Cerebral Cortex*, bhv352.
- Baum, M., & Savulescu, J. (2013). Behavioral Biomarkers: What Are They Good For? *Bioprediction, Biomarkers, and Bad Behavior*, 12–41. <https://doi.org/10.1093/acprof:oso/9780199844180.003.0002>

- Behzadi, Y., Restom, K., Liau, J., & Liu, T. T. (2007). A Component Based Noise Correction Method (CompCor) for BOLD and Perfusion Based fMRI. *NeuroImage*, *37*(1), 90–101. <https://doi.org/10.1016/j.neuroimage.2007.04.042>
- BOP. (2018). *First Step Act Overview*. <https://www.bop.gov/inmates/fsa/overview.jsp>
- Brett, M., Anton, J.-L., Valabregue, R., & Poline, J.-B. (2002). Region of Interest Analysis Using an SPM Toolbox [Abstract]. *Neuroimage*, *16*. [https://doi.org/10.1016/S1053-8119\(02\)90013-3](https://doi.org/10.1016/S1053-8119(02)90013-3)
- Calhoun, V. D., Stevens, M. C., Pearlson, G. D., & Kiehl, K. A. (2004). fMRI analysis with the general linear model: Removal of latency-induced amplitude bias by incorporation of hemodynamic derivative terms. *NeuroImage*, *22*(1), 252–257. <https://doi.org/10.1016/j.neuroimage.2003.12.029>
- Camchong, J., Stenger, A., & Fein, G. (2013). Resting-state synchrony during early alcohol abstinence can predict subsequent relapse. *Cerebral Cortex (New York, N.Y.: 1991)*, *23*(9), 2086–2099. <https://doi.org/10.1093/cercor/bhs190>
- Campbell, C. & Eastman, N. (2014). The limits of legal use of neuroscience. In W. Sinnott-Armstrong, I. Singh, & J. Savulescu (Eds.), *Bioprediction, Biomarkers, and Bad Behavior: Scientific, Legal, and Ethical Challenges* (pp. 91–117). Oxford University Press.
- Cecil, K. M., Brubaker, C. J., Adler, C. M., Dietrich, K. N., Altaye, M., Egelhoff, J. C., Wessel, S., Elangovan, I., Hornung, R., Jarvis, K., & Lanphear, B. P. (2008). Decreased Brain Volume in Adults with Childhood Lead Exposure. *PLoS Medicine*, *5*(5), e112. <https://doi.org/10.1371/journal.pmed.0050112>

- Chai, X. J., Castañón, A. N., Öngür, D., & Whitfield-Gabrieli, S. (2012). Anticorrelations in resting state networks without global signal regression. *Neuroimage*, *59*(2), 1420-1428
- Chamberlain, S. R., & Sahakian, B. J. (2007). The neuropsychiatry of impulsivity. *Current Opinion in Psychiatry*, *20*(3), 255–261. <https://doi.org/10.1097/YCO.0b013e3280ba4989>
- Choy, O., Raine, A., & Hamilton, R. H. (2018). Stimulation of the Prefrontal Cortex Reduces Intentions to Commit Aggression: A Randomized, Double-Blind, Placebo-Controlled, Stratified, Parallel-Group Trial. *The Journal of Neuroscience: The Official Journal of the Society for Neuroscience*, *38*(29), 6505–6512.
<https://doi.org/10.1523/JNEUROSCI.3317-17.2018>
- Craig, A. D. B. (2009). How do you feel--now? The anterior insula and human awareness. *Nature Reviews. Neuroscience*, *10*(1), 59–70. <https://doi.org/10.1038/nrn2555>
- Delfin, C., Krona, H., Andiné, P., Ryding, E., Wallinius, M., & Hofvander, B. (2019). Prediction of recidivism in a long-term follow-up of forensic psychiatric patients: Incremental effects of neuroimaging data. *PLOS ONE*, *14*, e0217127.
<https://doi.org/10.1371/journal.pone.0217127>
- Desmarais, S. L., Johnson, K. L., & Singh, J. P. (2016). Performance of recidivism risk assessment instruments in US correctional settings. *Psychological Services*, *13*(3), 206.
- Devinsky, O., Morrell, M. J., & Vogt, B. A. (1995). Contributions of anterior cingulate cortex to behaviour. *Brain: A Journal of Neurology*, *118* (Pt 1), 279–306.
<https://doi.org/10.1093/brain/118.1.279>
- Douglas, K. S., & Reeves, K. A. (2010). Historical-Clinical-Risk Management-20 (HCR-20) Violence Risk Assessment Scheme: Rationale, application, and empirical overview. In *Handbook of violence risk assessment* (pp. 147–185). Routledge/Taylor & Francis Group.

- Ermer, E., Cope, L. M., Nyalakanti, P. K., Calhoun, V. D., & Kiehl, K. A. (2012). Aberrant paralimbic gray matter in criminal psychopathy. *Journal of abnormal psychology, 121*(3), 649.
- Farrer, C., & Frith, C. D. (2002). Experiencing oneself vs another person as being the cause of an action: The neural correlates of the experience of agency. *NeuroImage, 15*(3), 596–603. <https://doi.org/10.1006/nimg.2001.1009>
- Fink, B. C., Steele, V. R., Maurer, M. J., Fede, S. J., Calhoun, V. D., & Kiehl, K. A. (2016). Brain potentials predict substance abuse treatment completion in a prison sample. *Brain and behavior, 6*(8), e00501.
- Focquaert, F. (2018). Neurobiology and crime: A neuro-ethical perspective. *Journal of Criminal Justice. https://doi.org/10.1016/j.jcrimjus.2018.01.001*
- Fox, M. D., & Greicius, M. (2010). Clinical applications of resting state functional connectivity. *Frontiers in Systems Neuroscience, 4. https://doi.org/10.3389/fnsys.2010.00019*
- Friston, K. J., Holmes, A. P., Worsley, K. J., Poline, J.-P., Frith, C. D., & Frackowiak, R. S. J. (1994). Statistical parametric maps in functional imaging: A general linear approach. *Human Brain Mapping, 2*(4), 189–210. <https://doi.org/10.1002/hbm.460020402>
- Freire, L., Roche, A., & Mangin, J.-F. (2002). What is the best similarity measure for motion correction in fMRI time series? I. *IEEE Transactions on Medical Imaging, 21*, 470–484. <https://doi.org/10.1109/TMI.2002.1009383>
- Fu, Z., Tu, Y., Di, X., Biswal, B. B., Calhoun, V. D., & Zhang, Z. (2017). Associations between functional connectivity dynamics and BOLD dynamics are heterogeneous across brain networks. *Frontiers in human neuroscience, 11*, 593.

- Gendreau, P., Little, T., & Goggin, C. (1996). A meta-analysis of the predictors of adult offender recidivism: What works!. *Criminology*, 34(4), 575-608.
- Greiner, L. E., Law, M. A., & Brown, S. L. (2015). Using dynamic factors to predict recidivism among women: A four-wave prospective study. *Criminal Justice and Behavior*, 42(5), 457-480.
- Haarsma, G., Davenport, S., White, D. C., Ormachea, P. A., Sheena, E., & Eagleman, D. M. (2020). Assessing risk among correctional community probation populations: predicting reoffense with mobile neurocognitive assessment software. *Frontiers in psychology*, 10, 2926.
- Hare, R. D., Hart, S. D., & Harpur, T. J. (1991). Psychopathy and the DSM-IV criteria for antisocial personality disorder. *Journal of abnormal psychology*, 100(3), 391.
- Hare, R. D. (2003). *The psychopathy checklist-Revised*. Toronto, ON, 412.
- Hare, R. D., & Neumann, C. S. (2008). Psychopathy as a clinical and empirical construct. *Annu. Rev. Clin. Psychol.*, 4, 217-246.
- Hare, R. D., & Neumann, C. S. (2009). Psychopathy: Assessment and forensic implications. *The Canadian Journal of Psychiatry*, 54(12), 791-802.
- Harris, G. T., Rice, M. E., & Quinsey, V. L. (1993). Violent recidivism of mentally disordered offenders: The development of a statistical prediction instrument. *Criminal Justice and Behavior*, 20(4), 315-335. <https://doi.org/10.1177/0093854893020004001>
- Harsay, H. A., Spaan, M., Wijnen, J. G., & Ridderinkhof, K. R. (2012). Error Awareness and Salience Processing in the Oddball Task: Shared Neural Mechanisms. *Frontiers in Human Neuroscience*, 6. <https://doi.org/10.3389/fnhum.2012.00246>

- Heagerty, P. J., & Zheng, Y. (2005). Survival model predictive accuracy and ROC curves. *Biometrics*, *61*(1), 92–105. <https://doi.org/10.1111/j.0006-341X.2005.030814.x>
- Hemphill, J. F., Hare, R. D., & Wong, S. (1998). Psychopathy and recidivism: A review. *Legal and Criminological Psychology*, *3*, 139–170. <https://doi.org/10.1111/j.2044-8333.1998.tb00355.x>
- Holroyd, C. B., & Coles, M. G. H. (2002). The neural basis of human error processing: Reinforcement learning, dopamine, and the error-related negativity. *Psychological Review*, *109*(4), 679–709. <https://doi.org/10.1037/0033-295X.109.4.679>
- Hu, Y., Salmeron, B. J., Gu, H., Stein, E. A., & Yang, Y. (2015). Impaired functional connectivity within and between frontostriatal circuits and its association with compulsive drug use and trait impulsivity in cocaine addiction. *JAMA Psychiatry*, *72*(6), 584–592. <https://doi.org/10.1001/jamapsychiatry.2015.1>
- Hunt, K. S., & Easley, B., (2017) United State Sentencing Commission: The effects of aging on recidivism among federal offenders.
- Janes, A. C., Farmer, S., Peechatka, A. L., Frederick, B. de B., & Lukas, S. E. (2015). Insula-Dorsal Anterior Cingulate Cortex Coupling is Associated with Enhanced Brain Reactivity to Smoking Cues. *Neuropsychopharmacology: Official Publication of the American College of Neuropsychopharmacology*, *40*(7), 1561–1568. <https://doi.org/10.1038/npp.2015.9>
- Janes, A. C., Pizzagalli, D. A., Richardt, S., Frederick, B. deB., Chuzi, S., Pachas, G., Culhane, M. A., Holmes, A. J., Fava, M., Evins, A. E., & Kaufman, M. J. (2010). Brain Reactivity to Smoking Cues Prior to Smoking Cessation Predicts Ability to Maintain Tobacco

Abstinence. *Biological Psychiatry*, 67(8), 722–729.

<https://doi.org/10.1016/j.biopsych.2009.12.034>

Jurjako, M., Malatesti, L., & Brazil, I. A. (2018). Some Ethical Considerations About the Use of Biomarkers for the Classification of Adult Antisocial Individuals. *International Journal of Forensic Mental Health*, 0(0), 1–15. <https://doi.org/10/gffnqw>

Kaeble, D., & Cowhig, M. (2018). *Correctional Populations in the United States, 2016*. 14.

Kennealy, P. J., Skeem, J. L., Walters, G. D., & Camp, J. (2010). Do core interpersonal and affective traits of PCL-R psychopathy interact with antisocial behavior and disinhibition to predict violence? *Psychological Assessment*, 22, 569–580.

<https://doi.org/10.1037/a0019618>

Kerns, J. G., Cohen, J. D., MacDonald, A. W., Cho, R. Y., Stenger, V. A., & Carter, C. S.

(2004). Anterior cingulate conflict monitoring and adjustments in control. *Science (New York, N.Y.)*, 303(5660), 1023–1026. <https://doi.org/10.1126/science.1089910>

Kiehl, K. A., Liddle, P. F., & Hopfinger, J. B. (2000). Error processing and the rostral anterior cingulate: An event-related fMRI study. *Psychophysiology*, 37(2), 216–223.

Kiehl, Kent A. (2006). A cognitive neuroscience perspective on psychopathy: Evidence for paralimbic system dysfunction. *Psychiatry Research*, 142(2–3), 107–128.

<https://doi.org/10.1016/j.psychres.2005.09.013>

Kiehl, K. A., & Hoffman, M. B. (2011). The criminal psychopath: History, neuroscience, treatment, and economics. *Jurimetrics*, 51, 355.

Kiehl, K. A., Anderson, N. E., Aharoni, E., Maurer, J. M., Harenski, K. A., Rao, V., ... & Steele, V. R. (2018). Age of gray matters: Neuroprediction of recidivism. *NeuroImage: Clinical*, 19, 813-823.

- Kosson, D. S., Budhani, S., Nakic, M., Chen, G., Saad, Z. S., Vythilingam, M., Pine, D. S., & Blair, R. J. R. (2006). The role of the amygdala and rostral anterior cingulate in encoding expected outcomes during learning. *NeuroImage*, *29*(4), 1161–1172.
<https://doi.org/10.1016/j.neuroimage.2005.07.060>
- Kurth, F., Zilles, K., Fox, P. T., Laird, A. R., & Eickhoff, S. B. (2010). A link between the systems: Functional differentiation and integration within the human insula revealed by meta-analysis. *Brain Structure & Function*, *214*(5–6), 519–534.
<https://doi.org/10.1007/s00429-010-0255-z>
- Large, M., & Niessen, O. (2017). The limitations and future of violence risk assessment. *World Psychiatry*, *16*(1), 25–26. <https://doi.org/10/gdzzrr>
- Latessa, E. J., & Lovins, B. (2010). The Role of Offender Risk Assessment: A Policy Maker Guide. *Victims & Offenders*, *5*(3), 203–219.
<https://doi.org/10.1080/15564886.2010.485900>
- Leistico, A. M., Salekin, R. T., DeCoster, J., & Rogers, R. (2008). A large- scale meta-analysis relating the Hare measures of psychopathy to antisocial conduct. *Law and Human Behavior*, *32*, 28–45. <https://doi.org/10.1007/s10979-007-9096-6>
- Li, N., Ma, N., Liu, Y., He, X. S., Sun, D. L., Fu, X. M., ... & Zhang, D. R. (2013). Resting-state functional connectivity predicts impulsivity in economic decision-making. *Journal of Neuroscience*, *33*(11), 4886–4895.
- Ling, S., Umbach, R., & Raine, A. (2019). Biological explanations of criminal behavior. *Psychology, Crime & Law*, *25*(6), 626–640.
<https://doi.org/10.1080/1068316X.2019.1572753>

- Liu, J., Xu, X., Wu, K., Piao, Z., Huang, J., Guo, Y., Li, W., Zhang, Y., Chen, A., & Huo, X. (2011). Association between lead exposure from electronic waste recycling and child temperament alterations. *Neurotoxicology*, *32*(4), 458–464.
<https://doi.org/10.1016/j.neuro.2011.03.012>
- Liu, J., Zubieta, J. K., & Heitzeg, M. (2012). Sex differences in anterior cingulate cortex activation during impulse inhibition and behavioral correlates. *Psychiatry Research: Neuroimaging*, *201*(1), 54–62.
- Lystad, R. P., & Pollard, H. (2009). Functional neuroimaging: A brief overview and feasibility for use in chiropractic research. *The Journal of the Canadian Chiropractic Association*, *53*(1), 59–72.
- MacKenzie, D. L. (2006). *What works in corrections: Reducing the criminal activities of offenders and delinquents*. Cambridge University Press.
https://books.google.com/books?hl=en&lr=&id=gyBniA_PCA0C&oi=fnd&pg=PA3&dq=mackenzie+reducing+criminal+activity&ots=WM4Y5gFYD7&sig=SMR54DHpqWMAaUndWi0u2o52EZk
- Mathalon, D. H., Whitfield, S. L., & Ford, J. M. (2003). Anatomy of an error: ERP and fMRI. *Biological Psychology*, *64*(1–2), 119–141. [https://doi.org/10.1016/s0301-0511\(03\)00105-4](https://doi.org/10.1016/s0301-0511(03)00105-4)
- Menon, V., & Uddin, L. Q. (2010). Saliency, switching, attention and control: A network model of insula function. *Brain Structure & Function*, *214*(5–6), 655–667.
<https://doi.org/10.1007/s00429-010-0262-0>
- Menon, V. (2015). Salience Network. In *Brain Mapping* (pp. 597–611). Elsevier.
<https://doi.org/10.1016/B978-0-12-397025-1.00052-X>

- Meynen, G. (2018). Forensic psychiatry and neurolaw: Description, developments, and debates. *International Journal of Law and Psychiatry*. <https://doi.org/10/gfgqbf>
- Miglin, R., Bounoua, N., Goodling, S., Sheehan, A., Spielberg, J. M., & Sadeh, N. (2019). Cortical thickness links impulsive personality traits and risky behavior. *Brain sciences*, 9(12), 373.
- Molero-Chamizo, A., Martín Riquel, R., Moriana, J. A., Nitsche, M. A., & Rivera-Urbina, G. N. (2019). Bilateral Prefrontal Cortex Anodal tDCS Effects on Self-reported Aggressiveness in Imprisoned Violent Offenders. *Neuroscience*, 397, 31–40. <https://doi.org/10.1016/j.neuroscience.2018.11.018>
- Mortensen, J. A., Evensmoen, H. R., Klensmeden, G., & Håberg, A. K. (2016). Outcome Uncertainty and Brain Activity Aberrance in the Insula and Anterior Cingulate Cortex Are Associated with Dysfunctional Impulsivity in Borderline Personality Disorder. *Frontiers in Human Neuroscience*, 10, 207. <https://doi.org/10.3389/fnhum.2016.00207>
- Nadelhoffer, T., & Sinnott-Armstrong, W. (2012). Neurolaw and Neuroprediction: Potential Promises and Perils: Neurolaw and Neuroprediction. *Philosophy Compass*, 7(9), 631–642. <https://doi.org/10.1111/j.1747-9991.2012.00494.x>
- Nadelhoffer, T., Bibas, S., Grafton, S., Kiehl, K. A., Mansfield, A., Sinnott-Armstrong, W., & Gazzaniga, M. (2012). Neuroprediction, violence, and the law: Setting the stage. *Neuroethics*, 5(1), 67-99.
- Ojala, K. P., Tiihonen, J., Repo-Tiihonen, E., Tikkanen, R., & Virkkunen, M. (2015). Basal insulin secretion, PCL-R and recidivism among impulsive violent alcoholic offenders. *Psychiatry research*, 225(3), 420-424.

- Olver, M. E., & Wong, S. C. P. (2015). Short- and long-term recidivism prediction of the PCL-R and the effects of age: A 24-year follow-up. *Personality Disorders, 6*(1), 97–105.
<https://doi.org/10.1037/per0000095>
- Orr, C., & Hester, R. (2012). Error-related anterior cingulate cortex activity and the prediction of conscious error awareness. *Frontiers in human neuroscience, 6*, 177.
- Pardini, D. A., Raine, A., Erickson, K., & Loeber, R. (2014). Lower Amygdala Volume in Men is Associated with Childhood Aggression, Early Psychopathic Traits and Future Violence. *Biological Psychiatry, 75*(1). <https://doi.org/10.1016/j.biopsych.2013.04.003>
- Paulus, M. P., Tapert, S. F., & Schuckit, M. A. (2005). Neural activation patterns of methamphetamine-dependent subjects during decision making predict relapse. *Archives of General Psychiatry, 62*(7), 761–768. <https://doi.org/10.1001/archpsyc.62.7.761>
- Pierce, M., Hayhurst, K., Bird, S. M., Hickman, M., Seddon, T., Dunn, G., & Millar, T. (2017). Insights into the link between drug use and criminality: Lifetime offending of criminally-active opiate users. *Drug and Alcohol Dependence, 179*, 309–316.
<https://doi.org/10.1016/j.drugalcdep.2017.07.024>
- Philippi, C. L., Pujara, M. S., Motzkin, J. C., Newman, J., Kiehl, K. A., & Koenigs, M. (2015). Altered Resting-State Functional Connectivity in Cortical Networks in Psychopathy. *The Journal of Neuroscience, 35*(15), 6068–6078. <https://doi.org/10.1523/JNEUROSCI.5010-14.2015>
- Piotrowska, P. J., Stride, C. B., Croft, S. E., & Rowe, R. (2015). Socioeconomic status and antisocial behaviour among children and adolescents: A systematic review and meta-analysis. *Clinical Psychology Review, 35*, 47–55.
<https://doi.org/10.1016/j.cpr.2014.11.003>

- Poels, V. (2007). Risk assessment of recidivism of violent and sexual female offenders. *Psychiatry, Psychology and Law, 14*(2), 227-250.
- Poldrack, R. A., Monahan, J., Imrey, P. B., Reyna, V., Raichle, M. E., Faigman, D., & Buckholtz, J. W. (2018). Predicting Violent Behavior: What Can Neuroscience Add? *Trends in Cognitive Sciences, 22*(2), 111–123. <https://doi.org/10.1016/j.tics.2017.11.003>
- Poldrack, R. A., Huckins, G., & Varoquaux, G. (2020). Establishment of Best Practices for Evidence for Prediction: A Review. *JAMA Psychiatry, 77*(5), 534–540. <https://doi.org/10.1001/jamapsychiatry.2019.3671>
- Power, J. D., Barnes, K. A., Snyder, A. Z., Schlaggar, B. L., & Petersen, S. E. (2013). Steps toward optimizing motion artifact removal in functional connectivity MRI; a reply to Carp. *NeuroImage, 76*. <https://doi.org/10.1016/j.neuroimage.2012.03.017>
- Reynolds, B. W., Basso, M. R., Miller, A. K., Whiteside, D. M., & Combs, D. (2019). Executive function, impulsivity, and risky behaviors in young adults. *Neuropsychology, 33*(2), 212.
- Romero-Martínez, Á., Bressanutti, S., & Moya-Albiol, L. (2020). A systematic review of the effectiveness of non-invasive brain stimulation techniques to reduce violence proneness by interfering in anger and irritability. *Journal of clinical medicine, 9*(3), 882.
- Ryan, J. J., & Ward, L. C. (1999). Validity, reliability, and standard errors of measurement for two seven-subtest short forms of the Wechsler Adult Intelligence Scale—III. *Psychological Assessment, 11*(2), 207.
- Serin, R. C. (1996). Violent recidivism in criminal psychopaths. *Law and Human Behavior, 20*, 207–217. <https://www-jstor-org.gcsu.idm.oclc.org/stable/1394084>
- Siever, L. J. (2008). Neurobiology of Aggression and Violence. *The American Journal of Psychiatry, 165*(4), 429–442. <https://doi.org/10.1176/appi.ajp.2008.07111774>

- Singh, J. P., Grann, M., & Fazel, S. (2011). A comparative study of violence risk assessment tools: A systematic review and metaregression analysis of 68 studies involving 25,980 participants. *Clinical psychology review*, 31(3), 499-513.
- Sinha, R., & Li, C.-S. R. (2007). Imaging stress- and cue-induced drug and alcohol craving: Association with relapse and clinical implications. *Drug and Alcohol Review*, 26(1), 25–31. <https://doi.org/10.1080/09595230601036960>
- Soares, J. M., Magalhães, R., Moreira, P. S., Sousa, A., Ganz, E., Sampaio, A., Alves, V., Marques, P., & Sousa, N. (2016). A Hitchhiker's Guide to Functional Magnetic Resonance Imaging. *Frontiers in Neuroscience*, 10. <https://doi.org/10.3389/fnins.2016.00515>
- Sohn, J. S., Raine, A., & Lee, S. J. (2020). The utility of the Psychopathy Checklist-Revised (PCL-R) facet and item scores in predicting violent recidivism. *Aggressive behavior*, 46(6), 508-515.
- Spunt, R. P., Lieberman, M. D., Cohen, J. R., & Eisenberger, N. I. (2012). The phenomenology of error processing: The dorsal ACC response to stop-signal errors tracks reports of negative affect. *Journal of Cognitive Neuroscience*, 24(8), 1753–1765. https://doi.org/10.1162/jocn_a_00242
- Starr, S. B. (2014). Evidence-based sentencing and the scientific rationalization of discrimination. *Stan. L. Rev.*, 66, 803.
- Steele, V. R., Claus, E. D., Aharoni, E., Harenski, C., Calhoun, V. D., Pearlson, G., & Kiehl, K. A. (2014). A Large Scale (N = 102) Functional Neuroimaging Study of Error processing in a Go/NoGo Task. *Behavioural Brain Research*, 268, 127–138. <https://doi.org/10.1016/j.bbr.2014.04.001>

- Steele, V. R., Claus, E. D., Aharoni, E., Vincent, G. M., Calhoun, V. D., & Kiehl, K. A. (2015). Multimodal imaging measures predict rearrest. *Frontiers in Human Neuroscience*, 9. <https://doi.org/10.3389/fnhum.2015.00425>
- Stoeckel, L. E., Chai, X. J., Zhang, J., Whitfield-Gabrieli, S., & Evins, A. E. (2016). Lower gray matter density and functional connectivity in the anterior insula in smokers compared with never smokers. *Addiction Biology*, 21(4), 972–981. <https://doi.org/10.1111/adb.12262>
- Steele, V. R., Fink, B. C., Maurer, J. M., Arbabshirani, M. R., Wilber, C. H., Jaffe, A. J., Sidz, A., Pearlson, G. D., Calhoun, V. D., Clark, V. P., & Kiehl, K. A. (2014). Brain potentials measured during a Go/NoGo task predict completion of substance abuse treatment. *Biological Psychiatry*, 76(1), 75–83. <https://doi.org/10.1016/j.biopsych.2013.09.030>
- Taxman, F. S. (2002). Supervision-exploring the dimensions of effectiveness. *Fed. Probation*, 66, 14.
- Thomson, N. D., Vassileva, J., Kiehl, K. A., Reidy, D., Aboutanos, M., McDougale, R., & DeLisi, M. (2019). Which features of psychopathy and impulsivity matter most for prison violence? New evidence among female prisoners. *International journal of law and psychiatry*, 64, 26-33.
- van Veen, V., & Carter, C. S. (2002). The anterior cingulate as a conflict monitor: FMRI and ERP studies. *Physiology & Behavior*, 77(4–5), 477–482. [https://doi.org/10.1016/s0031-9384\(02\)00930-7](https://doi.org/10.1016/s0031-9384(02)00930-7)
- Walsh, Z. (2013). Psychopathy and criminal violence: The moderating effect of ethnicity. *Law and Human Behavior*, 37, 303–311. <https://doi.org/10.1037/lhb0000017>

- Walters, G. D., Wilson, N. J., & Glover, A. J. J. (2011). Predicting recidivism with the Psychopathy Checklist: Are factor score composites really necessary? *Psychological Assessment, 23*, 552–557. <https://doi.org/10.1037/a0022483>
- Wei, Z., Yang, N., Liu, Y., Yang, L., Wang, Y., Han, L., Zha, R., Huang, R., Zhang, P., Zhou, Y., & Zhang, X. (2016). Resting-state functional connectivity between the dorsal anterior cingulate cortex and thalamus is associated with risky decision-making in nicotine addicts. *Scientific Reports, 6*. <https://doi.org/10.1038/srep21778>
- Whitfield-Gabrieli, S., & Nieto-Castanon, A. (2012). Conn: A functional connectivity toolbox for correlated and anticorrelated brain networks. *Brain Connectivity, 2*(3), 125–141. <https://doi.org/10.1089/brain.2012.0073>
- Yang, M., Wong, S. C. P., & Coid, J. (2010). The efficacy of violence prediction: A meta-analytic comparison of nine risk assessment tools. *Psychological Bulletin, 136*(5), 740–767. <https://doi.org/10.1037/a0020473>
- Zheng, D., Chen, J., Wang, X., & Zhou, Y. (2019). Genetic contribution to the phenotypic correlation between trait impulsivity and resting-state functional connectivity of the amygdala and its subregions. *Neuroimage, 201*, 115997.
- Zijlmans J., Marhe R., Bevaart F., Van Duin L., Luijckx M. A., Franken I., Tiemeier H., Popma A. (2021). The predictive value of neurobiological measures for recidivism in delinquent male young adults. *J Psychiatry Neurosci, 46*(2):E271-E280.

APPENDICES

Appendix A: CV

Corey H. Allen

71 Howard St. SE, Unit 5309, Atlanta, GA 30317
(918) 231-9996 – Callen63@student.gsu.edu

Education

Georgia State University	Atlanta, GA
<i>Ph.D. Candidate, Neuroscience Institute, GPA: 4.00</i>	Aug. 2016-Defense Scheduled June 2021
Neuroethics Concentration	
Proposed Dissertation: <i>The Neuroprediction of Recidivism: Out-of-Sample Validation and Extension of the Error-Monitoring Model</i>	
Regis University - Magna Cum Laude	Denver, CO
<i>Bachelor of Science in Neuroscience, GPA: 3.86</i>	2015
Honors Thesis: <i>Neurons and Narratives: Living in a Wittgensteinian World</i>	
Independent Research: <i>Philosophical Ideals and the Political Spectrum</i>	
<i>Bachelor of Arts in Philosophy, GPA: 3.86</i>	2015
Capstone: <i>The Phenomenology of Cycling</i>	

Research Experience

Georgia State University	Atlanta, GA
<i>Graduate Research Assistant in Cooperation, Conflict, & Cognition Lab.</i>	Aug. 2016-Present
Projects:	
-Testing risk of recidivism via task based and resting-state fMRI data.	
-Testing third-party punishment motives, including effects of neuroscientific framing on criminal punishment and treatment decisions.	
-Characterizing latent structure of mental state attributions of moral agency.	
-Exploring the ethical-legal implications of neuroprediction for punishment and treatment.	
University of Colorado Anschutz Medical Campus	Denver, CO
<i>Research Assistant in TMS and Movement Sciences Lab.</i>	Jan. 2014 Jan. 2017
Projects:	
-Conducted meta-analysis on the safety of transcranial magnetic stimulation in children.	
<i>Lab Technician</i>	Jan. 2014-Dec. 2014
Duties:	
-Determined patient motor threshold via EMG and transcranial magnetic stimulation and conducted rTMS for clinical trials and therapy in various demographics (with/without MRI guide).	

-Analyzed torque development during range of motion movement in Parkinson's patients.

Regis University

Denver,

CO

Lab Technician in Neuroscience and Psychology Department.

Jan. 2013-May 2015

Duties:

- Conducted stereotaxic surgery on mice in order to research oxidative stress in Parkinson's models.
- Created, gained IRB support, and conducted research on philosophical ideals and political bias.
- Created guide on how to quantify facial emotion via EMG for department faculty.
- Collected and analyzed behavioral data on empathy in mice populations.

St. John Medical Center

Tulsa, OK

Stroke Clinic Intern in Heyman Stroke Center.

Summer 2012

Duties:

- Conducted neurological assessments on stroke patients, examined CT/MRI scans, and gathered background information relating to potential stroke and other health issues.

Publications

Aharoni, E., Abdulla, S., **Allen, C. H.**, and Nadelhoffer, T. (in press). Ethical Implications of Neurobiologically Informed Risk Assessment for Criminal Justice Decisions: A Case for Pragmatism. *MIT Press*.

Allen, C. H., & Aharoni, E. (2020). Current Trends in Cognitive Neuroscience and Criminal Punishment. In F. Focquaert, E. Shaw, & B. Waller (Eds.) *The Routledge Handbook of the Philosophy and Science of Punishment*. Routledge.

Aharoni, E., Anderson, N. E., Barnes, J. C., **Allen, C. H.**, & Kiehl, K. A. (2019). Mind the gap: Toward an integrative science of the brain and crime. *BioSocieties*.

Nahmias, E., **Allen, C. H.**, & Loveall, B. (2019). When Do Robots Have Free Will? Exploring the Relationships Between (Attributions of) Consciousness and Free Will. In B. Feltz, M. Missal, & A. Sims (Eds.) *Free Will, Causality, and Neuroscience*. Cognitive Science Series. Brill Publishers.

Allen C. H., Vold, K., Felsen, G., Blumenthal-Barby, J. S., Aharoni, E. (2019). Reconciling the opposing effects of neurobiological evidence on criminal sentencing judgments. *PLoS ONE* 14(1): e0210584. <https://doi.org/10.1371/journal.pone.0210584>

Allen, C. H., Kluger, B. M., & Buard, I. (2017). Safety of Transcranial Magnetic Stimulation in Children: A Systematic Review of the Literature. *Pediatric Neurology*.

Manuscripts in Review or Preparation

Allen, C. H., Aharoni, E., Harenski, C.L., Harenski, K. A., & Kiehl, K. A. (in prep). Hemodynamic model from 442 inmates improves predictions of rearrest.

Allen, C. H., Aharoni, E., Gullapalli, A., Harenski, C.L., Harenski, K. A., & Kiehl, K. A. (in prep). Limbic activity

predicts reoffending in women: A partial validation and extension.

Allen, C. H., Aharoni, E., Harenski, C., & Kiehl, K. A. (in prep). Functional connectivity measures in the salience network improves predictions of rearrest: a resting state analysis.

Nahmias, E., **Allen, C. H.**, Aharoni, E. (in prep). In support of a communicative theory of punishment: the role of understanding in decreased punitive inclinations.

Work in the Media

Allen, C. H., Nahmias, E., & Aharoni, E. (2021, March). Neuro-Interventions as Punishment? The Neuroethics Blog. <http://www.theneuroethicsblog.com/2021/03/neuro-interventions-as-punishment.html>

Allen, C. H., & Aharoni, E. (2019, April). Should Brain Scans Influence How Heavily Criminals are Punished? Newsweek. <https://www.newsweek.com/should-brain-scans-influence-how-heavily-criminals-are-punished-1383297>

Allen, C. H., (2018, April). The Effects of Neuroscientific Framing on Legal Decision Making. The Neuroethics Blog. <http://www.theneuroethicsblog.com/2018/04/the-effects-of-neuroscientific-framing.html>

Academic Meeting Presentations and Other Academic Works

Allen, C. H., Aharoni, E., Harenski, C. L., Harenski, K. A., & Kiehl, K. A. (2021, March). Functional connectivity measures in the salience network improve predictions of rearrest: a resting state analysis. Poster presented at the annual meeting of the Cognitive Neuroscience Society.

Aharoni, E., **Allen, C. H.**, Gullapalli, A., Harenski, C. L., Harenski, K. A., & Kiehl, K. A. (2021, March). Limbic activity predicts reoffending in women: A partial validation and extension. Poster presented at the annual meeting of the Cognitive Neuroscience Society.

Allen, C. H., Nahmias E., & Aharoni, E. (2020, October). Moral Intuitions Regarding NIBS Interventions in Criminal Offenders. Video presentation at the meeting of the International Neuroethics Society.

Allen, C. H., Abdulla, S., Nadelhoffer, T., & Aharoni, E. (2019, October). Ethical Implications of Neurobiologically Informed Risk Assessment for Criminal Justice Decisions: A Case for Pragmatism. Poster presented at the meeting of the International Neuroethics Society, Chicago, IL.

Allen, C. H. (2019, September). Behavioral Inhibition: Connections with Cognitive Neuroscience and the Neuroprediction of Recidivism. Invited lecture given at the College of Arts and Sciences, 3000 Level Behavioral Psychology, Georgia State University, Atlanta, GA.

Allen, C. H. (2019, June). The Neuroprediction of Recidivism: Out-of-Sample Validation and Extension of the Error Monitoring Model. Dissertation proposal defended at CCC Lab, Georgia State University, Atlanta, GA.

Allen, C. H. (2019, April). Justice at all costs? Transparency about the costs of incarceration decreases lay and law student sentencing recommendations. Invited presentation given at College of Law, Georgia State University, Atlanta, GA.

Allen, C. H. (2019, March). The Neuroprediction of Recidivism: Validation and Extension of the Error Monitoring Model. Oral presentation given at Neuroscience Institute Breakfast Lecture Series, Georgia State University, Atlanta, GA.

Allen, C. H. (2018, November). Neurobiologically Informed Risk Assessment: The Neuroprediction of Recidivism. Oral presentation given at Hard Data Cafe, Georgia State University, Atlanta, GA.

Allen, C. H., Watzek, J., Kleider-Offutt, H. M., Brosnan, S. F., & Aharoni, E. (2018, November). Justice at all costs? Transparency about the costs of incarceration decreases lay sentencing recommendations. Poster session presented at the annual meeting of the Society for Judgment and Decision Making, New Orleans, LA.

Nahmias, E., **Allen, C. H.,** & Loveall, B. (2018, July). When Robots and Aliens Have Free Will: Exploring the Relationships Between (Attributions of) Consciousness, Rationality, Free Will, and Blame. Poster session presented by Eddy Nahmias at the annual meeting of Society for Philosophy and Psychology, Ann Arbor, MI.

Allen, C. H., Felson, G., Blumenthal-Barby, J., Vold, K., & Aharoni, E. (2017, November). Effects of framing on criminal punishment and involuntary commitment. Poster session presented at the annual meeting of the International Neuroethics Society, Washington, D.C.

Nahmias, E., **Allen, C. H.,** & Loveall, B. (2017, November). When Robots Have Free Will: Exploring the Relationships Between (Attributions of) Consciousness and Free Will. Keynote speech presented by Eddy Nahmias at X-Phi Workshop Osnabruck, Germany.

Allen, C. H., Felson, G., Blumenthal-Barby, J., Vold, K., & Aharoni, E. (2017, April). Testing Effects of Framing on Punishment Decisions Involving Violence Risk Assessment. Poster session presented at the Second Century Initiative Poster Day, Georgia State University, Atlanta, GA.

Allen, C. H., Felson, G., Blumenthal-Barby, J., Vold, K., & Aharoni, E. (2017, March). Testing Effects of Framing on Punishment Decisions Involving Violence Risk Assessment. Oral presentation given at Hard Data Cafe, Georgia State University, Atlanta, GA.

Allen, C. H. (2015). Neurons and Narratives: Living in a Wittgensteinian World. *All Regis University Theses*. 637. <https://epublications.regis.edu/theses/637>

Allen, C. H. (2015, May). Neurons and Narratives: Living in a Wittgensteinian World. Honors Thesis defended within the Neuroscience and Philosophy Department, Regis University, Denver, CO.

Allen, C. H. (2015, May). The Phenomenology of Cycling. Oral presentation given at the Philosophy Capstone Consortium, Regis University, Denver, CO.

Allen, C. H. (2014). Philosophical Ideals and the Political Spectrum. Poster session presented at the Neuroscience and Psychology Department Poster Day, Regis University, Denver, CO.

Allen, C. H. (2014). Torque Development in Parkinson's Patients. Oral presentation given at the Neuroscience Department, Regis University, Denver, CO.

Teaching and Academic Leadership

Georgia State University*Instructor of Record*

Course:

-Sensation and Perception

Atlanta, GA
Aug.-May 2021**Community Educational Outreach****Denver, CO***Tutor*

Duties:

Jan.-May 2013

- Tutored recent parolees in goal of obtaining GEDs and/or steady jobs.
- Taught General Chemistry, Biology, Earth Sciences, Trigonometry, Algebra, and English.
- Lectured on electronic competency: resumes, job interviews, and applying to jobs in the digital age.

Philosophy Club*Co-Head*

Duties:

Denver, CO
2014-2015

- Chose weekly discussion topics/readings & lectured on them, leading the group discussion.

Awards, Recognitions, and Scholarships**External**

International Neuroethics Society Travel Stipend (\$250) - 2019

Society for Judgment and Decision Making Poster Award, First Place (\$750) - 2018

International Neuroethics Society Elsevier Poster Award (\$100) - 2017

Duke Institute for Brain Sciences (project personnel - \$3,000) - 2017

Georgia State University

2CI Neuroethics Fellowship (guaranteed for four years - \$25,000) – 2016, 2017, 2018, 2019, 2020

Atlanta, GA**Regis University**

The Francis J. Malecek Award for Excellence in Philosophy – One male/female per graduating class

Admitted and graduated in Regis University Honors Program – Limited to 40 per year

Honors Scholarship (five students per year) – 2014, 2015

Dean's List (GPA of 3.75 or higher) – 2011, 2012, 2013, 2014, 2015

Board of Trustees Scholarship – 2011, 2012, 2013, 2014, 2015

Denver, CO**Skills****Software** - MATLAB, giftICA, SPM, CONN, FSL, R, BrainSight, EndNote, AcqKnowledge, SPSS, Qualtrics, mTurk**Hardware** - Stereotaxic surgery, MagStim TMS, BioPac**Procedures** - fMRI/sMRI/rsfMRI/DTI data preprocessing and analysis, rTMS, sp/ppTMS, statistical analyses, survey design and administration